Inferring the Global Financial Network from High-Dimensional Time-Series of Stock Returns

Sachapon Tungsong

First Supervisor: Professor Tomaso Aste

Second Supervisor: Dr. Fabio Caccioli

A dissertation submitted in partial fulfillment

of the requirements for the degree of

Doctor of Philosophy

of

University College London.

Department of Computer Science

University College London

September 29, 2018

Statement of Declaration

I, Sachapon Tungsong, confirm that the work presented in this thesis is my own. Where information has been derived from other sources, I confirm that this has been indicated in the work.

Abstract

Connectedness in a financial network refers to the structure of interlinkages among the financial institutions which encompasses three aspects: which institutions are linked, how many of the institutions are linked, and the magnitude of the linkages.

This research measures time-varying connectedness in the global financial network using the following two frameworks: (1) vector autoregression-forecast error variance decomposition (VAR-FEVD) and (2) information filtering network-based algorithm LoGo-TMFG. In the first framework we construct a *full* connectedness network where each of the financial institutions is linked to the others using VAR. On the contrary, in the second framework we construct a *sparse* connectedness network where only significant links are kept and insignificant links are put to zeros using LoGo-TMFG, which is a novel sparse modeling algorithm.

We show that both frameworks reveal strong variations of connectedness during past crises, but the connectedness measure computed on the sparse network can distinguish major crises better than that computed on the full network. This suggests that sparse modeling using the LoGo-TMFG algorithm increases the signal-to-noise ratio in the data and improves interpretability of the connectedness measure, which leads to better statistical inference of the result.

In the first framework we analyze bank returns in North America, the European Union, and Southeast Asia from 2005 to 2016. We find that the North American system has the highest connectedness, suggesting that it is the most interconnected system. We perform Granger causality and transfer entropy tests which indicate that the connectedness of the North American system led that of the EU and Southeast Asia. Through our analysis we make technical improvements to the VAR-FEVD methodology and deal with the issues of outliers and overfitting of the VAR model.

In the second framework we study rolling windows of high dimensional datasets

comprising companies in the financial sector (GICS 40) globally from 1990 to 2016. Analyzing the global financial network as a system of ten economic regions, we find that the regions become more interconnected over time as evidenced by the increase in the number and size of inter-regional links. In addition, the regions are more interconnected during crises than during normal periods. North America and Europe, the two dominant regions, were connected to all other regions over the sample period from 1990 to 2016 and the links between the two regions were much stronger than those between the other regions. We find that North America, especially the U.S., was dominated by banks (GICS 4010) as they were the most impactful and vulnerable industry throughout the entire sample period. For the other regions, the dominant industry alternates between diversified financials (GICS 4020) and banks (GICS 4010). In this framework we contribute to the literature by addressing high dimensionality in financial data using the novel LoGo-TMFG algorithm which is the first application of the algorithm in connectedness measurement. In addition, our datasets are unique and much larger than those in other studies, where each rolling window contains up to 4,310 financial companies. By analyzing rolling windows of data, each of which contains companies that were active during the three-year period, we address the survival bias issue that many other studies do not.

Our research findings are beneficial especially for policy makers, e.g., the central banks, who can use our connectedness metrics to enhance systemic risk monitoring. Practitioners in the macro research or macro trading desks at a bank or asset manager can also make use of both the methodologies we used as well as the research findings.

Impact Statement

This PhD thesis has academic impacts in that it adds to the area of systemic risk research, specifically to the improvements of the methodologies used in measuring connectivity, which has been rapidly growing since the Global Financial Crisis. First, we improve the existing VAR-FEVD methodology and apply it onto new datasets that have not been studied before.

Second, our application of the LoGo-TMFG algorithm in systemic risk and onto such large and complete datasets is novel. We demonstrate that analyzing large and noisy financial datasets can be done with the LoGo-TMFG and will provide more interpretable results than those discussed in existing research. With their wide-ranging applicability, both the improved VAR-FEVD and LoGo-TMFG algorithms can definitely be beneficial for measuring connectivity in big datasets in other fields within finance and outside of finance.

Organizations outside of academia can make use of the results and research methodology discussed in this PhD thesis. As our analyses are done on the global financial network, institutions in both the public and private sectors globally can infer from the thesis information that might be useful for their day-to-day business.

In order to increase reachability, we disseminate our research both formally through journal publications, conferences, talks, and consulting work, and informally through conversations with friends and acquaintances. A part of my PhD thesis was published in the Journal of Network Theory in Finance in the June 2018 issue. In addition, I presented my PhD research in conferences including the European Winter Meeting of the Econometric Society 2015, Computing in Economics and Finance 2015 & 2016, and IMA Conference on Mathematics in Finance 2015.

Acknowledgements

I would like to thank my primary supervisor Tomaso Aste for his invaluable academic guidance and support with respect to my PhD studentship and my general well-being throughout the PhD. I would like to thank my second supervisor Fabio Caccioli for our research discussions, new ideas, and suggestions to improve our papers which are a part of my PhD thesis. Both Tomaso and Fabio are very positive and have been extremely generous with their time guiding me throughout my PhD.

I am grateful for the studentship provided by EPSRC and for the Dean's Prize granted by UCL's Department of Computer Science over the course of my PhD.

I thank my classmates for their humor, camaraderie, and for sharing with me knowledge and life stories. My experience in the PhD program would not have been as enriched and fun without them.

Finally, I would like to thank my mom, dad, and sister for believing in me and for providing unconditional love and support. Thanks for always being there for me.

Contents

List of Figures

List of Tables

Chapter 1

Introduction

1.1 Motivation

The Global Financial Crisis of 2007-2008 highlighted the need for academics, practitioners, and policy makers to take a closer look at systemic risk and how to measure it accurately. During the crisis, contagion proved to be a dangerous factor which accelerated the transmission of financial troubles from one financial institution to the others, causing a number of financial institutions to fail.

In the wake of such extreme event, various tools from a variety of scientific disciplines including network theory, statistics, econometrics, and machine learning have been employed to measure financial connectedness. The challenge in accurately measuring connectedness and systemic risk remains, despite the wealth of existing literature pioneered by Adrian and Brunnermeier [2016] and Brownlees and Engle [2016]. Each of the existing connectedness metrics helps explain only a portion of the complex financial interconnectedness, provided that there are many ways financial institutions can be connected to one another. For instance, banks may have direct connections through cross equity holding, joint business projects, and interbank lending. Indirect connections between banks include similarity in business models, trading, investment and risk management strategies, and common exposures to economic fluctuations such as the credit downgrade of the US government. Indirect connections are often reflected in the co-movement of the banks' share prices due to fluctuations in the economy [Allen and Babus, 2008]. Due to the multidimensional nature of the relationships between financial institutions, it is impossible for a single metric to capture the extent and complexity of financial connectedness. It is thus important to measure connectedness from

different angles, each of which is based on different type of financial connections. In addition, one must analyze jointly different metrics of connectedness to have a more complete understanding of the relationships between financial institutions.

Despite the role of financial institutions in the past crises, there is little empirical research that covers the entire global financial network. The main reason for the lack of empirical work on global financial connectedness is the network's high dimensionality [Demirer et al., 2017]. Diebold and Yilmaz [2014] had to limit their analysis to a small number of US firms, which is incomplete, given the global nature of the financial sector. The largest network existing research has investigated is the world's top 150 banks by [Demirer et al., 2017], which again is only a fraction of the global financial sector.

1.2 Research objectives

This research attempts to fill the gap in existing literature by quantifying time-varying connectedness at different levels of granularity in the **global** financial network. We use publicly available data, such as stock returns, instead of relying on proprietary information, such as interbank lending, which are unavailable to the public. We believe that market data, to a certain degree, carry information about connectedness between financial institutions. By quantifying the connectedness, we attempt to understand how exogenous shocks can be amplified by the endogenous dynamics of the financial network. We analyze companies in the global financial sector (GICS 40) [1] which includes banks (GICS 4010), diversified financials (GICS 4020), insurance (GICS 4030), and real estate (GICS 4040) from ten economic regions of the world: North America, South America, Africa, Europe, the Middle East, West Asia, South Asia, East Asia, Southeast Asia, and Australia.

In the context of network construction, we view the global financial network as an endogenous system that is susceptible to exogenous shocks, whose transmission from one institution to another is dictated by the structure and size of connectedness between the financial institutions. With this view, we conduct our analysis at different levels of granularity with the aim to investigate the following:

1. **pairwise connectedness** for each pair of financial companies. We quantify con-

[1] The Global Industry Classification Standard (GICS) is a standardized classification system for equities developed jointly by Morgan Stanley Capital International (MSCI) and Standard and Poor's.

nectedness between pairs of financial institutions and investigate if financial institutions headquartered in the same geographical regions have stronger connectivity than those from different geographical regions.

2. **system-wide or total connectedness**. We aim to quantify total connectedness within each of the economic regions and analyze how it evolves over time, from normal to crisis periods. In addition, we investigate how total connectedness of one region is compared to that of another. We hope to uncover lead-lag relationship between the regional connectivities by using causality tests such as Granger causality and transfer entropy.

3. **inter-regional connectedness** between two economic regions and between each of the economic regions and the rest. We hope to understand the strength of connectivity between two regions and to what extent each region affects and is affected by the rest of the world. In addition, we aim to identify which regions are the most impactful and vulnerable.

4. **inter-industrial connectedness** between two industries and between each industry and the rest of the financial sector. We aim to identify which of the four industries is the most impactful and/or vulnerable as well as to understand the connectivity strength between two industries.

1.3 Methodological frameworks

The existing literature on financial contagion can be broadly classified into two categories: network models and econometric models. First, network models, which can be calibrated with balance-sheet data, aim to describe various propagation mechanics of financial contagion. Pioneering literature in this category are Allen and Gale [2000] and Eisenberg and Noe [2001]. Second, econometric models which aims to measure connectedness or spillover exclusively from market data, without making assumptions about the distress propagation dynamics between the financial institutions. Prominent examples of literature in this category include Adrian and Brunnermeier [2016], Brownlees and Engle [2016], and Billio et al. [2012]. In addition, recent empirical work which relies on econometric models especially VAR and FEVD includes Diebold and Yilmaz [2009, 2012, 2014], Demirer et al. [2017], and Geraci and Gnabo

[2018]. This research falls into the second category—we quantify from market data connectedness at different granularities using the two following frameworks:

1. **vector autoregression-forecast error variance decomposition (VAR-FEVD)**, where we construct a *full* connectedness network in which each and every financial firm is linked to the others and estimate connectedness via decomposing the forecast error variance for each firm,

2. **information filtering network-based algorithm LoGo-TMFG**, where a *sparse* network is constructed by keeping only significant links and putting insignificant links to zero. We then estimate connectedness based on information theoric quantities such as conditional mutual information and conditional transfer entropy.

1.3.1 VAR-FEVD framework

In this framework we build on the framework proposed by Diebold and Yilmaz [2009, 2012, 2014] who use the well-known multivariate time series analysis tools—VAR and FEVD—to quantify connectedness from market data.

The VAR-FEVD framework views the financial institutions as an endogenous system in which the stock return of each firm $\mathbf{y}_t$ is a linear function of its own lags and the lagged returns of the other firms in the system,

$$\mathbf{y}_t = \mathbf{A}\mathbf{y}_{t-1} + \mathbf{u}_t,$$

where $\mathbf{y}_t = (y_{1t}, ..., y_{Kt})'$ is a $K \times 1$ vector of centered K variables, $\mathbf{A}$ is a fixed $K \times K$ matrix of VAR coefficients, and $\mathbf{u}_t = (u_{1t}, ..., u_{Kt})'$ is a K-dimensional white noise process. The endogenous system is subject to external shocks, e.g., a severe economic downturn, which are accounted for in the error term $\mathbf{u}_t$.

Through the error term $\mathbf{u}_t$ and the endogenous relationship between the stock returns $\mathbf{A}$, we analyze how the effects from an external shock are transmitted through the system. We decompose the shock occurred to a firm which then gets transmitted to other firms to obtain pairwise impact from the former to each of the latter. The process is called forecast error variance decomposition (FEVD), i.e., we decompose the variance of the forecast error produced by the VAR process. Finally, we take the average of the pairwise impacts in order to quantify how much the banking system as

a whole is affected when an external shock occurred to a single bank. This gives us the total connectedness or system-wide connectedness metric. Note that the network in this framework is not sparse.

There are several issues to consider when one measures connectedness empirically. Of particular interest to us are the issues of outliers and high dimensionality of data, whose impacts are more pronounced in rolling-window analyses. Extreme outliers will largely affect our analysis as long as they are included in the current rolling window. High dimensional data typically result in underdetermined inverse problems, large standard errors of parameter estimators, and overfitting in which the model describes noise instead of the underlying relationship between the variables. In this research we will address the sensitivity to outliers issue in the data preprocessing step where we apply exponential weights onto the data, giving higher weights to more recent data points. Overfitting and high variance due to the curse of dimensionality is addressed in the estimation step by using ridge regression instead of the standard OLS.

1.3.2 Information filtering network-based LoGo-TMFG

One of the drawbacks of the VAR-FEVD framework is that it is unable to handle large datasets in which the number of observations is small compared to the number of variables. As the global financial sector comprises as many as 4,310 active companies between 2014 and 2016, the VAR to model for this dataset will be overparameterized which results in unreliable parameter estimates and forecasts.

Common issues when dealing with large datasets are non-invertible covariance matrices and overparameterization which leads to other issues such as overfitting and unreliable estimates and forecasts. It is often the case that a model with fewer parameters has stronger predictive power and can better describe the statistical variability of data than overparameterized models. One way to obtain such a parsimonious model is to use sparsity modeling.

The starting point for sparsity modeling is to formulate the global financial network as a Gaussian Markov Random Field (GMRF), a construct in which the financial institutions' stock returns are assumed to be jointly Gaussian and the relationships between the financial institutions are described by a precision matrix. The LoGo-TMFG algorithm, proposed by Barfuss et al. [2016], yields a sparse precision matrix in which

where the zero elements indicate conditional independence between the financial institutions. In the LoGo-TMFG framework, a network is represented by a triangulated maximally planar graph (TMFG), which is made up of a number of four-node cliques (4-cliques) and separators which are three-node cliques (3-cliques). LoGo-TMFG constructs the global sparse precision matrix from a simple sum of local inverse covariances, reducing the large-scale problem of finding the global inverse of a full covariance matrix to summing the inverses of significantly smaller local covariance matrices.

From the estimated inverse covariances, we compute five connectedness metrics including number of links, conditional mutual information, conditional transfer entropy, impact, and vulnerability. These metrics address different granularities of connectedness, e.g., between financial companies, between economic regions, between industries within the financial sector, and the system-wide connectedness, similar to the connectedness metrics from the VAR-FEVD framework.

1.4 Main contributions

The main contributions of this thesis are in both the methodological approach and actual empirical analyses. On the methodology part, we propose technical improvements to the VAR-FEVD which lead to superior results compared to the standard VAR. We also add to the graphical lasso literature by providing an empirical proof that the algorithm yields unreliable results for our large datasets and illustrate that the novel LoGo-TMFG algorithm leads to better outcome in this case. In addition, we propose "impact" and "vulnerability" which are computed from conditional transfer entropies as additional connectedness metrics. On the empirical analysis part, we apply VAR-FEVD on unique datasets and conduct causality tests on the resulting total connectedness metrics, which provides valuable insight on the lead-lag relationship between connectedness in different economic regions. Moreover, we analyze the entire global financial network using LoGo-TMFG, which is the first both in terms of the dataset and application of the algorithm, resulting in new, useful findings.

Our research findings are beneficial for policy makers, e.g., the central banks, with respect to systemic monitoring. We believe practitioners in the macro research or macro trading desks at a bank or asset manager can also make use of our research results and methodologies.

1. Connectedness measurement using the VAR-FEVD framework

Our contributions are three folds. First, we contribute to the technical aspect of VAR estimation, yielding better identification of crisis events, which leads to more accurate and insightful interpretation of the results. More specifically, we mitigate the problem of sensitivity to outliers by applying exponential weights on the data, putting higher weights on more recent data points. We also perform ridge regression in order to minimize the standard error of the VAR coefficients, as the problem of large standard errors is generally associated with large-scale systems.

Second, we apply the VAR-FEVD methodology on new datasets for the first time. We study the structures of connectedness in the three banking systems, namely North America, the European Union, and Southeast Asia. While related studies such as Diebold and Yilmaz [2009] and Demirer et al. [2017] analyze a global network composed of banks from many regions, we investigate individually the NA, EU and ASEAN banking systems and show that, despite the regions' geographical distances, they are affected in various degrees by major financial crises originated in dominant regions such as the North America and the EU. In addition, conducting our analysis this way allows us to observe that the NA connectedness is generally the highest, followed by the EU and ASEAN.

Third, we perform a Granger causality and transfer entropy tests on the connectedness time series generated from the VAR-FEVD method. This is to investigate the causal relationships among the connectedness structures of the aforementioned three banking systems. To the best of our knowledge, this causality study is the first of its kind. Our findings indicate that the connectivity within North America is generally the highest and leads those of the EU and Southeast Asia, and the connectivity within the EU is the second highest and leads that of Southeast Asia. That is, high level of connectivity within North America is believed to induce high level of connectivities within Europe and Southeast Asia.

2. Connectedness measurement using the information filtering network-based LoGo-TMFG algorithm

Our contributions from this research are as follows. First, we address high dimen-

sionality in financial data using the novel LoGo-TMFG which is a sparsity modeling algorithm. This is the first application of the LoGo-TMFG algorithm in the context of connectedness and systemic risk measurement. We show that the LoGo-TMFG yields more superior results to those from the well-known graphical lasso algorithm. Graphical lasso infers a disconnected network from our large datasets which is unrealistic. This is quite common among the ℓ_1-based methods which tend to over-sparsify the network (Zhao and Yu [2006] and Heinavaara et al. [2016]). Barfuss et al. [2016], the LoGo-TMFG is faster, taking approximately 0.56 times as long as graphical lasso with LARS solver for a small dataset and 0.16 times as long for a larger dataset.

Second, our global financial datasets are larger than those in any other studies to date. In addition to the full samples covering the periods from 1990 to 1999 and from 2000 to 2016, we analyze twenty five rolling windows, each of which features three years (approx. 750 trading days) of daily stock returns for a large number of financial companies, i.e., between 1,680 companies in 1990-1992 to 4,310 in 2014-2016. To the best of our knowledge, published research to date that empirically measures financial connectedness has not used datasets of this size. A key reason for the lack of empirical work on global financial connectedness is the high dimensionality of the network [Demirer et al., 2017]. Because there are very many important financial institutions globally, using unrestricted VAR and related analyses on a large global dataset is intractable. Diebold and Yilmaz [2014] were forced to limit their analysis to a small number of purely US institutions. The subsequent work of [Demirer et al., 2017] which addressed high dimensionality using LASSO-VAR covered only the world's 150 top banks, which is much smaller than our datasets.

Third, we deal with the survival bias by analyzing 25 three-year rolling windows, each of which contains financial companies which were active during the period. While time series data over long periods exclude companies that are new, short-lived, and bankrupt, our rolling windows include such companies, which most likely have had significant contributions to network connectedness and systemic risk.

We find that the magnitude of the temporal and contemporaneous connectedness, measured respectively by conditional transfer entropy and mutual information, increased over the entire sample period (1990-2016), suggesting that the financial system became more interconnected over time. Banks outnumbered other types of insti-

tutions between 1990 and 2010 and diversified financial companies outnumbered the others from 2010 onward. In the US and North America for all years (1990-2016) and in South America for the majority of years, banks had the highest impact and vulnerability. This is consistent with the findings in [Billio et al., 2012] in which banks appear to transmit shocks significantly more than other types of financial institutions. Diversified financials generally had the highest impact and vulnerability in Europe, the Middle East, South Asia, East Asia, Southeast Asia, and Australia while in Africa and West Asia, banks and diversified financials took turns being the highest impactful and vulnerable industry.

1.5 Publications

The following publications were completed over the course of this thesis.

1. "Relation between regional uncertainty spillovers in the global banking system" (co-authored with Caccioli, F. and Aste, T.), arXiv: 1702.05944, published in the March 2018 issue of the **Journal of Network Theory in Finance**

2. "Variance decomposition of forecast errors as a linkage measure: A banking network application" in the **European Winter Meeting of the Econometric Society 2015** and in **Computing in Economics and Finance 2016** (co-authored with Caccioli, F. and Aste, T.)

3. "Inferring financial network structures using VAR with stochastic volatility" in **IMA Conference on Mathematics in Finance 2015**

4. "Estimating spillover in the global banking network: VAR with exponential smoothing and ridge regression" (co-authored with Caccioli, F. and Aste, T.) in **Computing in Economics and Finance 2015 Conference**

1.6 Thesis outline

This thesis is organized as follows. In **Chapter 2** we provide a literature review on financial contagion and quantification of connectedness and discuss challenges in quantifying connectedness and how we tackle them in this research.

In **Chapter 3** we provide a summary of vector autoregression (VAR) and forecast error variance decomposition (FEVD) which are two of the main tools we use in

quantifying connectedness. In **Chapter 4** we discuss Granger causality and transfer entropy and the findings in Barnett et al. [2009] who showed that the two measures are equivalent for Gaussian variables. **Chapter 5** contains empirical results from using our improved VAR-FEVD framework to measure network connectedness in the North American, the EU, and the ASEAN banking systems. More specifically, we discuss pairwise and system-wide connectedness metrics and test for lead-lag relationships between network connectedness of the three banking systems.

Chapter 6 discusses Gaussian Markov Random Fields (GMRF) and provides an overview of sparsity algorithms for connectedness estimation based on a GMRF including graphical lasso and LoGo-TMFG. **Chapters 7 and 8** contain empirical results obtained from analyzing high dimensional datasets of global financial institutions using the sparsity modeling algorithm LoGo-TMFG. While in **Chapter 7** we view the global network as a system of ten economic regions, in **Chapter 8** we view the global network as a system of four financial industries; however, for both Chapters we compute five network connectedness metrics: number of links, conditional mutual information, conditional transfer entropy, impact, and vulnerability which are computed from conditional transfer entropy and mutual information. Finally, we conclude our research in **Chapter 9**.

Chapter 2

Background: Systemic risk, quantification of connectedness, and challenges

Summary: In this chapter we define and discuss the concepts of systemic risk, contagion, and connectedness. We then provide a literature review on financial contagion and quantification of connectedness. Lastly, we discuss challenges surrounding quantification of connectedness and how we tackle those challenges in this research.

2.1 Systemic risk, contagion, and connectedness

Systemic risk is a risk that an event will lead to a breakdown of the entire financial system rather than simply the failure of individual parts [1]. In the financial context, systemic risk captures the risk of a cascading failure, caused by complex interlinkages within the financial system, resulting in a severe economic downturn.

As systemic risk materializes, contagion takes place [Martinez-Jaramillo et al., 2010]. Contagion is the main mechanism through which financial troubles become so widespread that a crisis reaches a systemic level. Smaga [2014] defines contagion effect as the probability that the instability of a given institution will spread to other parts of the financial system with negative effects, leading to a system-wide crisis.

In this research we will be focusing on how to quantify contagion in order to answer the question of how severe the repercussion is, or what level of systemic risk

[1] This definition is given by the Systemic Risk Centre of the London School of Economics and Political Sciences (LSE).

is induced, when an extreme event occurs. Two factors contributing to the severity of contagion are the magnitude of the initial shock and the structure of interlinkages among the institutions in the network. If we take the size of the initial shock as given, the task of quantifying contagion reduces to determining the structure of interlinkages which involves determining which institutions are connected, how many institutions are connected, and the extent or magnitude of interconnectedness. Because interlinkages provide channels through which contagion is transmitted from one institution to another, their structure determines how many institutions will be affected by the shock and which institutions are hit the hardest. As such, a good interlinkage structure is one that enables the sytem to withstand shocks while a bad interlinkage structure acts as a catalyst to the initial shock. Throughout this research, we will sometimes refer to interlinkages within the financial system as interconnectedness or simply connectedness.

2.2 Literature on financial contagion and quantification of connectedness

Literature on financial contagion can be broadly classified into two categories: (1) **Network models** which aim to describe various causal mechanics of financial contagion, which can be calibrated with balance-sheet data and (2) **Econometric models** which aim at identifying spillover effects exclusively from market data, without making assumptions about the dynamics of distress propagation between banks.

2.2.1 Network models

Network models aim to describe various propagation mechanics of financial contagion and can be calibrated with balance-sheet data. The work of Allen and Gale [2000] pioneered literature in the this category. The authors showed how the stability of banking system is affected at equilibrium by the pattern of interconnections between banks. Another well-known work is by Eisenberg and Noe [2001], who analyzed how financial losses propagate through the interbank network using clearing vectors of payments in a network of interbank claims. In addition, Furfine [2003], Nier et al. [2007], Gai and Kapadia [2010], Cont et al. [2010], Upper [2011], Battiston et al. [2012], and Bardoscia et al. [2015] explored extensively the relation between an interbank network structure and its stability in the context of non-equilibrium network models. Beale

et al. [2011] demonstrated that a tension between individual risk and systemic risk exists—what makes a bank individually less risky might increase the risk of a systemic failure. More recently, the literature has been extended beyond interbank lending networks to the study of networks of overlapping portfolios as discussed in Huang et al. [2013], Caccioli et al. [2014], and Corsi et al. [2016].

Although models in this category have been insightful to understand the dynamics of financial contagion, and in some cases they have been applied to real data (see Upper [2011] for a review of existing literature), there are clear challenges to their applicability. First, there is a lack of reliable data on banks' balance sheets, which makes it hard to calibrate the models[2]. Second, to obtain a reliable assessment of systemic risk one has to capture all relevant types of interconnections between banks because the interaction between different contagion channels can significantly change the stability of the system [Caccioli et al., 2015].

2.2.2 Econometric models

Literature in this category aims to measure connectedness or spillover exclusively from market data, using econometric models, without making assumptions about the distress propagation dynamics between the financial institutions. The advantage of this approach with respect to network modeling is that market data are readily available, and that different types of interconnections between banks have already been aggregated by the market. However, the drawback is that this approach does not provide an explanation of how stress propagates between banks, and that it relies on the underlying assumption of market efficiency, which is not realistic [Shiller, 2003]. Nevertheless, one can assume that, although markets are not efficient, prices do reflect to some extent the aggregate information (or expectations) about the underlying assets. Prominent examples of literature in this category include Adrian and Brunnermeier [2016] who propose ΔCoVaR as a measure of systemic risk and Brownlees and Engle [2016] who introduce SRISK as a measure of systemic risk contribution of a firm. Less recent empirical work includes Diebold and Yilmaz [2009, 2012, 2014], Caceres et al. [2010], Billio et al. [2012], Claeys and Vasicek [2014], Lucas et al. [2014]. Dungey et al.

[2] Admati et al. [2013] report that banks tend to find ways to get around regulations in order to invest in mortgage-backed securities and derivatives via structured-investment vehicles which are off balance sheet items. Such leeway allowed by regulations creates regulatory boundaries, making it difficult for outsiders to know what banks actually report.

[2005] provide a summary of empirical models of contagion up to 2005.

Of particular relevance for the first empirical analysis in Chapter 5 of this PhD thesis is the work of Diebold and Yilmaz [2009, 2012, 2014], who merge network theory to the well-known multivariate econometric tools, namely VAR and FEVDs, and influenced subsequent studies such as McMillan and Speight [2010], Bubák et al. [2011], Fujiwara and Takahashi [2012], Klößner and Wagner [2014], Alter and Beyer [2014], Chau and Deesomsak [2014], Fengler and Gisler [2015], Demirer et al. [2017], and Geraci and Gnabo [2018]. This strand of contributions uses vector autoregression (VAR) and forecast error variance decompositions (FEVDs) to quantify unpredictability of each of the variables in the network. In addition, the VAR-FEVD method allows for disentanglement of the contribution to unpredictability due to endogenous interdependencies from that due to exogeneous shocks.

In this research we take a somewhat complementary approach to inferring interdependencies between financial institutions from market data, which belongs to this category of literature. We will refer to interdependency interchangeably as network connectedness, total connectedness, system-wide connectedness or total spillover.

2.3 Challenges in quantification of connectedness and how this thesis overcomes them

2.3.1 Proprietary data

The greatest difficulty faced by research into financial interconnectedness and stability has been associated with data availability [Geraci and Gnabo, 2018]. Data on bank cross-exposures are inaccessible, proprietary information which is why very few studies including Furfine [2003], Upper and Worms [2004], and Degryse and Nguyen [2004] quantify direct connectedness using interbank lending data. We avoid using proprietary data and instead use listed banks' stock prices which can be accessed through various databases. To infer connectedness from market data, we do not make an assumption that market is efficient but we do believe that stock prices reflect to some extent the aggregate information about the banks including their performances and direct and indirect connections they may have. It is worth emphasizing that using market data allows us to capture both direct and indirect connections between the banks, which

we would not be able to achieve by using interbank data because they reflect only direct connections between the banks.

2.3.2 Survival bias

Literature on survival bias is found mostly in the context of measuring mutual fund performance. As mutual fund databases tend to include only active funds [Rohleder et al., 2010], a good overall performance measured from such data is likely to be a result of failing funds being excluded from the dataset.

In the context of this research, a survival bias is a statistically incorrect conclusion obtained from analyzing only financial institutions that made it past the crises and were active over a specified sample period. We recognize that over the past few decades, some financial institutions ceased to exist due to mergers, acquisitions, or bankruptcy while others came into existence.

The problem with survival bias is that the number of active financial institutions is underestimated while performance in terms of returns is overestimated. We find that a data sample covering the period from 1990 to 2016 include a much smaller number of active financial institutions than a data sample covering the period from 1990 to 1993.

Unlike mutual fund databases, stock databases generally have data for both active and defunct stocks. We attempt to include defunct stocks in our study by performing rolling-window analysis where each window covers a period of 750 days or 3 years of daily data in Chapters 7 and 8[3]. By decreasing the window size, short-lived stocks are more likely to be included in our study and survival bias is reduced.

2.3.3 High dimensionality

High dimensionality refers to a characteristic of data in which the number of unknown parameters p is of much larger order than sample size n. As the financial markets becomes more complex and data are abundant, solving financial problems including portfolio allocation, asset pricing and risk management becomes extremely challenging. To optimize the return or to manage the risk of a portfolio, many approaches require estimating the covariance matrix of the asset returns in the portfolio. If we have 200 financial securities to be selected for asset allocation, the corresponding covariance

[3]We use 750 days to ensure we have enough observations in a window to reveal the true pattern in the data and that the problem is not ill conditioned. Later we discuss in Section 5.2.2 that various rolling-window sizes, e.g., 250, 300, 500, and 750 days do not significantly change the results.

matrix has 20,200 parameters to estimate. As covariance matrices pervade every facet of financial econometrics, from asset allocation, asset pricing, and risk management, to derivative pricing and proprietary trading, it is crucial to obtain an accurate estimation for them.

The curse of dimensionality was first recognized and discussed by Bellman [1961], which indicates that to estimate an arbitrary function with a given level of accuracy the number of observations n needed grows exponentially with respect to the number of input variables p of the function. This is because as the number of input variables increases, the number of parameters usually increases in a very rapid way, often exponentially. More generally, the curse of dimensionality refers to all undesirable characteristics and consequences that come with high-dimensional data in the context of behavior and performances of learning algorithms.

High-dimensional spaces show surprising geometrical properties that are counter-intuitive [Verleysen and François, 2005]. Among these properties, the concentration of norm phenomenon has the most impact on the design of data analysis tools. For example, standard Euclidean norms may become unselective in high-dimensional spaces, and the Gaussian kernels, commonly used in many tools, may become inappropriate too. The curse of dimensionality prevents the use of most conventional modelling techniques and forces us to look for more specific solutions.

In order to deal with consequences of the curse of dimensionality, a range of dimensionality reduction measures have been proposed. Two most common ways to handle the curse of dimensionality are to sparsify the graph which represents the links between the variables, and to reduce the data space dimensionality through appropriate linear or nonlinear data projection methods.

a. Graph sparsification

Graph sparsification refers to the approximation of a graph by a subgraph that is sparse, i.e., has less than a quadratic number of edges. The idea of graph sparsification is to approximate a given graph G by a sparse graph S on the same set of vertices. If S is close to G in some appropriate metric, then S can be used as a proxy for G in computations without incurring too much error. Because S has a small number of edges, computation with and storage of S should be cheaper [Spielman and Srivastava, 2009]. Graph sparsification was introduced by Benczúr and Karger [1996] who used a near linear time

procedure which takes as input an undirected graph G on n vertices and constructs a weighted subgraph S with $O(n \log n/\varepsilon^2)$ edges. A stronger class of graph sparsifiers called spectral sparsifiers was introduced by Spielman and Teng [2011], which led to the development of a number of efficient algorithms for constructing cut and spectral sparsifiers [Batson et al., 2014].

b. Dimensionality reduction

Dimensionality reduction through linear data projection methods are done via tools such as Principal Component Analysis (PCA) and Linear Discriminant Analysis (LDA). PCA, the most traditional tool used for dimension reduction, projects data on a lower-dimensional space, choosing axes to keep the maximum of the data initial variance. LDA finds a linear combination of features that separates two or more classes of objects. The drawback of linear data projection is that nonlinear relationship between the initial variables may be lost in the preprocessing step.

In order to capture the nonlinear relationship, kernel trick is employed to map the data to higher dimensional space, then apply PCA on the transformed data. The method is called Kernel PCA. Another nonlinear projection method is based on the concept of "distance preservation." The idea of the distance preservation methods is to find a lower dimensional representation of data where the pairwise distances are preserved with respect to the original data space. Sammon mapping, Curvilinear Component Analysis (CCA), Curvilinear Distance Analysis (CDA), and Isomap belong in this category.

Dimensionality reduction techniques help identify and remove as much irrelevant and redundant data as possible, which in turns allows learning algorithms to operate more efficiently and effectively.

To mitigate the curse of dimensionality, this research employ tools which belong in the graph sparsification category. In Chapter 5, we use regularization, specifically ridge regression in the context of VAR-FEVD for NA (10 banks), ASEAN (39 banks), and the EU (62 banks) banking networks. We expand our dataset to cover a much larger global financial network in Chapters 7 and 8 which contains 914 financial institutions that were active in 1990-1999 and 1,127 global financial institutions that were active in 2000-2016. We also analyze 25 rolling windows which cover the three-year rolling periods, e.g., 1990-1992, 1991-1993, ..., 2014-2016. The number of active financial

institutions in each window ranges from the smallest, 1,680 companies in 1990-1992, to the largest, 4,396 companies in 2009-2011.

Given the number of companies above, to continue using the VAR-FEVD model on the global financial datasets will lead to over-parameterization, especially when we take into consideration both lag *and* current returns. That is, the number of covariates in our VAR regressions will exceed the number of observations for each firm. As such, sparsity modeling is necessary to analyze the global financial network datasets. We use LoGo-TMFG which is a novel sparsity algorithm based on information filtering network for the empirical analyses in Chapters 7 and 8.

Chapter 3

Background: Econometric models for estimation of connectedness

Summary: This chapter summarizes from current literature, including Sims [1980], Greene [2003], Lutkepohl [2006], and Tsay [2010], the econometric analysis tools that are widely used for estimation of connectedness: the vector autoregressive (VAR) model and forecast error variance decomposition (FEVD). In addition, we provide a recap of the discussion in Diebold and Yilmaz [2014], which demonstrates how FEVD is linked to concepts from network theory.

3.1 Vector Autoregression (VAR)

The VAR models, introduced by Sims [1980], are a natural extension of the univariate autoregressive (AR) model to multivariate time series. In an AR model, there is a single linear equation of a single variable, where the current value of the variable is explained by its own lagged values. In a VAR model there are K linear equations describing K variables. Each variable in a VAR model is endogenous, i.e., it is explained by its own lagged values as well as by lagged values of the other $K-1$ variables in the system. Exogenous shocks are captured by the error terms, which may be contemporaneously correlated with one another but are not serially correlated. Being an endogenous model, VAR may give rise to the issue of incompleteness of the system, i.e., there are other factors than the variables in the system that affect the variables in the system. However, such omitted variables are accounted for by the error terms.

The reduced-form VAR(1) model for K variables describes a relationship between the current observation of each of the K variables and the first lags of all K variables .

It is a system of equations in which the i-th equation describes the linear relationship between the i-th dependent variable $y_{i,t}$ and the explanatory variables which are the first lags of all variables $\{y_{1,t-1},...,y_{K,t-1}\}$.

Following Lutkepohl [2006], the VAR(1) model can be expressed in matrix notation as

$$\boldsymbol{y}_t = \boldsymbol{A}\boldsymbol{y}_{t-1} + \boldsymbol{u}_t. \tag{3.1}$$

where $\boldsymbol{y}_t = (y_{1t},...,y_{Kt})'$ is a $K \times 1$ vector of demeaned K variables, $\boldsymbol{A}$ is a fixed $K \times K$ matrix of VAR coefficients, and $\boldsymbol{u}_t = (u_{1t},...,u_{Kt})'$ is a K-dimensional white noise process. $\mathbb{E}\boldsymbol{u}_t = \boldsymbol{0}, \mathbb{E}(\boldsymbol{u}_t\boldsymbol{u}_t') = \boldsymbol{\Sigma_u}$ is non-singular and may be non-diagonal, i.e., contemporaneous correlation among $\{u_1,...,u_K\}$ is allowed. However, there is no serial correlation $\mathbb{E}(\boldsymbol{u}_t\boldsymbol{u}_s') = \boldsymbol{0}$ for $s \neq t$.

When including p lags of each variables, we obtain a VAR(p) model where each lag $i = 1,2,...p$ has the corresponding $K \times K$ matrix $\boldsymbol{A_i}$ of VAR coefficients:

$$\boldsymbol{y}_t = \boldsymbol{A}_1\boldsymbol{y}_{t-1} + ... + \boldsymbol{A}_p\boldsymbol{y}_{t-p} + \boldsymbol{u}_t \tag{3.2}$$

The VAR(p) process with $p > 1$ can be written in the Kp-dimensional VAR(1) form [Lutkepohl, 2006] as in the Equation (3.3) below, which is simpler to analyze than the form in Equation (3.2).

$$\boldsymbol{Y}_t = \boldsymbol{A}\boldsymbol{Y}_{t-1} + \boldsymbol{U}_t, \tag{3.3}$$

where

$$\boldsymbol{Y}_t := \underbrace{\begin{bmatrix} \boldsymbol{y}_t \\ \boldsymbol{y}_{t-1} \\ \vdots \\ \boldsymbol{y}_{t-p+1} \end{bmatrix}}_{(Kp\times 1)}, \quad \boldsymbol{A} := \underbrace{\begin{bmatrix} \boldsymbol{A}_1 & \boldsymbol{A}_2 & \cdots & \boldsymbol{A}_{p-1} & \boldsymbol{A}_p \\ \boldsymbol{I}_K & \boldsymbol{0}_K & \cdots & \boldsymbol{0}_K & \boldsymbol{0}_K \\ \boldsymbol{0}_K & \boldsymbol{I}_K & \cdots & \boldsymbol{0}_K & \boldsymbol{0}_K \\ \vdots & & \ddots & \vdots & \vdots \\ \boldsymbol{0}_K & \boldsymbol{0}_K & \cdots & \boldsymbol{I}_K & \boldsymbol{0}_K \end{bmatrix}}_{(Kp\times Kp)}, \quad \boldsymbol{U}_t := \underbrace{\begin{bmatrix} \boldsymbol{u}_t \\ \boldsymbol{0}_K \\ \vdots \\ \boldsymbol{0}_K \end{bmatrix}}_{(Kp\times 1)},$$

provided that $\boldsymbol{y}_t = (y_{1t}, ..., y_{Kt})'$ is a $K \times 1$ vector of demeaned K variables, $\mathbf{0}_K$ is a $K \times K$ matrix of zeros, and $\boldsymbol{I}_K$ is a $K \times K$ identity matrix.

3.1.1 Moving average (MA) representation

Under stationarity [1], the $Kp \times 1$ vector $\boldsymbol{Y}_t$ has the following moving average (MA) or Wold representation [Lutkepohl, 2006]:

$$\begin{aligned} \boldsymbol{Y}_t &= \boldsymbol{U}_t + \boldsymbol{A}\boldsymbol{U}_{t-1} + \boldsymbol{A}^2\boldsymbol{U}_{t-2} + ... \\ &= \sum_{i=0}^{\infty} \boldsymbol{A}^i \boldsymbol{U}_{t-i}, \end{aligned} \tag{3.4}$$

where $\boldsymbol{Y}_t$ is expressed in terms of past and present error vector $\boldsymbol{U}_t$. The MA representation of $\boldsymbol{y}_t$ can be obtained by premultiplying Equation 3.4 by the $(K \times Kp)$ matrix $\boldsymbol{J} := [\underbrace{\boldsymbol{I}_K, \mathbf{0}_K, \ldots, \mathbf{0}_K}_{K \times Kp}]$.

$$\boldsymbol{y}_t = \boldsymbol{J}\boldsymbol{Y}_t = \sum_{i=0}^{\infty} \boldsymbol{J}\boldsymbol{A}^i\boldsymbol{J}'\boldsymbol{J}\boldsymbol{U}_{t-i} = \sum_{i=0}^{\infty} \boldsymbol{\Phi}_i \boldsymbol{u}_{t-i}, \tag{3.5}$$

where the $K \times K$ matrices $\boldsymbol{\Phi}_i$, $i = 0, ..., p$ is defined as $\boldsymbol{\Phi}_i := \boldsymbol{J}\boldsymbol{A}^i\boldsymbol{J}'$. Note that $\Phi_0 = \boldsymbol{J}\boldsymbol{A}^0\boldsymbol{J}' = \boldsymbol{I}_K$, $\boldsymbol{U}_t = \boldsymbol{J}'\boldsymbol{J}\boldsymbol{U}_t$ and $\boldsymbol{u}_t = \boldsymbol{J}\boldsymbol{U}_t$.

3.1.2 Forecast error variance decomposition (FEVD)

FEVD is a structural analysis tool associated with VAR, which is used to determine how much of the forecast error variance of one variable is explained by the exogenous shock occurred another variable in the VAR system. In other words, $FEVD_{ij}$ is the portion of the variability of the error in forecasting a variable y_j that is due to the variability in the structural shock to the error term u_i, associated with variable y_i [2]. The summary of FEVD in this section is based on Lutkepohl [2006].

---

[1] $\boldsymbol{Y}_t$ is stationary if $\det(\boldsymbol{I}_{Kp} - \boldsymbol{A}z) \neq 0$ for $|z| \leq 1$. y_t is stationary if $\det(\boldsymbol{I}_K - \boldsymbol{A}_1 z - ... - \boldsymbol{A}_p z^p) \neq \mathbf{0}$ for $|z| \leq 1$

[2] For example, if there are two variables in our system, namely GDP and interest rate, for a given forecast horizon, there will be four FEVDs: (1) the percentage of the variance of the error made in forecasting GDP that is due to a specific shock to the error term in the interest rate equation, (2) the percentage of the variance of the error made in forecasting interest rate that is due to a specific shock to the error term in the GDP equation, (3) the percentage of the variance of the error made in forecasting interest rate that is due to a specific shock to the error term in the interest rate equation, and (4) the percentage of the variance of the error made in forecasting GDP that is due to a specific shock to the error term in the GDP equation.

Recall the MA form of VAR in Equation (3.5), i.e., $\boldsymbol{y}_t = \sum_{i=0}^{\infty} \boldsymbol{\Phi}_i \boldsymbol{u}_{t-i}$. We decompose $\boldsymbol{\Sigma}_u$, which is the covariance matrix of $\boldsymbol{u}$, into a product of the lower triangular $\boldsymbol{P}$ and its transpose $\boldsymbol{P}'$, i.e., $\boldsymbol{\Sigma}_u = \boldsymbol{P}\boldsymbol{P}'$ and substitute $\boldsymbol{\Theta}_i = \boldsymbol{\Phi}_i \boldsymbol{P}$ and $\boldsymbol{w}_{t-i} = \boldsymbol{P}^{-1}\boldsymbol{u}_{t-i}$ into Equation (3.5) and obtain

$$\boldsymbol{y}_t = \sum_{i=0}^{\infty} \boldsymbol{\Phi}_i \boldsymbol{P}\boldsymbol{P}^{-1}\boldsymbol{u}_{t-i} = \sum_{i=0}^{\infty} \boldsymbol{\Theta}_i \boldsymbol{w}_{t-i}. \tag{3.6}$$

Note that while the components u_{it} and u_{jt} in $\boldsymbol{u}_t$ may be correlated, the components w_{it} and w_{jt} in $\boldsymbol{w}_t$ are orthogonal. That is, $\boldsymbol{P}^{-1}$ orthogonalizes $\boldsymbol{u}_t$, resulting in the orthogonalized error term $\boldsymbol{w}_t$ whose covariance matrix $\boldsymbol{\Sigma}_w$ is orthogonal:

$$\boldsymbol{\Sigma}_w = \mathbb{E}(\boldsymbol{P}^{-1}\boldsymbol{u}\boldsymbol{u}'(\boldsymbol{P}^{-1})') = \boldsymbol{P}^{-1}\boldsymbol{\Sigma}_u(\boldsymbol{P}^{-1})' = \boldsymbol{I}_K. \tag{3.7}$$

$\boldsymbol{y}_{t+1}$ and its forecast value $\boldsymbol{y}_t(1)$ given the information at time t are, respectively,

$$\boldsymbol{y}_{t+1} = \boldsymbol{\mu} + \boldsymbol{\Theta}_0 \boldsymbol{w}_{t+1} + \boldsymbol{\Theta}_1 \boldsymbol{w}_t + \boldsymbol{\Theta}_2 \boldsymbol{w}_{t-1} + \ldots, \tag{3.8}$$

$$\boldsymbol{y}_t(1) = \boldsymbol{\mu} + \boldsymbol{\Theta}_1 \boldsymbol{w}_t + \boldsymbol{\Theta}_2 \boldsymbol{w}_{t-1} + \ldots \tag{3.9}$$

The 1-step ahead forecast error for $\boldsymbol{y}$ given the information at time t is the difference between the actual value and forecast value of $\boldsymbol{y}_{t+1}$ given the information at time t

$$\boldsymbol{y}_{t+1} - \boldsymbol{y}_t(1) = \boldsymbol{\Theta}_0 \boldsymbol{w}_{t+1}. \tag{3.10}$$

In matrix form, the 1-step ahead forecast error for $\boldsymbol{y}$ is

$$\begin{bmatrix} y_{1,t+1} - y_{1,t}(1) \\ y_{2,t+1} - y_{2,t}(1) \\ y_{3,t+1} - y_{3,t}(1) \\ \vdots \\ y_{K,t+1} - y_{K,t}(1) \end{bmatrix} = \begin{bmatrix} \theta_{11,0} & \theta_{12,0} & \ldots & \theta_{1K,0} \\ \theta_{21,0} & \theta_{22,0} & \ldots & \theta_{2K,0} \\ \theta_{31,0} & \theta_{32,0} & \ldots & \theta_{3K,0} \\ & \vdots & & \\ \theta_{K1,0} & \theta_{K2,0} & \ldots & \theta_{KK,0} \end{bmatrix} \begin{bmatrix} w_{1,t+1} \\ w_{2,t+1} \\ w_{3,t+1} \\ \vdots \\ w_{K,t+1} \end{bmatrix} \tag{3.11}$$

For each component y_i of $\boldsymbol{y}$, the 1-step ahead forecast error and the variance of the

1-step forecast error are

$$y_{i,t+1} - y_{i,t}(1) = \theta_{i1,0} w_{1,t+1} + \theta_{i2,0} w_{2,t+1} + \ldots + \theta_{iK,0} w_{K,t+1} \tag{3.12}$$

$$var(y_{i,t+1} - y_{i,t}(1)) = \theta_{i1,0}^2 + \theta_{i2,0}^2 + \ldots + \theta_{iK,0}^2 = \sum_{k=1}^{K} \theta_{ik,0}^2 = MSE(y_{i,t}(1)). \tag{3.13}$$

We then decompose the forecast error variance of each variable y_j into contributions from a one-standard deviation shock associated with each of the variables y_i in the system:

$$FEVD_{ij,1} = \frac{\theta_{ji,0}^2}{\sum_{k=1}^{K} \theta_{jk}^2} = \frac{\theta_{ji,0}^2}{MSE(y_{j,t}(1))}. \tag{3.14}$$

For h-step ahead FEVD derivation, please refer to A.2.

3.2 The intersection of network theory and VAR

As discussed in Diebold and Yilmaz [2014] the spillover or connectedness table, Table 3.1, is put together using the h-step ahead FEVDs. The table helps visualize pairwise connectedness for each pair of banks and total connectedness for the entire system.

Diebold and Yilmaz [2014] successfully merged the well-known multivariate econometric analysis tools VAR and FEVDs to concepts from network theory by showing that the spillover table is analogous to a weighted adjacency matrix, a concept from network theory, which measure pairwise directed links. They propose the following connectedness metrics using as inputs the c_{ij}^h elements from Table 3.1.

Table 3.1: Diebold and Yilmaz's h-step ahead spillover table where $c_{ij}^h = FEVD_{ji}^h$ for $h = 1, 2, \ldots$

	x_1	x_2	$\ldots$	x_K	To others
x_1	c_{11}^h	c_{12}^h	$\ldots$	c_{1K}^h	$\sum_{j=1}^{K} c_{1j}^h, j \neq 1$
x_2	c_{21}^h	c_{22}^h	$\ldots$	c_{2K}^h	$\sum_{j=1}^{K} c_{2j}^h, j \neq 2$
$\vdots$	$\vdots$	$\vdots$	$\ddots$	$\vdots$	$\vdots$
x_K	c_{K1}^h	c_{K2}^h	$\ldots$	c_{KK}^h	$\sum_{j=1}^{K} c_{Kj}^h, j \neq K$
From others	$\sum_{i=1}^{K} c_{i1}^h, i \neq 1$	$\sum_{i=1}^{K} c_{i2}^h, i \neq 2$	$\ldots$	$\sum_{i=1}^{K} c_{iK}^h, i \neq K$	$\frac{1}{K} \sum_{i,j=1}^{K} c_{ij}^h, i \neq j$

Pairwise connectedness or pairwise spillover

Pairwise connectedness (c_{ij}^h) represents the magnitude of link or connection from variable i to variable j. In the variance decomposition jargon, c_{ij}^h is the share of forecast error variance of variable j coming from a shock to variable i. It is worth noting that generally $c_{ij}^h \neq c_{ji}^h$, that is, the contribution from variable i to variable j does not generally equal the contribution from variable j to variable i.

Directional connectedness (inward and outward)

Total directional connectedness can be further categorized into two metrics: inward connectedness and outward connectedness which are equivalent to a node's in-degree and out-degree respectively. Inward connectedness to Bank j, denoted $c_{:,j}$, is the sum of bilateral connectedness from all other banks to Bank j,

$$c_{:,j} = \sum_{i=1}^{K} c_{ij} \tag{3.15}$$

Outward connectedness from variable i, denoted $c_{i,:}$, is the sum of bilateral connectedness from variable i to all other variables,

$$c_{i,:} = \sum_{j=1}^{K} c_{ij}. \tag{3.16}$$

One can subtract the inward connectedness from the outward connectedness to obtain net connectedness for each bank. If the bank has positive net connectedness, it is a net impacter. On the other hand, if it has a negative net connectedness, it is a net impactee.

Total connectedness or total spillover

Total connectedness or total spillover ($\frac{1}{K}\sum_{i,j=1}^{K} c_{ij}^h,\ i \neq j$) is a system-wide measure of connectedness. It is equal to the average of the inward connectedness of all variables in the network, or equivalently the average of the outward connectedness of all variables. In other words, total connectedness is the average level of spillover in the network and is equivalent to a node's mean degree. A total connectedness value of 0.4 means that on average, 40 percent of the forecast error variance of the variables in the system comes from interdependency or connectedness of the variables in the system. Higher values of total connectedness correspond with higher contagion within the network and stronger

connection among variables in the network.

3.2.1 Variable ordering in VAR, the resulting FEVDs, and total connectedness

The ordering of the endogenous variables in the VAR system has an impact on the resulting FEVDs. That is, two different orderings of the endogenous variables give rise to different FEVD values. A shock to the first variable in the system affects the forecast errors of all other variables, a shock to the second variable does not affect the forecast error of the first variable but affects the forecast errors of the third to last variables, and so on. If we follow this recursive relationship, it is clear that a shock to the last variable in the system has no effect on the other variables but itself. Hence, each ordering of the endogenous variables results in an upper triangular FEVD matrix with the first element on the main diagonal equals 100. Each endogenous variable has the maximum impact onto the network when it is the first variable in the system. On the contrary, each endogenous variable has the minimum impact onto the network (i.e., the only impact it has is onto itself but not to the other variables) when it is the last variable in the system.

In several occasions, one may be able to order the endogenous variables based on their importance supported by economic theory. Often times, to impose certain variable ordering involves making restrictive assumptions which we try to avoid in carrying out this research. One way to get around the issues associated with variable ordering is to take the average of N FEVD matrices from N random orderings of the variables, where N is sufficiently large [3].

Another way to solve the problem of variable ordering is to use the generalized variance decomposition (GVD) framework of Koop et al. [1996] and Pesaran and Shin [1998] to compute order-invariant FEVDs, as demonstrated in Diebold and Yilmaz [2012, 2014].

Although FEVDs are affected by variable ordering, the aggregate metric such as total connectedness is robust to Cholesky ordering; that is, the difference between total connectedness estimates across orderings is often quite small [Diebold and Yilmaz, 2014].

[3] If N is too small, the range of each FEVD value and metrics derived from it can be significantly underestimated [Klößner and Wagner, 2014].

Chapter 4

Background: Granger causality & transfer entropy

Summary: In this chapter we summarize the well-known Granger causality which is a part of the VAR analysis and the concepts of entropy, mutual information, and transfer entropy which come from information theory. Granger causality and transfer entropy are used for causality tests in Chapter 5 while entropy, mutual information, and transfer entropy are among the analytical tools used in Chapters 7 and 8. Chapters 5, 7 and 8 are original empirical work and are the main contribution of this PhD thesis. This chapter concludes with a discussion on the equivalence of Granger causality and transfer entropy, which are the main findings in Barnett et al. [2009].

4.1 Granger causality

Granger causality is a concept of causation defined by Granger [1969] based on a simple idea that a cause occurs before an effect and if a variable x causes a variable y, x must occur before y and should help improving predictions of y.

As discussed in Lutkepohl [2006], Granger causality requires all relevant information up to and including period t is known in its most demanding definition. Let Ω_t be all such relevant information, $y_t(h|\Omega_t)$ the optimal, minimum MSE h-step ahead predictor of y_{t+h}, based on the information set Ω_t, $\Sigma_y(h|\Omega_t)$ the corresponding h-step ahead forecast MSE for y, and $\Omega_t \setminus \{x_s|s \leq t\}$ the set of all relevant information excluding past and present history of x_t. The process x_t is said to Granger-cause y_t if, for at

least one forecast horizon $h \in \{1,2,...\}$,

$$\Sigma_y(h|\Omega_t) < \Sigma_y(h|\Omega_t \setminus \{x_s|s \leq t\}). \tag{4.1}$$

That is, x_t is Granger-causes y_t if including x_t in predicting y_t yields lower MSE than that obtained when excluding x_t for at least one forecast horizon $h \in \{1,2,...\}$. In other words, if y_{t+h} can be more efficiently predicted when x_t is taken into account, then x_t is Granger causal for y_t. On the contrary, *Granger non-causality* implies that the forecast of y_t obtained from including x_t in the set of predictor variables is the same as the forecast of y_t obtained without including x_t in the set of predictor variables.

In general, not all the relevant information in the universe is available which makes impossible the formulation of the optimal predictor given Ω_t. A less demanding definition of Granger causality is often used in practice [Lutkepohl, 2006]. That is, the information in the past and present of the process, denoted $\{y_s, x_s|s \leq t\}$, is considered as opposed to all the information in the universe, Ω_t. Furthermore, in the context of Granger causality analysis, emphasis is generally given to comparing optimal *linear* predictors as opposed optimal predictors.

The definition of Granger causality does not cover instantaneous correlation or instantaneous causality between x_t and y_t, which are commonly observed in practice. If $u_{1,t}$, the innovation to x_t and $u_{2,t}$ the innovation to y_t are correlated, there is instantaneous causality between x_t and y_t. That is, instantaneous causality refers to the causation that exists between observations of x_t and y_t that occur at the same time. In general, if x is Granger-causal for y but there is no instantaneous causation between x and y, one may conclude that the "real" causality is stronger.

4.1.1 Granger causality, instantaneous linear feedback, and total independence

Suppose we model two stationary stochastic process x_t and y_t using: (1) the univariate AR model and (2) the multivariate VAR model.

Model 1: The univariate autoregressive (AR) model

$$x_t = \sum_{p=1}^{\infty} c_{1,p} x_{t-p} + e_{1t}, \text{var}(e_{1t}) = \gamma_1, \tag{4.2}$$

$$y_t = \sum_{p=1}^{\infty} c_{2,p} y_{t-p} + e_{2t}, \text{var}(e_{2t}) = \gamma_2. \tag{4.3}$$

Model 2: The multivariate vector autoregressive (VAR) model

$$x_t = \sum_{p=1}^{\infty} a_{11,p} x_{t-p} + \sum_{p=1}^{\infty} a_{12,p} y_{t-p} + u_{1t}, \text{var}(u_{1t}) = \sigma_1, \tag{4.4}$$

$$y_t = \sum_{p=1}^{\infty} a_{21,p} x_{t-p} + \sum_{p=1}^{\infty} a_{22,p} y_{t-p} + u_{2t}, \text{var}(u_{2t}) = \sigma_2 \tag{4.5}$$

where the error terms u_{1t} and u_{2t} are not serially correlated but are allowed to be contemporaneously correlated with covariance matrix $\Sigma = \begin{bmatrix} \sigma_1 & \sigma_{12} \\ \sigma_{12} & \sigma_2 \end{bmatrix}$, whose off-diagonal entries are $\sigma_{12} = \text{cov}(u_{1t}, u_{2t})$ [1].

Granger proposed an intuitive conclusion that if σ_1 is less than γ_1 by some statistical measure, then y_t is said to have a causal effect on x_t. However, formulation of a test statistic was not specified in Granger [1969]. Geweke [1982] viewed Granger causality as a measure of linear feedback, and proposed three measures of linear feedback, a measure of linear dependence, and the formulations of the measures as follows.

The linear feedback from y_t to x_t, or the Granger causal effect of y_t on x_t is represented by

$$F_{y \to x} = \ln \frac{\gamma_1}{\sigma_1}. \tag{4.6}$$

If $F_{y \to x} = 0$, y has no causal effect on x and if $F_{y \to x} > 0$ y has causal effect on x [2].

The instantaneous linear feedback between x and y is $F_{x.y} = \ln \frac{\sigma_1 \sigma_2}{|\Sigma|}$, where $|\Sigma|$ is the determinant of the matrix Σ. There is no instantaneous linear feedback between x and y ($F_{x.y} = 0$) if $\sigma_{12} = 0$, implying $|\Sigma| = \sigma_1 \sigma_2$. On the contrary, there exists instantaneous

[1] It is worth emphasizing that γ_1 measures the inaccuracy of the autoregressive forecast of x_t based on its lagged values, while σ_1 measures the inaccuracy of forecasting x_t based on the lagged values of both x_t and y_t. If x_t and y_t are independent, $a_{12,p} = a_{21,p} = 0$, $\sigma_{12} = 0$, $\gamma_1 = \sigma_1$, and $\gamma_2 = \sigma_2$.

[2] Similarly, Granger causal effect of x on y is represented by $F_{x \to y} = \ln \frac{\gamma_2}{\sigma_2}$ and x has Granger causal effect on y iff $F_{x \to y} > 0$.

linear feedback between x and y ($F_{x.y} > 0$), if $\sigma_{12} \neq 0$.

A related concept which is the total (linear) dependence between x and y is given by $F_{x,y} = \ln \frac{\gamma_1 \gamma_2}{|\Sigma|}$. $F_{x,y} = 0$ if x and y are independent and $F_{x,y} > 0$ if x and y are not independent. In sum, $F_{x,y} = F_{y \to x} + F_{x \to y} + F_{x.y}$, that is, the total interdepencence between the two time series x_t and y_t comprises three components: two directional causal effects due to temporal interactions, and the instantaneous linear feedback due to exogenous factors, e.g., a common driving factor.

Often we will have that x_t Granger causes y_t and y_t Granger causes x_t. In this case we have a feedback system, indicating that the variables x and y are related. We can make further statement about the direction of net information transfer between x_t and y_t using the equivalence of Granger causality and transfer entropy which will be discussed in Section 4.3.

4.2 Entropy, mutual information, and transfer entropy

4.2.1 One-dimensional random variable

Shannon [1948] introduces the concept of entropy and defines entropy of a random variable X, denoted $H(X)$, as a measure of uncertainty about X . Given $p(x)$ the probability that $X = x$, $H(X) = -\sum_x p(x) \log p(x)$. The joint entropy for X and Y, $H(X,Y) = -\sum_{x,y} p(x,y) \log p(x,y)$, where $p(x,y)$ is the probability that $X = x$ and $Y = y$, measures the uncertainty associated with the set of variables X and Y.

Based on Shannon [1948], the conditional entropy $H(Y|X)$, is a measure of what X does not say about Y, which, in other words, is "the amount of uncertainty remaining about Y after X is known" is given by

$$H(Y|X) = H(X,Y) - H(X). \tag{4.7}$$

Mutual information, denoted $I(X;Y)$, refers to the concept of mutual dependence between two random variables X and Y [Shannon, 1948]. $I(X;Y)$ quantifies the amount of information obtained about X through Y which is equal to $I(Y;X)$ the amount of information obtained about Y through X. Mutual information is essentially "what X says about Y" or "what Y says about X" or the reduction in uncertainty that knowing either variable provides about the other. Based on Wyner [1978], the value of mutual

information is derived from the entropies involving the two random variables:

$$I(X;Y) = H(X) - H(X|Y) = H(Y) - H(Y|X) \tag{4.8}$$

$$= H(X) + H(Y) - H(X,Y) = H(X,Y) - H(X|Y) - H(Y|X) \tag{4.9}$$

The Venn diagram below illustrates the relationship among $H(X)$, $H(Y)$, $H(X,Y)$, $H(X|Y)$, $H(Y|X)$, and $I(X;Y)$. Note that $H(X,Y)$ is analogous to the union of two sets, $I(X;Y)$ is analogous to the intersection of two sets, $H(X|Y)$ is analogous to $X - Y$ and $H(Y|X)$ is analogous to $Y - X$. In addition, $H(X) \geq H(X|Y)$ and $H(Y) \geq H(Y|X)$.

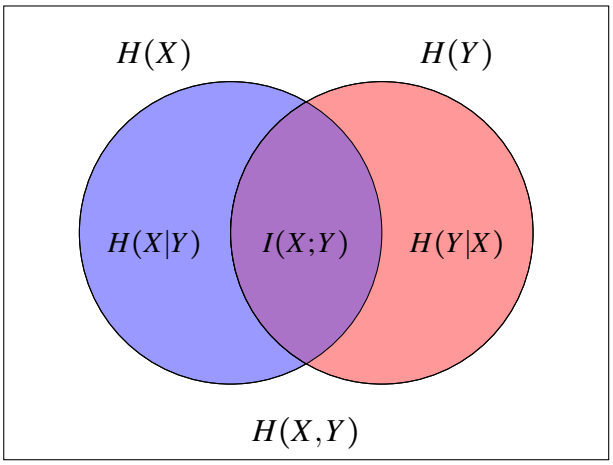

The transfer entropy from X to Y, denoted $TE(X \to Y)$, measures the uncertainty on Y accounted for by the past of X, given the past of Y [Schreiber, 2000]. In other words, transfer entropy $TE(X \to Y)$ quantifies the reduction of uncertainty on the variable Y that is provided by the knowledge of the past of the variable X taking in consideration the information from the past of Y. Based on Schreiber [2000], $TE(X \to Y)$ is equal to the mutual information between Y and the past of X, conditioned on the past of Y. As such, one could view transfer entropy as conditional mutual information.

$$TE(X \to Y) = I(Y;X^{-}|Y^{-}) \tag{4.10}$$

$$= H(Y|Y^{-}) - H(Y|Y^{-},X^{-}) \tag{4.11}$$

$$= H(Y,Y^{-}) + H(Y^{-},X^{-}) - H(Y,Y^{-},X^{-}) - H(Y^{-}), \tag{4.12}$$

where $X^{-} = \{X_{t-1},...,X_{t-K}\}$ and $Y^{-} = \{Y_{t-1},...,Y_{t-L}\}$ are the past of X and Y, K the number of lags for X and L the number of lags for Y.

4.2.2 Multidimensional random variable

The review in this section is summarized from Barnett et al. [2009]. For n-dimensional multivariate normal variables X, transfer entropy is given by

$$H(X) = \frac{1}{2}\log((2\pi e)^n|\Sigma_X|), \tag{4.13}$$

where $|\bullet|$ denotes determinant of a matrix and Σ_X is the covariance of X. Likewise, for m-dimensional multivariate normal variables Y, transfer entropy is given by $H(Y) = \frac{1}{2}\log((2\pi e)^m|\Sigma_Y|)$. The joint set of variables $X, Y \in \mathbb{R}^{n+m}$ has the joint entropy $H(X,Y)$, and the conditional entropy $H(Y|X)$:

$$H(X,Y) = \frac{1}{2}\log((2\pi e)^{n+m}|\Sigma_{X,Y}|), \tag{4.14}$$

$$H(Y|X) = \frac{1}{2}\log((2\pi e)^m|\Sigma_{Y|X}|), \tag{4.15}$$

where $\Sigma_{X,Y}$ is the joint covariance matrix and $\Sigma_{Y|X}$ is the conditional covariance of Y given X, which is equal to the covariance of the residual from regressing Y on X.

The mutual information $I(X;Y)$ and transfer entropy $TE(X \to Y)$ are given by

$$I(X;Y) = \frac{1}{2}(\log|\Sigma_Y| - \log|\Sigma_{Y|X}|), \tag{4.16}$$

$$TE(X \to Y) = \frac{1}{2}(\log|\Sigma_{Y|Y^-}| - \log|\Sigma_{Y|Y^-,X^-}|). \tag{4.17}$$

4.3 Equivalence of Granger causality and transfer entropy

Barnett et al. [2009] discuss the equivalence of Granger causality and the more recent concept of transfer entropy under Gaussian assumptions. While Granger causality is a statistical notion of causal influence based on VAR prediction, transfer entropy is a tool from information theory used to measure information transfer between jointly dependent processes. The concept of transfer entropy from Y to X was formulated by Schreiber [2000] as the degree to which Y disambiguates the future of X beyond the degree to which X already disambiguates its own future.

Given X, Y, and the conditioning variable Z, the transfer entropy of Y to X given

Z is non-negative and is defined as

$$TE(Y \to X|Z) \coloneqq H(X|X^-,Z^-) - H(X|X^-,Y^-,Z^-), \tag{4.18}$$

where $H(\cdot)$ denotes entropy and X^-,Y^-,Z^- denote the past values of X,Y,Z. For jointly multivariate Gaussian variables X,Y,Z the transfer entropy of Y to X is

$$TE(Y \to X|Z) \coloneqq \frac{1}{2}\ln\left(\frac{|\Sigma_{X|X^-,Z^-}|}{|\Sigma_{X|X^-,Y^-,Z^-}|}\right) \tag{4.19}$$

The concept of Granger causality for multivariate variables X and Y as proposed by Geweke [1982] is as follow. Given the regression models for X and Y:

$$X_t = \alpha_t + (X_{t-1} + \ldots + X_{t-p} + Z_{t-1} + \ldots + Z_{t-r})A + u_t \tag{4.20}$$

$$X_t = \tilde{\alpha}_t + (X_{t-1} + \ldots + X_{t-p} + Y_{t-1} + \ldots + Y_{t-q} + Z_{t-1} + \ldots + Z_{t-r})\tilde{A} + \tilde{u}_t, \tag{4.21}$$

$$F_{Y\to X|Z} = \ln\left(\frac{|\Sigma_u|}{|\Sigma_{\tilde{u}}|}\right) = \ln\left(\frac{|\Sigma_{X|X^-,Z^-}|}{|\Sigma_{X|X^-,Y^-,Z^-}|}\right). \tag{4.22}$$

Comparing $TE(Y \to X|Z)$ in Equation (4.19) and $F_{Y\to X|Z}$ in Equation (4.22), we find that Granger causality and transfer entropy are equivalent up to a factor of 2 for jointly Gaussian processes X,Y,Z:

$$F_{Y\to X|Z} = 2TE(Y \to X|Z). \tag{4.23}$$

In information theory, one can compare $TE(Y \to X|Z)$ with $TE(X \to Y|Z)$ to understand which is the prevalent verse of information transfer. If $TE(Y \to X|Z) > TE(X \to Y|Z)$, the direction of the information transfer goes from Y to X. On the contrary, if $TE(X \to Y|Z) > TE(Y \to X|Z)$, the direction of the information transfer goes from X to Y. As previously shown that transfer entropy and Granger causality are positively related, one can also compare $F_{Y\to X|Z}$ with $F_{X\to Y|Z}$ to infer information transfer direction. If $F_{Y\to X|Z} > F_{X\to Y|Z}$, the direction of the information transfer goes from Y to X and if $F_{X\to Y|Z} > F_{Y\to X|Z}$, the direction of the information transfer goes from X to Y [Barnett et al., 2009].

Chapter 5

Empirical analysis: Connectedness estimation using VAR-FEVD

Summary: In this chapter we quantify connectedness in the North American (NA) banking system, the European Union (EU) banking system, and the Southeast Asian (ASEAN) banking system, by analyzing banks' stock returns from 2005 to 2015 using our improved VAR-FEVD methodology. Our analysis covers two levels of granularity: pairwise connectedness and total, system-wide connectedness. For pairwise analysis, we focus on discussing the properties of pairwise connectedness which are the ij-elements in the spillover table, Table 3.1. For system-wide analysis, we compute total connectedness for each banking system as an endogenous system in which the stock return of each bank is a function of its own lag and the lags of all other banks in the system. Then we perform Granger causality and transfer entropy tests on the three total connectedness measures in order to investigate lead-lag relationships between the three systems. A portion of this chapter has been published in the Journal of Network Theory in Finance as Tungsong et al. [2018].

5.1 Related literature

Diebold and Yilmaz [2009, 2012, 2014, 2015a] and Yilmaz [2010] were the first to use the VAR-FEVD framework to measure network spillover, directional spillover, and pairwise spillover. The Diebold-Yilmaz Spillover Index was introduced in Diebold and Yilmaz [2009] via the study of volatility spillovers within a network of 19 global equity markets between 1992 and 2007. While Yilmaz [2010] focused on return and volatility spillovers in 10 East Asian countries between 1993 and 2008, Diebold and Yil-

maz [2012] investigated volatility spillovers between four asset classes including stock, bond, commodity, and FX using U.S. market data between 1999 and 2010. Diebold and Yilmaz [2014] studied connectedness within the network of 13 major U.S. financial institutions and showed that their connectedness measures computed using VAR-FEVD are analogous to a network's adjacency matrix, in which each element represents the link between a pair of nodes. Diebold-Yilmaz total connectedness, which is the sum of all FEVDs divided by the number of nodes, is equivalent to a node's mean degree in the context of a weighted and directed network. Diebold and Yilmaz [2015b] analyzed the Trans-Atlantic network of major U.S. and European banks using Generalized VAR which allows the shocks to be correlated and appropriately accounted for. Demirer et al. [2017] studied the network of global banks which prompts the application of LASSO-VAR to address the high dimensional nature of the problem. According to Demirer et al. [2017], there is little empirical research on global bank connectedness due to the curse of dimensionality associated with analyzing large networks.

The VAR-FEVD framework has been used, improved, and modified by other authors in their research including the following. McMillan and Speight [2010] measured return and volatility spillovers between three major FX pairs including EURUSD, EURGBP, and EURJPY while Fujiwara and Takahashi [2012] analyzed stock indices of 12 global economies using the methodology in Diebold and Yilmaz [2009]. Bubák et al. [2011] used vector heterogeneous autoregressive model (VHAR) with multivariate GARCH errors to measure the dynamics of volatility spillover between Central European currencies and the EURUSD. Klößner and Wagner [2014] improved the methodology in Diebold and Yilmaz [2009] by proposing a new divide-and-conquer strategy to significantly reduce computing time while obtaining the full range of results from all orderings of variables. Chau and Deesomsak [2014] modified the methodology in Diebold and Yilmaz [2012] and constructed the Financial Stress Spillover Index (FSSI) to measure spillovers across the U.S. equity, debt, banking, and foreign exchange markets. Alter and Beyer [2014] used a VAR with exogenous variables (VARX) model on CDS spreads to assess the systemic effect of an unexpected shock to the creditworthiness of a sovereign or bank index. Awartani and Maghyereh [2013] investigated the dynamic spillover of return and volatility between oil and equities in the Gulf Cooperation Council Countries between 2004 and 2012. Zhou et al. [2012] used generalized

VAR-FEVD framework to measure directional volatility spillovers between the Chinese and world equity markets. Antonakakis [2012] used dynamic correlations and VAR-FEVD to analyze return co-movements and volatility spillovers between major exchange rates before and after the introduction of the euro.

5.2 Methodology

5.2.1 The VAR(1) and FEVD

In this research we model stock returns as jointly normally distributed following a stationary multivariate autoregressive process as described by VAR. In particular, we view the financial network as an endogenous system in which the stock return of each financial institution is a linear function of its lags and the lags of the returns of other financial institutions in the system. The financial network may be perturbed by an exogenous shock originally occurred to one financial institution, whose effect is spilled over to the other institutions through various channels of contagion. Connectedness is an aggregate measure of how strongly linked the financial network is. The larger and more numerous the channels of contagion, the more connected is the network, and the more affected the network is by an exogenous shock.

To measure connectedness in a financial network, we would like to forecast future returns of each financial institution and analyze the forecast errors i.e. the unpredictability of the model, which represent uncertainty faced by the financial system. Following Diebold and Yilmaz [2009, 2012, 2014], we decompose the forecast error associated with a financial institution into effects from each of the other financial institutions in the system. The aforementioned decomposed effects are pairwise, representing connectedness between any two financial institutions. By aggregating pairwise connectedness we obtain system-wide or total connectedness which is a measure of how the financial system as a whole is affected when an external shock occurred to a financial institution.

We find that the VAR of order 1 i.e. VAR(1) best fits our dataset based on the BIC and HQ information criteria. In classical VAR estimation, the coefficients A in Equation 3.1 is estimated using ordinary least squares (OLS) method, where the following

sum of squares is minimized with respect to $\boldsymbol{A}$:

$$(y_t - \boldsymbol{A}y_{t-1})'(y_t - \boldsymbol{A}y_{t-1}). \tag{5.1}$$

OLS is performed, one by one, on each equation from y_{1t} to y_{Kt} which belong to a system of simultaneous equations y_t. We then decompose the forecast variances obtained from the VAR estimation and uncover the network structure of each of the three banking systems as per Section 3.1.2.

Although the classical VAR is appropriate for systems with small numbers of variables, it can be overparameterized as the number of endogenous variables increases. As a consequence, the classical VAR usually generates imprecise forecasts in high dimensional systems, which are commonly observed in practice.

We propose improvements upon the classical VAR estimation, which was used in the pioneering work of Diebold and Yilmaz [2009, 2012, 2014], in Sections 5.2.2 and 5.2.3 below. First, we propose giving the data points exponential decay weights, where smaller weights are assigned to more remote observations, to mitigate the effects associated with outliers in a rolling-window estimation. Second, we handle increased dimensionality using ridge regression, which is a regularization method.

5.2.2 Technical Improvement 1: Exponential smoothing

Equal weighting of time series data is counterintuitive because it implies that events (prices or returns) occurring further in the past are as informative as those occurring more recently. On the contrary, more recent events are more informative than those further in the past in both descriptive and forecasting contexts. If each data point receives equal weighting, the impact of a distant outlier remains significant as long as it is included in the rolling window.

Pozzi et al. [2012] showed that exponential weighting is useful in characterizing dynamic dependency structure of a financial time series and discussed the importance of optimal tuning of weights, especially a tradeoff between alleviating the lasting effect of outliers and maximizing significance and robustness [1]. The optimal rolling-window

[1] The authors studied dynamic correlations of time series and pointed out that inappropriate weights given to the time series can destabilize the system of correlations, i.e., raise the condition number of the matrix, change the structure of the matrices' eigenvalues, and distort the distribution of coefficients.

size Δt and weight structure are jointly determined and the weights are defined as

$$w_t = w_0 \exp\left(\frac{t-\Delta t}{\theta}\right), \forall t \in 1,2,...,\Delta t, \tag{5.2}$$

where $\theta > 0$ is the weights' characteristic time which can vary for flexibility. For their study of 300 NYSE stocks, Pozzi et al. [2012] found the optimal relationship between θ and Δt to be

$$\theta = \frac{\Delta t}{3}. \tag{5.3}$$

In this research, we compute log returns for the stocks and multiply them by 100 for ease of reading, then we assign exponential weights to the log returns, using $\Delta t = 300, \theta = \frac{\Delta t}{3} = \frac{300}{3} = 100$. We have conducted our study with rolling windows of various sizes e.g. 250, 300, 500, and 750 days and found that different window sizes do not significantly change the results.

5.2.3 Technical Improvement 2: Ridge regression

In estimating the VAR model, we use ridge regression to regularize the coefficients $\boldsymbol{A}$ of the VAR, i.e., to shrink the elements of $\boldsymbol{A}$ towards zero. As our data are high dimensional, ridge regression helps prevent overfitting and mitigate the unreliability of VAR coefficients and forecasts due to the coefficients $\boldsymbol{A}$'s high variances. The ridge regression estimation problem is to minimize the following penalized sum of squares:

$$(y_t - \boldsymbol{A}y_{t-1})'(y_t - \boldsymbol{A}y_{t-1}) + \lambda \boldsymbol{A}'\boldsymbol{A}, \tag{5.4}$$

where λ is the tuning parameter or regularization parameter. In this research we perform ridge regression estimation on the scaled returns with tuning parameters $\lambda = 0.001, 0.01, 1, 100, 200, 500,$ and 1000 on each equation y_{it} in the VAR. We find that $\lambda < 100$ does not provide enough regularization and $\lambda = 100, 200, 500,$ and 1000 lead to similar results; in this thesis we discuss the results from $\lambda = 100$.

5.3 Data

We collect daily stock prices from January 2005 to October 2015 of banks headquartered in North America (NA), the European Union (EU), and Southeast Asia (ASEAN) from Compustat database. We include only the financial institutions in the sub-industry

"Banks" i.e. those having GICS [2] sub-industry code 40101010 and compute daily log returns for each bank. Our sample includes 10 publicly listed banks in NA (Canada and US), 66 banks in the EU and 39 banks in ASEAN. All banks in the NA banking system list their stocks in the New York Stock Exchange (NYSE), some of the bigger EU and ASEAN bank stocks also trade in the NYSE, but most of the EU and ASEAN banks stocks trade in their own national stock markets. Tables 5.1, 5.3, and 5.4 list the banks in the three regions and provide summary statistics.

Unlike Diebold and Yilmaz [2009] who view all financial institutions as belonging to one global system, we group the banks into three regional banking systems and test for causality among their spillover structures. There are economic reasons that support analyzing the banks based on their geographical regions as follows.

1. The three banking systems are geographically distant, which is likely to impede inter-regional business relationships as banks tend to have two-way lines with banks nearer to them than further away.

2. The banks' equities in the three banking systems trade in different stock markets which have significantly different trading hours. For example, as the ASEAN markets close, The EU markets open while the NYSE has not begun trading for the day. Putting all the banks together in one system would introduce time-zone related bias in our causality analysis.

3. Different stock markets are at different stages of development which influence the markets' trading environments, trading restrictions, types of market participants, and how prices reflect information.

4. Within each region banking regulations are fine-tuned in order to facilitate cross-border business transactions as well as increase competition. For example, it has been documented that the financial markets of Canada and the US had already been highly integrated prior to NAFTA, from which point they have become even more integrated [White, 1994]. In addition, the Canadian and American bank stocks in our sample trade in the same capital market (NYSE). As for the EU and ASEAN, bank stocks trade mostly in their own national stock markets, but

[2] The Global Industry Classification Standard (GICS) is a standardized classification system for equities developed jointly by Morgan Stanley Capital International (MSCI) and Standard and Poor's.

Table 5.1: List of actively traded banks that are headquartered in North America (Canada and the U.S.) between 2005-2015.

	Bank name	Country	Mean return (%, daily)	Volatility (%, daily)
1.	Canadian Imperial Bank (CIBC)	CAN	0.01	1.82
2.	Bank of Montreal (BMO)	CAN	0.01	1.69
3.	Royal Bank of Canada (RBC)	CAN	0.03	1.73
4.	Toronto Dominion Bank (TD)	CAN	0.03	1.65
5.	Bank of Nova Scotia (BNS)	CAN	0.01	1.72
6.	Citigroup (CITI)	USA	-0.08	3.70
7.	Bank of America Corp (BAC)	USA	-0.04	3.51
8.	Wells Fargo & Co (WFC)	USA	0.02	2.86
9.	JP Morgan Chase & Co (JPM)	USA	0.02	2.64
10.	US Bancorp (USB)	USA	0.01	2.32

the cross-country differences and trading restrictions are relatively low due to the economic community agreements (EU and ASEAN) that are in place.

Based on the above four reasons, it is intuitive to view one region as an endogenous system, analyze the structure of the unexplained or shock component of the system, and then analyze how the shock component of each system relates to that of another.

Table 5.1 lists all 10 banks headquartered in North America that were actively traded between 2005-2015 and summarizes their mean daily returns and daily volatilities. While both Canadian and American banks have similar average daily returns, the returns of the Canadian banks are less volatile than those of the American banks. Table 5.2 lists all 39 banks headquartered in Southeast Asia that were actively traded between 2005-2015 and summarizes their mean daily returns and daily volatilities. The Malaysian and Singaporean banks on average have lower volatilities than those based in other countries. Similarly Tables 5.3 and 5.4 list all 66 banks headquartered in the European Union that were actively traded between 2005-2015 and summarize their mean daily returns and daily volatilities. The Greek banks on average have higher volatilities than those based in the other countries.

Table 5.2: List of Southeast Asian headquartered banks that were actively traded in 2005-2015.

	Bank	Country	Market cap ($ billion)	Mean return (%, daily)	Volatility (%, daily)
1	Bank Rakyat Indonesia	IDN	20.43	0.07	2.56
2	Bank Permata	IDN	0.54	0.02	1.93
3	Bank Danamon	IDN	2.23	0.00	2.73
4	Bank Maybank Indonesia	IDN	0.79	0.00	2.67
5	Bank Cimb Niaga	IDN	1.07	0.02	2.51
6	Panin Bank	IDN	0.17	0.03	2.68
7	Bank Negara Indonesia	IDN	6.66	0.04	2.50
8	Bank Central Asia	IDN	23.21	0.08	2.06
9	Bank Mandiri	IDN	15.75	0.05	2.54
10	Public Bank	MYS	16.15	0.04	0.90
11	Malayan Banking	MYS	18.70	0.00	1.23
12	RHB Capital	MYS	3.73	0.03	1.58
13	AMMB Holdings	MYS	3.04	0.01	1.51
14	AFFIN Holdings	MYS	0.97	0.01	1.65
15	Alliance Financial Group	MYS	1.15	0.01	1.52
16	BIMB Holdings	MYS	1.35	0.03	2.13
17	CIMB Group Holdings	MYS	7.92	0.02	1.54
18	Hong Leong Bank	MYS	6.17	0.03	1.14
19	Philippine National Bank	PHL	1.20	0.03	2.39
20	Bank of Philippine Islands	PHL	6.97	0.03	1.79
21	China Banking Corp	PHL	1.36	0.04	1.39
22	Metropolitan Bank and Trust	PHL	4.67	0.05	2.12
23	Security Bank Corp	PHL	1.86	0.07	1.87
24	Rizal Commercial Bank Corp	PHL	0.94	0.03	2.19
25	Union Bank	PHL	1.22	0.05	1.77
26	BDO Unibank	PHL	7.33	0.05	2.04
27	United Overseas Bank	SGP	19.62	0.01	1.49
28	DBS Group Holdings	SGP	25.23	0.01	1.49
29	Oversea-Chinese Banking	SGP	22.71	0.02	1.33
30	Krung Thai Bank	THA	6.79	0.02	2.11
31	Siam Commercial Bank	THA	11.44	0.03	2.02
32	Bangkok Bank	THA	8.04	0.02	1.81
33	Bank of Ayudhya	THA	6.15	0.03	2.41
34	Kasikornbank	THA	10.94	0.04	1.97
35	TMB Bank	THA	3.12	-0.01	2.40
36	Kiatnakin Bank	THA	0.91	0.00	1.94
37	Tisco Financial Group	THA	0.96	0.02	2.11
38	Thanachart Capital	THA	14.3	0.03	2.13
39	CIMB Thai Bank	THA	0.76	-0.01	2.75

Table 5.3: List of EU headquartered banks that were actively traded in 2005-2015 (1).

	Bank name	Country	Mean return (%, daily)	Volatility (%, daily)
1	Oberbank Ag	AUT	0.02	0.38
2	Erste Group Bk Ag	AUT	-0.01	2.95
3	KBC Group Nv	BEL	0.00	3.50
4	Dexia Sa	BEL	-0.21	7.76
5	Hellenic Bank	CYP	-0.08	3.08
6	Komercni Banka As	CZE	0.01	2.10
7	IKB Deutsche Industriebank	DEU	-0.13	3.90
8	Commerzbank	DEU	-0.08	3.09
9	DVB Bank Ag	DEU	0.03	1.38
10	HSBC Trinkaus & Burkhardt	DEU	0.00	1.73
11	Comdirect Bank Ag	DEU	0.02	1.83
12	Deutsche Postbank Ag	DEU	0.00	2.15
13	Danske Bank As	DNK	0.01	2.11
14	Jyske Bank	DNK	0.02	1.94
15	Nordea Invest Fjernosten	DNK	0.01	1.43
16	Sydbank As	DNK	0.03	1.93
17	Banco Santander Sa	ESP	0.00	2.16
18	BBVA	ESP	-0.01	2.12
19	Banco Popular Espanol	ESP	-0.07	2.30
20	Bankinter	ESP	0.01	2.28
21	Banco De Sabadell Sa	ESP	-0.02	1.89
22	BNP Paribas	FRA	0.00	2.56
23	Natixis	FRA	-0.01	3.12
24	Societe Generale Group	FRA	-0.02	2.86
25	Credit Agricole Sa	FRA	-0.02	2.78
26	CIC (Credit Industriel Comm)	FRA	0.00	1.41
27	Barclays Plc	GBR	-0.03	3.23
28	HSBC Hldgs Plc	GBR	-0.02	1.72
29	Royal Bank of Scotland Group	GBR	-0.10	3.91
30	Standard Chartered Plc	GBR	0.00	2.44
31	Lloyds Banking Group Plc	GBR	-0.05	3.37
32	Piraeus Bank Sa	GRC	-0.22	5.04
33	Attica Bank Sa	GRC	-0.23	5.88
34	Eurobank Ergasias Sa	GRC	-0.31	5.52
35	National Bank of Greece	GRC	-0.20	4.81
36	Alpha Bank Sa	GRC	-0.15	4.69
37	Zagrebacka Banka	HRV	0.00	2.58
38	Privredna Banka Zagreb Dd	HRV	0.01	2.37
39	OTP Bank Plc	HUN	0.00	2.63

Table 5.4: List of EU headquartered banks that were actively traded in 2005-2015 (2).

	Bank name	Country	Mean return (%, daily)	Volatility (%, daily)
40	Unicredit Spa	ITA	-0.05	2.90
41	Credito Emiliano Spa	ITA	0.00	2.26
42	Intesa Sanpaolo Spa	ITA	0.00	2.61
43	Banca Popolare Di Sondrio	ITA	-0.01	1.83
44	Banca Carige Spa Gen & Imper	ITA	-0.10	2.39
45	Banco Desio Della Brianza	ITA	-0.02	1.76
46	Banco Popolare	ITA	-0.06	2.86
47	Banca Popolare Di Milano	ITA	-0.03	2.78
48	Banca Monte Dei Paschi Siena	ITA	-0.12	2.96
49	Bank of Siauliai Ab	LTU	-0.06	2.97
50	ING Groep Nv	NLD	-0.01	3.14
51	Van Lanschot Nv	NLD	-0.03	1.62
52	Mbank Sa	POL	0.05	2.34
53	Bank Handlowy W Warzawie Sa	POL	0.01	2.05
54	ING Bank Slaski Sa	POL	0.04	1.90
55	Bank BPH S.A.	POL	-0.09	4.48
56	Bank Millennium Sa	POL	0.03	2.62
57	Bank Plsk Kasa Opk Grp Pekao	POL	0.00	2.26
58	Bank Zachodni Wbk Sa	POL	0.04	2.15
59	Getin Holding Sa	POL	-0.02	3.16
60	Powszechna Kasa Oszczednosci	POL	0.00	2.02
61	Banco BPI Sa	PRT	-0.03	2.46
62	Banco Comercial Portugues Sa	PRT	-0.09	2.76
63	Svenska Handelsbanken	SWE	0.02	1.86
64	Skandinaviska Enskilda Bank	SWE	0.01	2.55
65	Nordea Bank Ab	SWE	0.02	2.05
66	Swedbank Ab	SWE	0.01	2.53

5.4 Empirical result: Pairwise analysis

In this section we will present, interpret, and discuss pairwise connectedness for the NA banking system between 2005 and 2016 which was estimated using the improved VAR-FEVD framework discussed in Section 5.2. The purpose of this section is to provide a background to help understand pairwise connectedness as we believe it is an important stepping stone for understanding the system-wide, total connectedness and appreciating how meaningful the metric is for measuring total connectivity.

5.4.1 Properties of FEVDs

The (i, j) element of an FEVD matrix represents pairwise connectedness from variable i to variable j. In econometric jargon, the (i, j) element is the proportion of forecast error variance of variable j that is due to a shock to variable i. As the proportion of forecast error variance of variable i that is due to a shock to variable j needs not to equal the proportion of forecast error variance of variable j that is due to a shock to variable i, FEVD matrices are not symmetric.

For each variable j, the sum of impacts on variable j's forecast error variance that come from shocks to all other variables including variable j equals 100. In other words, each column in the FEVD matrix sums to 100. Each row i in the FEVD matrix does not sum to 100 as it represents the impacts a shock to variable i has on all other variables' forecast error variances.

The ordering of the endogenous variables in the VAR system has an impact on the resulting FEVD matrix as discussed in Section 3.2.1 A shock to the first variable in the system affects the forecast errors of all other variables, a shock to the second variable does not affect the forecast error of the first variable but affects the forecast errors of the third to last variables, and so on. A shock to the last variable in the system has no effect on the other variables but itself. As a consequence, each ordering of endogenous variables results in an upper triangular FEVD matrix with the first element on the main diagonal equals 100. Each variable's impact onto the network is maximized when it is placed first and minimized when it is placed last.

To discuss the properties of FEVDs, we focus on empirical FEVD matrices for the NA banking system between 2005 and 2016. The NA FEVDs characterize pairwise links between 10 banks headquartered in Canada and the United States, whose equities

Table 5.5: NA banking network: 10-step ahead FEVDs from one random ordering of the 10 banks. This is the first window's forecast (for March 17, 2006) based on the first 300 days of train data (January 4, 2005-March 3, 2006). Estimation is done using ridge regularized VAR with exponential smoothing.

	RBC	CITI	BNS	BAC	TD	WFC	JPM	CIBC	USB	BMO
RBC	100.00	0.22	9.64	0.97	40.65	0.26	0.05	23.70	0.25	14.37
CITI	0.00	99.78	0.47	54.54	0.04	50.02	39.69	0.05	40.24	3.82
BNS	0.00	0.00	89.89	0.32	17.00	0.14	1.27	6.10	0.38	13.80
BAC	0.00	0.00	0.00	44.17	0.34	12.13	4.12	0.17	11.22	0.44
TD	0.00	0.00	0.00	0.00	41.98	0.04	0.12	0.35	0.92	6.07
WFC	0.00	0.00	0.00	0.00	0.00	37.40	3.41	0.07	5.14	0.02
JPM	0.00	0.00	0.00	0.00	0.00	0.00	51.33	2.57	2.06	0.86
CIBC	0.00	0.00	0.00	0.00	0.00	0.00	0.00	67.00	0.31	1.57
USB	0.00	0.00	0.00	0.00	0.00	0.00	0.00	0.00	39.50	3.49
BMO	0.00	0.00	0.00	0.00	0.00	0.00	0.00	0.00	0.00	55.57

are listed in stock exchanges in the U.S during the period between 2005 and 2016. Table 5.5 is the 10-day-ahead FEVD matrices from one random ordering of the 10 banks, in which Royal Bank of Canada (RBC) is placed first and the shock to RBC has impact on forecast error variances of all other banks in the network while Bank of Montreal (BMO) is placed last which results in it having no impact on forecast error variances of any other banks.

To avoid making an assumption about the ordering of the variables, we take the average of 200 FEVD matrices from 200 random orderings of variables. The resulting average FEVD matrix is still asymmetric but no longer triangular, with each element (i, j) representing the average of impacts that shocks to the i-th variable have on the forecast error variance of the j-th variable. Table 5.6 illustrates the average FEVD matrix computed from 200 random-ordered 10-day-ahead FEVD matrices for the NA banking network.

We are aware that Diebold and Yilmaz [2014] discussed the appeal of generalized variance decompositions (GVDs) in that they are independent of ordering. However, our own analysis, as well as that in Diebold and Yilmaz [2014], shows that the range of system-wide total connectedness, the average of the sum of pairwise connectedness, is very small across Cholesky orderings. We believe that the average of 200 Cholesky orderings yields robust results, similar to those from GVDs.

Table 5.6: NA banking network: 10-step ahead forecast error variance decompositions (FEVDs), averaged of 200 tables corresponding to 200 random orderings of the 10 banks. This is the first window's forecast (for March 17, 2006) obtained from analyzing the first 300 days of returns data (January 4, 2005-March 3, 2006) using ridge regularized VAR with exponential smoothing.

	RBC	CITI	BNS	BAC	TD	WFC	JPM	CIBC	USB	BMO
CIBC	78.64	4.48	8.34	5.51	4.37	0.08	0.08	0.11	1.19	0.24
BMO	3.69	70.65	3.35	8.05	6.53	1.11	0.42	0.29	0.40	1.85
RBC	7.38	3.45	70.73	14.01	2.14	0.08	0.22	0.12	0.19	0.11
TD	4.70	8.89	14.49	60.03	11.66	0.34	0.29	0.12	0.18	0.45
BNS	3.82	6.90	2.29	10.78	73.48	0.14	0.37	0.12	0.63	0.27
CITI	0.07	1.69	0.07	0.31	0.17	54.53	15.10	12.80	10.26	9.63
BAC	0.10	0.47	0.27	0.37	0.42	13.94	49.43	14.17	7.55	11.22
WFC	0.14	0.36	0.13	0.19	0.22	11.33	14.22	51.08	8.56	11.92
JPM	1.18	0.53	0.22	0.18	0.70	10.08	8.59	9.79	62.17	10.05
USB	0.27	2.58	0.12	0.57	0.31	8.37	11.27	11.40	8.86	54.27

5.4.2 Upperbound and lowerbound FEVDs

We mentioned briefly in Section 5.4.1 that impact of each variable onto the network is maximized when the variable is placed first, and minimized when it is placed last. If we place a variable i first, its impacts on each of the remaining variables are the same, independent of the ordering of the remaining variables [3]. We conjecture that these are the upperbound impacts of variable i on all other variables including itself. In order to gain insight into the upperbound of each bank's impact onto the network, we select 10 variable orderings corresponding to placing each of the 10 banks first. We then construct the upper bound FEVD matrix whose row i comes from an ordering in which Bank i is placed first, resulting in Bank i having the maximum impact onto the network.

The (i, j) element in the upperbound FEVD matrix for the NA network (Table 5.7a) represents the maximum impact a shock to variable i has on forecast error variance of variable j. An upperbound FEVD differs from a standard FEVD (Table 5.6) in three aspects: (1) the diagonal elements of the upperbound FEVD are equal to 100, (2) the columns of the upperbound FEVD do not sum to 100 and (3) the upperbound FEVD matrics are symmetric.

On the other hand, we construct the lowerbound FEVD matrix whose row i comes

[3] Supposed there are 3 banks in a banking network, the impact of A on B and A on C are the same in the two orderings $\{A,B,C\}$ or $\{A,C,B\}$

from an ordering in which Bank i is placed last, resulting in Bank i having the minimum impact onto the network. If we place variable i last, its impacts on all other variables are zero and the impact onto itself is maximized and is a constant, even though there is a change in the order of the remaining variables. We believe that these are the lowerbound of variable i's impact. In other words, the lowerbound impact of variable i is the impact onto itself when it is placed last.

	RBC	CITI	BNS	BAC	TD	WFC	JPM	CIBC	USB	BMO
CIBC	100	14.83	23.70	20.02	14.96	0.20	0.26	0.00	2.43	0.03
BMO	14.83	100	14.37	29.89	23.36	4.54	2.50	1.53	1.09	7.14
RBC	23.70	14.37	100	40.65	9.64	0.22	0.97	0.26	0.05	0.25
TD	20.02	29.89	40.65	100	34.51	0.01	1.21	0.01	0.68	1.59
BNS	14.96	23.36	9.64	34.51	100	0.69	1.82	0.08	2.47	1.38
CITI	0.20	4.54	0.22	0.01	0.69	100	55.10	50.25	39.73	40.44
BAC	0.26	2.50	0.97	1.21	1.82	55.10	100	57.27	37.05	48.92
WFC	0.00	1.53	0.26	0.01	0.08	50.25	57.27	100	39.11	49.31
JPM	2.43	1.09	0.05	0.68	2.47	39.73	37.05	39.11	100	38.90
USB	0.03	7.14	0.25	1.59	1.38	40.44	48.92	49.31	38.90	100

a Upperbound 10-step ahead FEVDs, each row i of the table comes from an ordering in which Bank i is placed first, resulting in Bank i having maximum impact onto the network.

	RBC	CITI	BNS	BAC	TD	WFC	JPM	CIBC	USB	BMO
CIBC	64.19	0.00	0.00	0.00	0.00	0.00	0.00	0.00	0.00	0.00
BMO	0.00	55.57	0.00	0.00	0.00	0.00	0.00	0.00	0.00	0.00
RBC	0.00	0.00	51.07	0.00	0.00	0.00	0.00	0.00	0.00	0.00
TD	0.00	0.00	0.00	37.61	0.00	0.00	0.00	0.00	0.00	0.00
BNS	0.00	0.00	0.00	0.00	57.64	0.00	0.00	0.00	0.00	0.00
CITI	0.00	0.00	0.00	0.00	0.00	34.53	0.00	0.00	0.00	0.00
BAC	0.00	0.00	0.00	0.00	0.00	0.00	30.18	0.00	0.00	0.00
WFC	0.00	0.00	0.00	0.00	0.00	0.00	0.00	32.23	0.00	0.00
JPM	0.00	0.00	0.00	0.00	0.00	0.00	0.00	0.00	44.78	0.00
USB	0.00	0.00	0.00	0.00	0.00	0.00	0.00	0.00	0.00	37.16

b Lowerbound 10-step ahead FEVDs, each row i of the table comes from an ordering in which Bank i is placed last, resulting in Bank i having minimum impact onto the network

Table 5.7: NA banking network: upper and lowerbounds 10-step ahead FEVDs. This is the first window's forecast (for March 17, 2006) based on 300 days of train data from January 4, 2005 to March 3, 2006 using ridge regularized VAR with exponential smoothing.

The lowerbound FEVD matrix for the NA banking network is shown in Table 5.7b. A lowerbound FEVD is another special case of FEVD matrix; it is diagonal whose elements (i,i) represent the minimum impact a shock to variable i has on the forecast

error variance of itself, and the columns of the lowerbound FEVD do not sum to 100. Subtracting each (i,i) element of the lowerbound FEVD from 100, we obtain the sum of impacts on bank i from all other banks in the network; we conjecture that the quantity is the maximum vulnerability of bank i. If we denote the lowerbound of variable i's impact I_L^i, the quantity $(100 - I_L^i)$ is the maximum vulnerability of variable i.

5.4.3 FEVDs vs. Pearson correlations

The Pearson product-moment correlation coefficient (r) is the standardized covariance between two variables which measures linear relationship between the two variables. The value of Pearson's r falls between -1 and 1 inclusive and the squared value of r is the coefficient of determination (R^2). Table 5.8 illustrates the squared correlations (coefficient of determination), multiplied by 100, between the equity returns of the 10 banks in the NA network between January 4, 2005-March 3, 2006.

Table 5.8: NA banking network: squared correlation (r^2) or coefficient of determination r^2, multiplied by 100. The values are obtained from 300 days of returns data from January 4, 2005-March 3, 2006.

	RBC	CITI	BNS	BAC	TD	WFC	JPM	CIBC	USB	BMO
CIBC	100	31.17	18.27	29.64	24.59	0.23	0.93	1.80	1.98	1.04
BMO	31.17	100	19.52	35.16	31.62	2.29	2.09	3.06	1.37	4.39
RBC	18.27	19.52	100	33.97	21.11	0.23	2.39	1.23	1.48	1.31
TD	29.64	35.16	33.97	100	39.64	0.33	2.62	1.39	1.61	2.86
BNS	24.59	31.62	21.11	39.64	100	0.68	2.16	1.03	2.49	1.20
CITI	0.23	2.29	0.23	0.33	0.68	100	44.16	40.47	42.43	34.76
BAC	0.93	2.09	2.39	2.62	2.16	44.16	100	48.47	44.89	43.76
WFC	1.80	3.06	1.23	1.39	1.03	40.47	48.47	100	40.86	44.61
JPM	1.98	1.37	1.48	1.61	2.49	42.43	44.89	40.86	100	41.31
USB	1.04	4.39	1.31	2.86	1.20	34.76	43.76	44.61	41.31	100

FEVDs differ from correlations in that the former convey both contemporaneous and temporal relationship between the variables while the latter reflect only contemporaneous relationship. In order to compare a squared correlation matrix to an upperbound FEVD matrix, we conducted two tests for the equivalence of two covariance matrices, namely the Box's M test and the F test. Our test statistic corresponding to the box's M test is 4.968 which is not significantly larger than the critical value of 73 ($\chi^2_{55}, \alpha = 55$). Also, our test statistic corresponding to the F test is 0.104 which is not

significantly larger than the critical value of 1.47 ($F(55,96), \alpha = 0.05$). The result indicates that the upperbound FEVD matrix (Table 5.7a) is not statistically distinguishable from the squared correlation matrix (Table 5.8). This indicates that FEVDs contain more information about contemporaneous relationship than that about temporal relationship between variables.

5.4.4 Rolling window analysis

To capture the dynamics in changing financial environments, we divide our data into 2415 windows, each window comprises 300 daily equity returns of 11 NA banks, and allow for time-variation of the VAR parameters. Table 5.9a is the average of 200 10-day-ahead FEVD matrices from 200 random orderings of 10 banks in the NA banking network using data between December 12, 2006-February 13, 2008. The FEVDs are computed from the forecast errors for February 28, 2008. Table 5.9b is the average of 200 10-day-ahead FEVD matrices from 200 random orderings of 10 banks in the NA banking network using data between December 12, 2006-February 13, 2008. The FEVDs are computed from the forecast errors for December 24, 2014.

Comparing Table 5.6 in Section 5.4.1 and Table 5.9a in this section, we see how the 10-day-ahead FEVDs corresponding to the forecast for February 28, 2008 have changed from those corresponding to the forecast for March 17, 2006. One particular observation worth noting is that clustering seems to have reduced in February 2008. In Table 5.6, the 10-day-ahead within-border FEVDs linking two Canadian banks or two American banks are significantly higher than cross-border FEVDs linking a Canadian bank to an American bank on March 17, 2006. However, the difference between the 10-day-ahead FEVDs linking two Canadian banks or two American banks and those linking a Canadian bank to an American bank seems to be significantly lower on February 28, 2008 as in Table 5.9a. Looking at the Tables 5.6, 5.9a, and 5.9b, we see that clustering decreased significantly in February 2008 from March 2006 but increased again in December 2014. This suggests that cross-border links were significantly stronger during crisis periods e.g. 2008 than non-crisis periods e.g. 2006, 2014.

The evolution of FEVDs can be uncovered by plotting pairwise FEVDs for each pair of banks over the forecast horizon. Figure 5.2 plots the pairwise FEVDs from and to Bank of Montreal (BMO) between 2005-2015. It is worth noting that the values

	RBC	CITI	BNS	BAC	TD	WFC	JPM	CIBC	USB	BMO
CIBC	48.87	9.28	8.53	9.10	8.68	4.14	3.74	2.52	3.53	3.54
BMO	8.34	41.57	8.81	8.38	9.55	5.65	4.03	3.02	4.40	3.47
RBC	7.76	9.09	32.04	11.61	12.79	6.47	5.73	4.12	5.34	5.18
TD	9.05	8.87	11.74	33.51	11.72	5.13	4.97	5.00	6.82	5.67
BNS	8.91	10.84	13.45	12.31	37.57	6.66	4.46	4.19	4.97	4.43
CITI	4.02	5.81	6.27	5.05	5.64	43.06	8.90	8.03	8.16	6.91
BAC	3.08	3.25	4.47	3.60	2.79	7.28	31.09	9.79	12.91	8.24
WFC	2.16	2.55	3.36	3.87	2.84	6.44	10.34	38.29	10.51	11.17
JPM	3.85	4.87	5.82	6.89	4.44	8.51	16.80	13.34	32.07	12.88
USB	3.96	3.86	5.52	5.68	3.98	6.66	9.95	11.68	11.30	38.50

a The 500th window's 10-step ahead average FEVDs (forecast for February 28, 2008 based on 300 days of train data between December 12, 2006-February 13, 2008).

	RBC	CITI	BNS	BAC	TD	WFC	JPM	CIBC	USB	BMO
CIBC	33.40	14.53	16.02	15.90	15.38	2.96	2.63	2.96	3.37	2.43
BMO	12.68	31.73	13.90	11.52	13.95	2.64	2.56	3.69	3.22	2.87
RBC	12.12	12.42	33.25	10.51	11.73	1.64	1.60	1.98	2.28	1.54
TD	14.03	11.50	12.04	29.74	13.26	3.56	4.58	4.14	4.78	3.31
BNS	14.54	15.28	14.39	14.50	30.48	3.84	3.58	4.83	4.22	3.40
CITI	2.83	2.73	1.95	3.39	3.11	33.81	16.54	10.84	16.70	13.31
BAC	1.90	1.92	1.42	3.20	2.12	13.73	30.22	10.04	13.24	10.67
WFC	2.44	3.31	1.98	3.31	3.41	8.90	10.26	34.19	10.79	13.98
JPM	3.55	3.56	3.12	4.70	3.69	17.18	16.48	13.67	29.83	13.52
USB	2.52	3.03	1.94	3.23	2.88	11.74	11.55	13.67	11.57	34.98

b The 2250th window's 10-step ahead average FEVDs (forecast for December 24, 2014 based on 300 days of train data between October 10, 2013-December 10, 2014).

Table 5.9: NA banking network: Comparing 10-step ahead average FEVDs for the 500th and the 2250th windows. Estimation is done using ridge regularized VAR with exponential smoothing.

of the FEVDs between BMO and another Canadian bank are generally higher (between 0.04 and 0.2) than those between BMO and an American bank (between 0 and 0.1). Moreover, the fluctuations over the horizon of FEVDs between BMO and another Canadian bank are significantly less than those of FEVDs between BMO and an American bank. In other words, the values of within-border FEVDs are more stable than those of cross-border FEVDs throughout different economic and financial episodes.

Figure 5.3 plots the FEVDs from and to JPMorgan Chase (JPM) between 2005-2015. Similarly, the values of FEVDs between JPM and another American bank are generally higher (between 0.05-0.2) than those between JPM and a Canadian bank

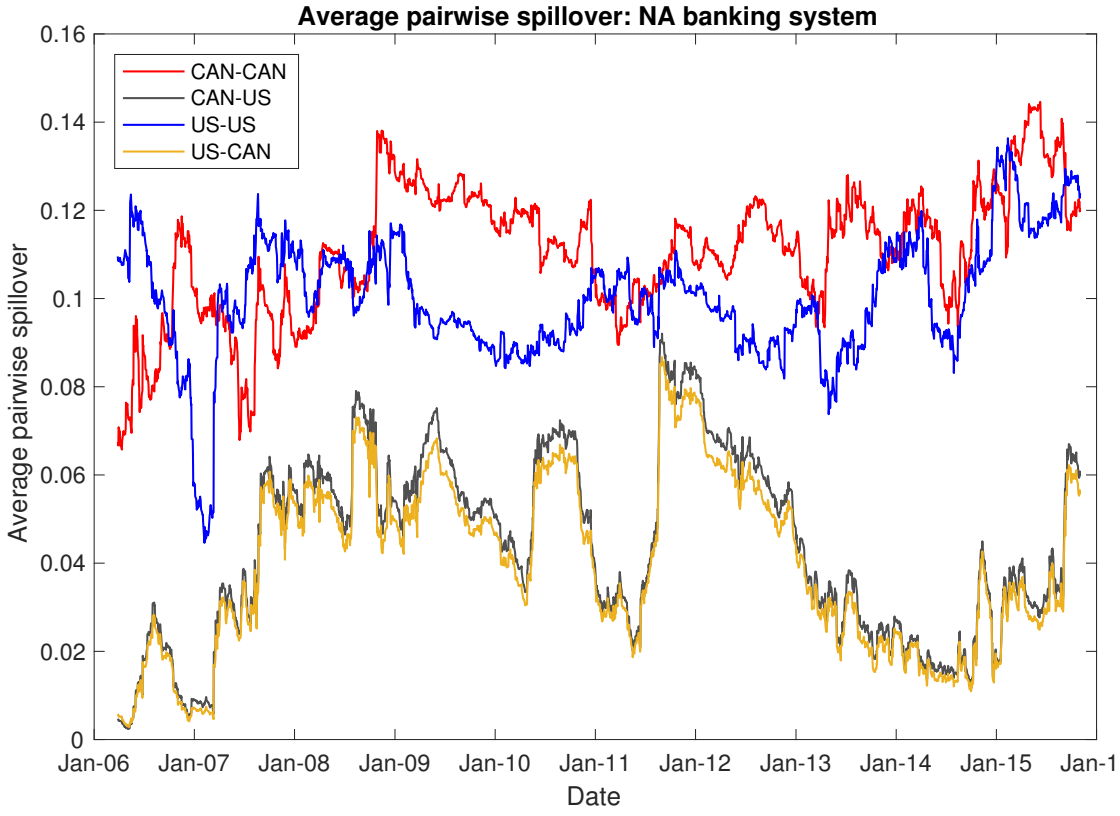

Figure 5.1: Average pairwise spillovers between regions in North America 2006-2015.

(between 0 and 0.1). There are also less fluctuations in the FEVDs between JPM and another American bank than in the FEVDs between JPM and a Canadian bank.

Figure 5.1 illustrates average pairwise links between the Canada and the U.S. Comparing the two within-border links (CAN-CAN, US-US), we find that the US-US link leads the CAN-CAN link. The CAN-US and US-CAN links are quite similar, with the CAN-US link being slightly higher than the US-CAN link, suggesting that on average, directional link from Canada to the U.S. is stronger than the U.S. to Canada. Comparing the American banks are more vulnerable to a shock coming from the Canadian side than vice versa. Comparing these vulnerability results with an independent indicator such as the credit ratings, market capitalizations, volatilities, and leverages of the banks given in Table 5.10, we conclude that the U.S. banks in general are more vulnerable to spillovers from the Canadian banks, receive lower credit ratings, have higher volatilities, and have higher market capitalization than the Canadian banks.

Figure 5.4 illustrates net spillovers for North American banks from 2005-2015.

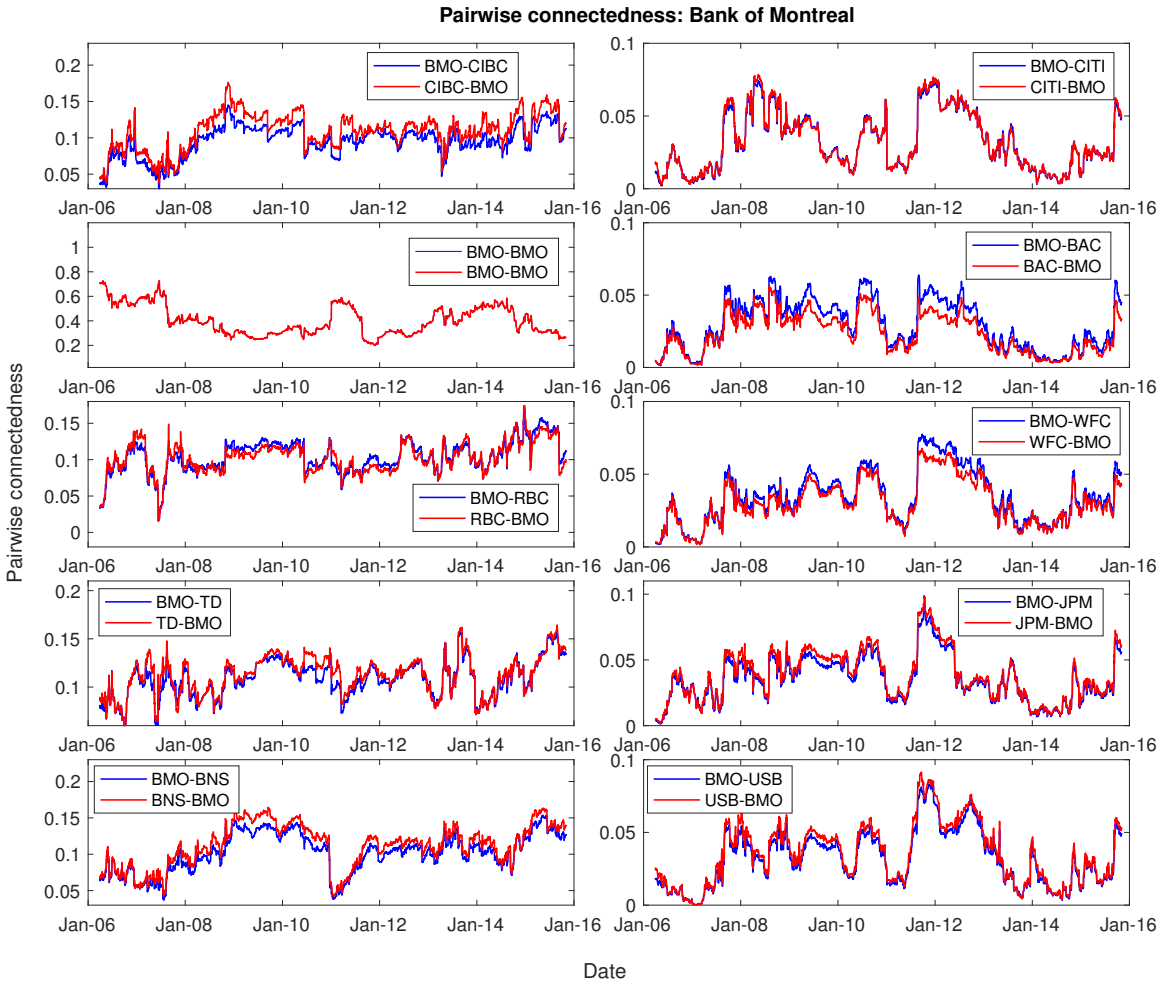

Figure 5.2: Pairwise spillovers from and to Bank of Montreal (BMO) between 2006-2015.

Table 5.10: North American banks: Current (2015) values of market capitalization, credit rating, average daily volatility, and leverage.

Bank	Market capitalization ($ billion)	Credit rating	Volatility (daily, %)	D/E ratio
CIBC	26.77	Aa3	1.81	0.81
BMO	25.84	Aa3	1.68	1.36
RBC	61.04	Aa3	1.72	2.43
TD	54.07	Aa1	1.64	1.82
BNS	40.54	Aa2	1.70	1.63
CITI	163.48	Baa1	3.72	1.89
BAC	146.56	Baa1	3.51	1.97
WFC	281.51	A2	2.86	1.39
JPM	238.24	A3	2.64	2.24
USB	76.11	A1	2.32	1.39

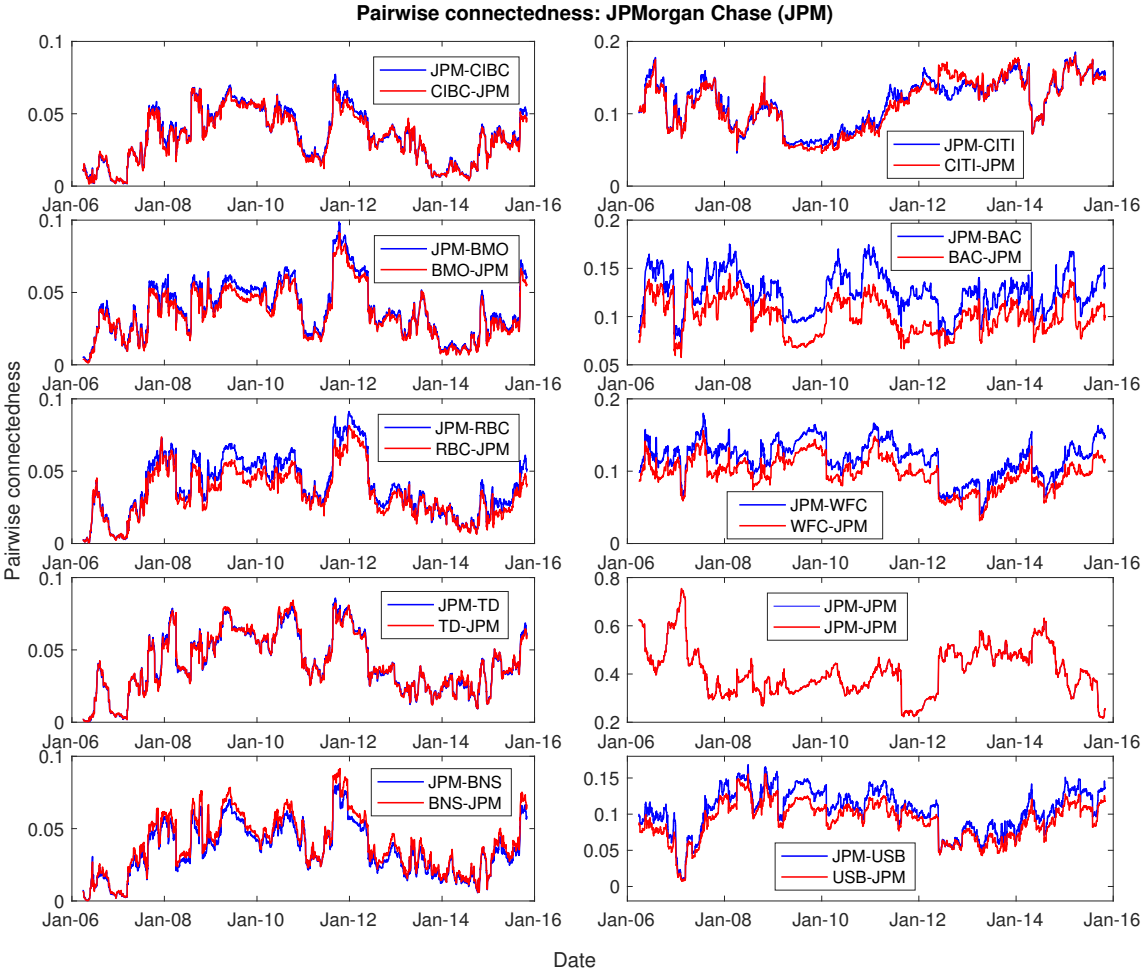

Figure 5.3: Pairwise spillovers from and to JPMorgan Chase (JPM) between 2006-2015.

A net spillover is calculated from the difference between the sum of outward and the sum of inward directional links. For example, the net spillover for CIBC is equal to the sum of directional links from CIBC to all other banks less the sum of directional links from all other banks to CIBC. The net spillovers of Canadian banks are closer to 0 between 2006 to 2008 and 2013 to 2015 but the division between the net receivers and net transmitters of shocks are more clear between 2009 and 2012. Bank of Montreal (BMO) appears to be a net receiver of shocks from all other banks nearly throughout the sample period of 2005-2015, except for a small period at the end of 2011. The net spillovers of the U.S. banks are closer to 0 between 2006 to 2007 and 2013 to 2015 but the division between the net receivers and net transmitters of shocks are more clear between 2008 and 2012. Bank of America Merrill Lynch (BAC) appears to be a net receiver throughout the 2005-2015 sample period.

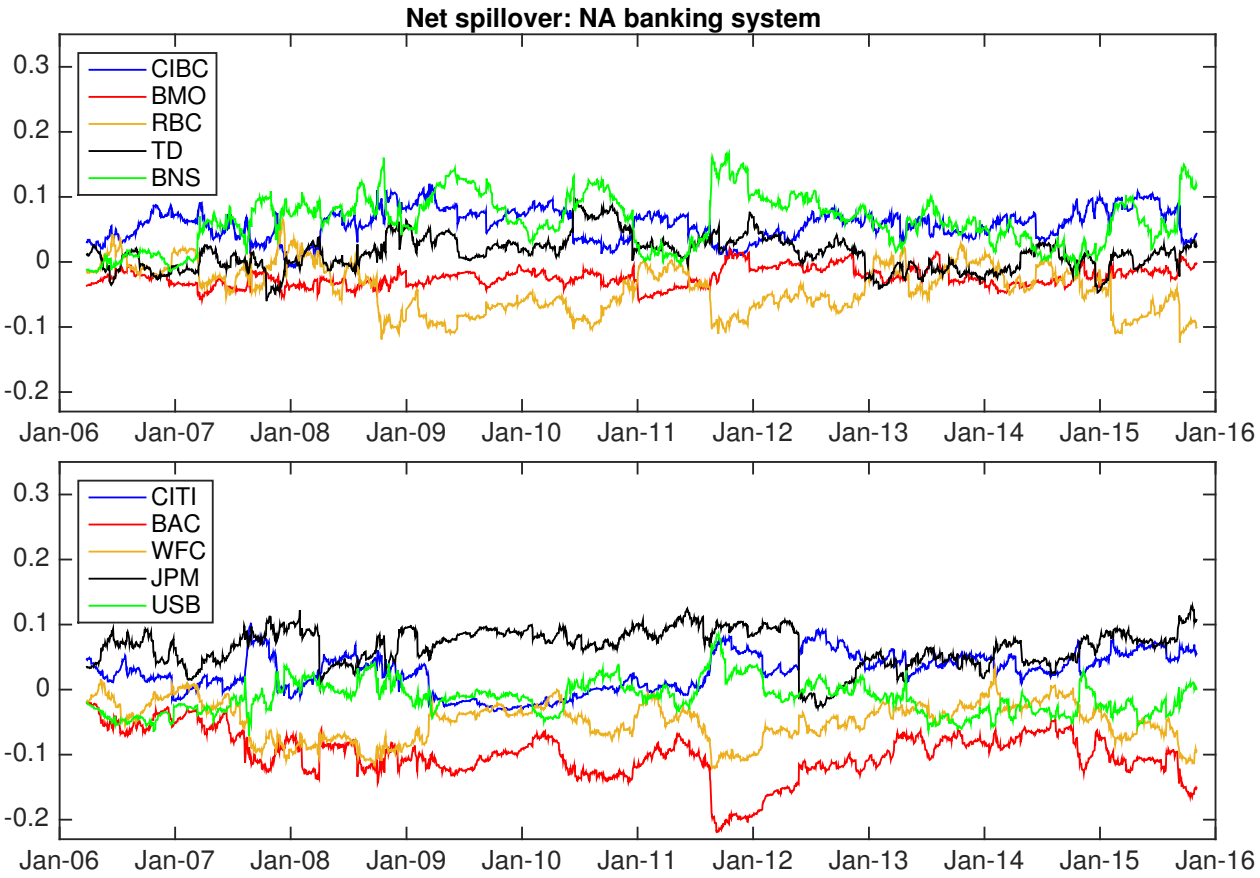

Figure 5.4: Net spillover (outward spillover less inward spillover) of each bank in North America 2006-2015.

Table 5.11 summarizes the maximum and minimum net spillovers for each of the 10 banks in the NA banking system. The net spillovers for 9 out of 10 banks fluctuate around 0, with the exception of Bank of America Merrill Lynch (BAC) being the only net receiver throughout the 2005-2016 sample period. This suggests that Bank of America Merrill Lynch is the most vulnerable bank, as it receives shocks from the other banks more than disperse its shock to the other banks in the network.

5.4.4.1 Clustering

An important finding in this section is clustering—banks based in the same country are more strongly linked than those from two different countries due to being commonly exposed to the same economic and regulatory environments. Throughout different economic and financial episodes, the links between banks based in the same countries fluctuate less than those between two banks from different countries. This suggests that the strength of cross-border links changes depending on the state of economy; however,

Table 5.11: Net spillover of each bank in North America over the period from 2006 to 2015

Bank	Min spillover	Mean spillover	Max spillover
CIBC	-0.0084	0.0578	0.1191
BMO	-0.0599	-0.0240	0.0178
RBC	-0.1241	-0.0413	0.0655
TD	-0.0588	0.0127	0.0992
BNS	-0.0208	0.0633	0.1672
CITI	-0.0335	0.0270	0.1016
BAC	-0.2192	-0.1000	-0.0204
WFC	-0.1207	-0.0485	0.0338
JPM	-0.0280	0.0661	0.1277
USB	-0.0708	-0.0131	0.0852

the strength of within-border links appears significantly more stable over time.

An intuitive explanation to this is that banks based in Canada are commonly exposed to the Canadian economic environment through, for instance, shared customer base, banking regulations, the state of the Canadian economy, interbank lending activities, and interbank trades of financial products. A Canadian bank and an American bank are commonly exposed to, for example, fluctuations in the NYSE in which both are listed, the American economic and regulatory environments in which the bank equities are traded, the cross-border interbank lending and interbank trades of financial products. The within-border links have a larger component arising from common exposure to real-sector fluctuations e.g. shared customer base, regulations, while cross-border links have a larger component arising from exposure to financial fluctuations.

5.5 Empirical result: System-wide analysis

In this section, we use our exponentially weighted, ridge-regularized VAR-FEVD methodology, hereafter known as “improved VAR”, discussed in Section 5.2 and measure time-varying network connectedness for three banking systems, namely North America (NA), the European Union (EU), and Southeast Asia (ASEAN). Specifically, we aggregate the pairwise connectedness between banks in each banking system to obtain a measure of total connectedness for the system. We then analyze lead-lag relationships among the three systems by performing Granger causality and transfer entropy tests on the network connectedness time series.

5.5.1 Total connectedness

Figures 5.5, 5.6, and 5.7 illustrate the total connectedness computed from the standard VAR and improved VAR models for the ASEAN, EU, and NA banking systems respectively. For all three systems, the total connectedness from the standard VAR (red marker) is generally smoother, less volatile, and varies within a smaller range than the total connectedness from the improved VAR (blue marker). Over the period from 2006 to 2015, the ASEAN total connectedness from the standard VAR varies between 0.32 and 0.53 while that from the improved VAR varies between 0.23 and 0.63. The EU total connectedness from the standard VAR varies between 0.47 and 0.72 and that from the improved VAR varies between 0.42 and 0.78. The NA total connectedness from the standard VAR varies between 0.38 and 0.72 while that from the improved VAR varies between 0.31 and 0.78.

It is evident in Figures 5.5, 5.6, and 5.7 that the effect of outliers is retained for the entire window length in the standard VAR case while for the improved VAR case the effect of outliers quickly diminishes. Because all data points are equally weighted in the standard VAR, the effects of outliers are retained until the rolling window move away from the outliers. In addition, in the improved VAR case we observe much clearer peaks which correspond to high connectivities of the system. The improved VAR estimation thus allows for better identification of point events i.e. events concentrated at specific times. On the contrary, the total connectedness obtained from standard VAR is much less informative than that obtained from the improved VAR—all the peaks in total connectedness from the standard VAR are less obvious than those from the improved VAR. If total connectedness from the standard VAR is used as the system's fragility or vulnerability measure, one will not be able to identify several peaks corresponding to extreme connectedness in the ASEAN banking system in 2009, 2010, 2011, 2013, and 2015, in the EU banking system in early and late 2007, 2010, 2013, and 2014, and in the NA banking system in 2006, 2007, 2008, 2010, end of 2011, 2013, 2014, and 2015.

In Diebold and Yilmaz [2009], global spillovers in equity index returns and volatilities were measured. They found that the return spillovers demonstrate "a gently increasing trend but no bursts, whereas volatility spillovers display no trend but clear bursts." Our results in Figures 5.5, 5.6, and 5.7 allow us to observe both trends and bursts in the return spillovers of all three banking systems. Thus, applying exponential

weights onto the data allows for clear peaks to be observed in the return spillovers, which was not visible in Diebold and Yilmaz [2009]. By using exponential weights our research improves Diebold and Yilmaz's methodology and enables us to better identify extreme connectedness and more accurately interpret the total connectedness graphs. In addition, the use of ridge regression reduces the variance of the VAR coefficient estimates, which in turn increases the reliability of the FEVDs, from which network connectedness is derived. In Figure 5.6, the sudden jump and drop in the EU total spillover from the standard VAR around January 2011 reflects such high variance problem.

Figure 5.8 illustrates the individual benefits of exponential weights and ridge regression in the context of total spillover estimation for the NA banking network. Using only ridge regression would help reduce the problem of high variability of the VAR coefficient estimates but would not produce the clear peaks in total spillover. On the other hand, applying only exponential weights would make the peaks in total spillover more visible but the VAR coefficients would still fluctuate widely as observed around August 2011. In other words, we obtain superior results (clearer peaks, lower estimation variances) when both exponential weights and regularization are applied simultaneously.

We were aware after the completion of our research that Demirer et al. [2017] uses the regularization technique LASSO in VAR estimation. We believe that LASSO can be used in our research instead of ridge regression and can potentially produce more interpretable pairwise results because the former does both variable selection and shrinkage while ridge regression does not do variable selection. The drawback of LASSO is the difficulty of implementation and significantly longer runtime, which makes it less appealing especially in the context of total, system-wide connectedness. Using LASSO or ridge regression is thus a decision to balance runtime, implementation difficulty, and interpretability of pairwise results. Because the differences between pairwise metrics from LASSO and ridge regression are averaged out when we compute total connectedness, we feel that ridge regression is more suitable for our research.

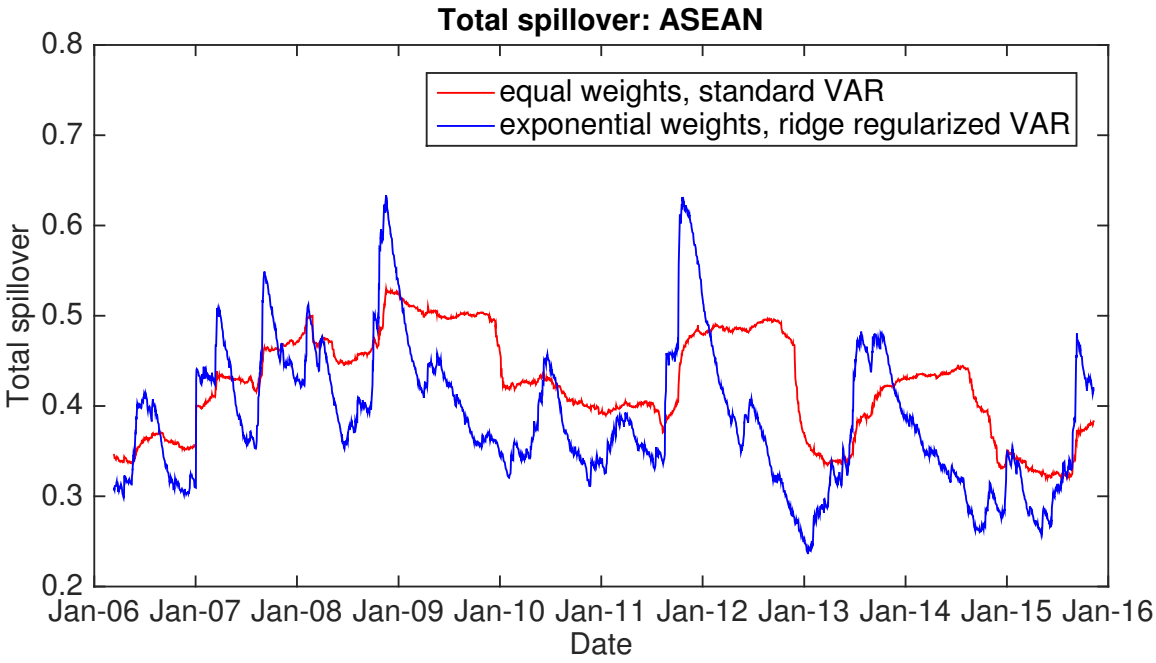

Figure 5.5: ASEAN banking system: Comparison between total spillover computed using classical VAR approach and the improved VAR approach with ridge penalization and exponential smoothing. 300-day rolling window.

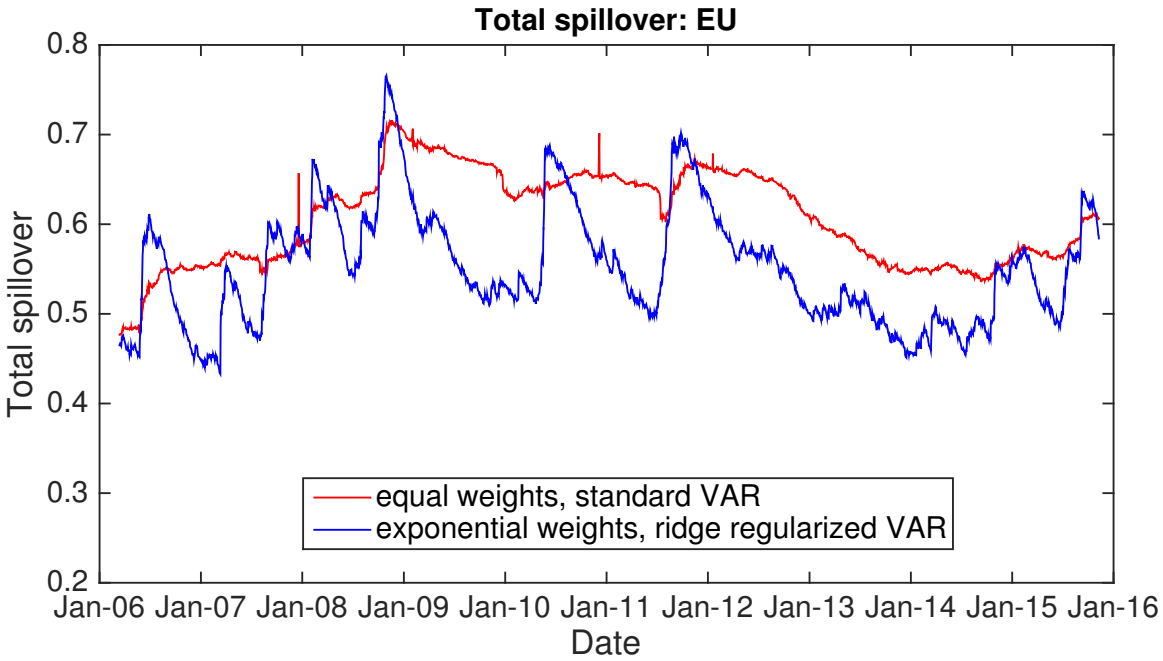

Figure 5.6: EU banking system: Comparison between total spillover computed using classical VAR approach and the improved VAR approach with ridge penalization and exponential smoothing. 300-day rolling window.

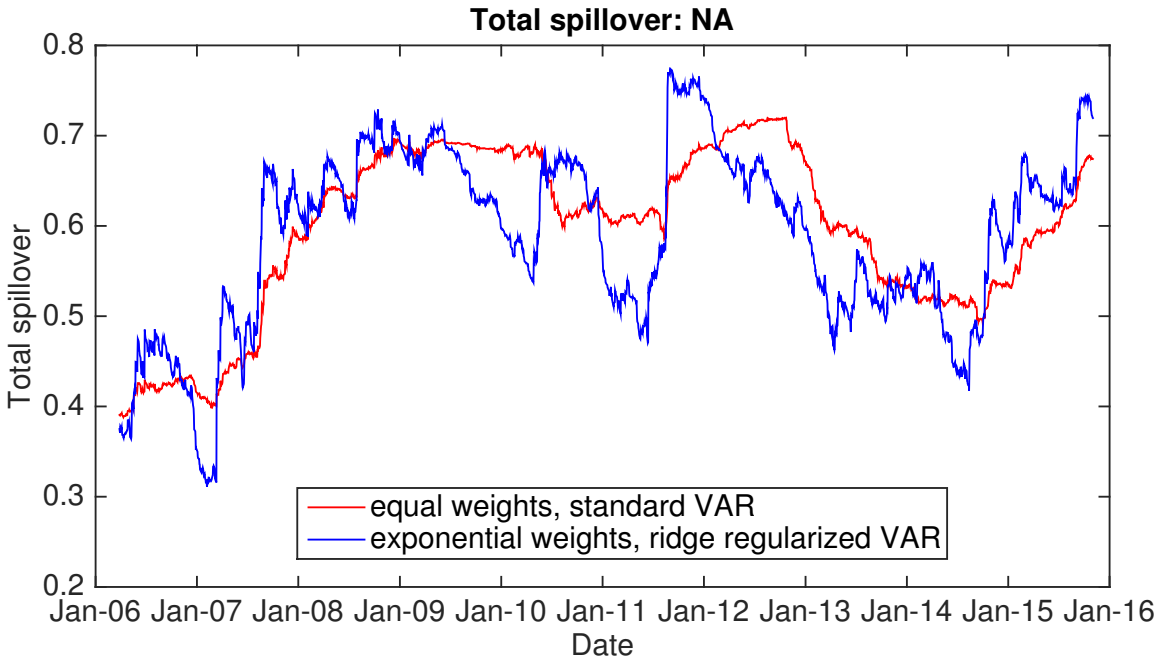

Figure 5.7: NA banking system: Comparison between total spillover computed using classical VAR approach and the improved VAR approach with ridge penalization and exponential smoothing. 300-day rolling window.

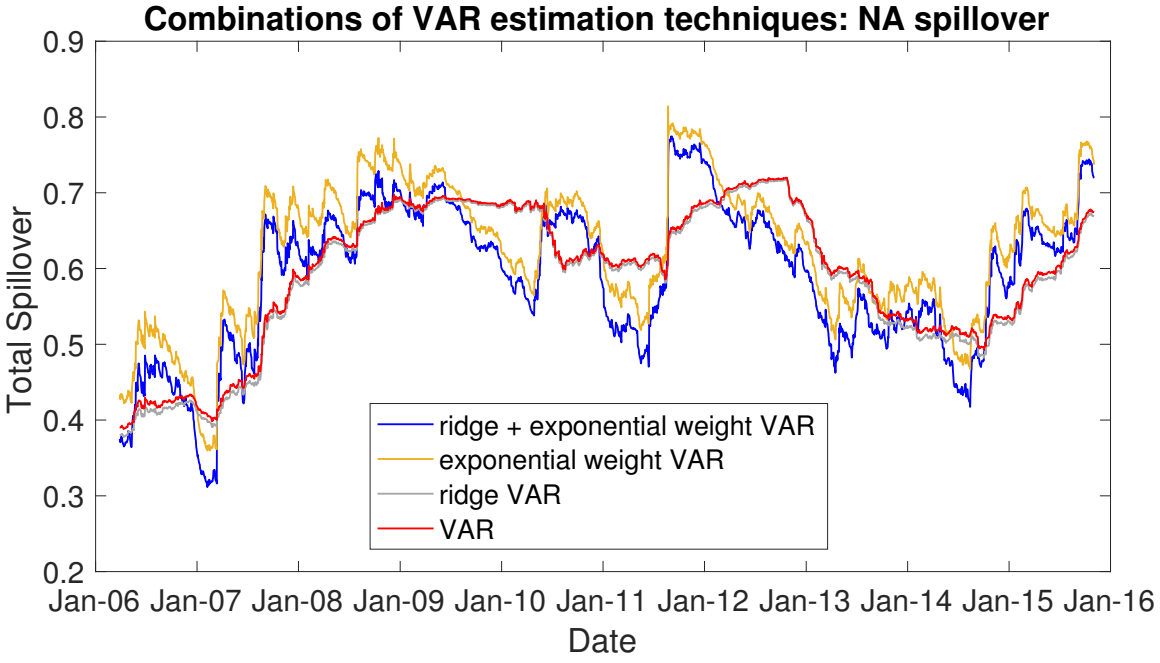

Figure 5.8: NA banking system: Comparison between total spillover computed using (1) improved VAR approach with ridge penalization and exponential smoothing, (2) VAR with exponential smoothing, (3) VAR with ridge penalization, and (4) classical VAR approach. 300-day rolling window.

Combining the ASEAN, EU, and NA total spillovers from the improved VAR models in Figures 5.5, 5.6, and 5.7 we obtain Figure 5.9 with major events labeled on the graph when they occurred. Over the period from 2006 to 2015, the values of the NA spillover are generally higher than those of the EU and ASEAN banking systems with the exceptions in 2006 to mid 2007, early 2011, early 2013 and mid 2014. More specifically, total connectedness in the NA banking system was the highest from mid-2007 onward, total connectedness in the EU banking system was the highest from 2005 to mid-2007 but was second highest from mid-2007 to 2016, and total connectedness in the ASEAN banking system was the lowest throughout the entire sample period. As the total spillover is a measure of total connectivity, it appears that the NA banking system is generally more interconnected and vulnerable to contagion than the EU and ASEAN banking systems.

From visual inspection of Figure 5.9, we found that total spillover within the NA banking system tends to lead those within the EU and ASEAN systems and total spillover within the EU system tends to lead that of the ASEAN system. This prompts us to perform linear and non-linear causality tests (Granger causality and transfer entropy tests detailed in Section 5.5.2) on the spillover time series of the three banking systems in order to investigate how connectivity and systemic vulnerability in each region influence the others.

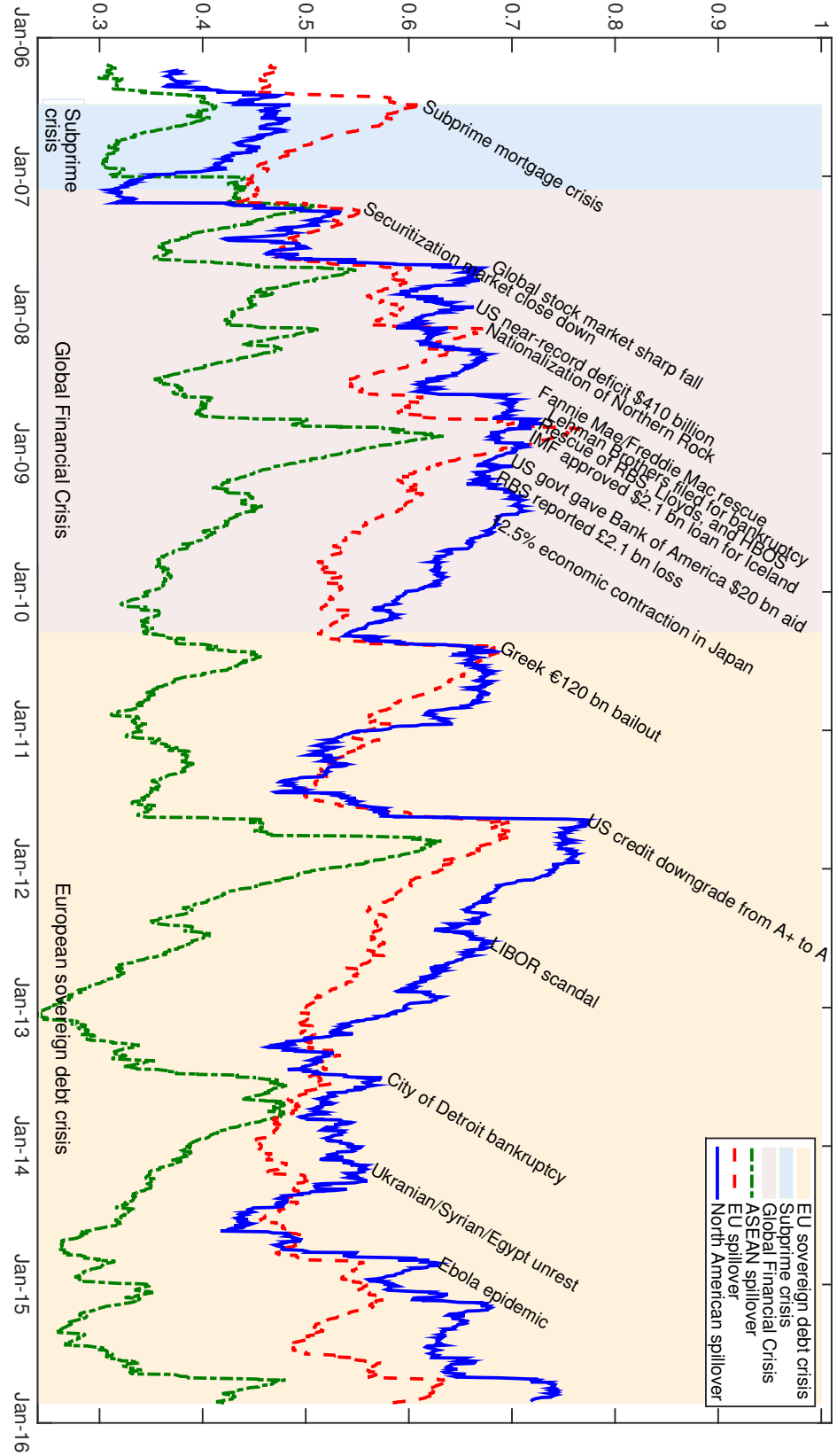

Figure 5.9: Total spillover in the three banking systems (as in Figs. 5.5, 5.6 and 5.7, blue solid lines) with indicated major events associated with peaks. (300-day rolling window).

5.5.2 Causality tests on regional spillovers

In order to test for lead-lag relationships among the NA, EU, and ASEAN total spillovers, we perform two causality tests, namely the Granger causality test and transfer entropy test. While Granger causality test is linear in nature, transfer entropy can be linear and non-linear.

5.5.2.1 Granger causality tests

We first analyze Granger causality relationships among the spillovers of the three banking systems over the full sample period from 2006 to 2015. Acknowledging that the stock market closing time in ASEAN leads that of the EU, which leads that of North America, we test for Granger causality over various lag horizons ranging from 1 day to 30 days.

Our findings in Table 5.12 indicate that the NA spillover Granger-causes the EU spillover over forecast horizons from 2-30 days but it does not Granger-cause the EU spillover over the forecast horizon of 1 day. In other words, 2 to 30-day lagged values of the NA spillover have significant predictive power on the EU spillover. In the reverse direction, the EU spillover Granger-causes the NA spillover over forecast horizons of 3-30 days but not over forecast horizons of 1-2 days.

The NA spillover Granger-causes the ASEAN spillover over forecast horizons of 2-30 days but not over forecast horizon of 1 day. In the reverse direction, the ASEAN spillover also Granger-causes the NA spillover over forecast horizons of 2-30 days but not over forecast horizon of 1 day. The EU spillover Granger-causes the ASEAN spillover over forecast horizons of 2-30 days but not over forecast horizon of 1 day. In the reverse direction, the ASEAN spillover also Granger-causes the EU spillover forecast horizons of 2-30 days but not over forecast horizon of 1 day.

For all three spillover pairs (NA-EU, NA-ASEAN, and EU-ASEAN), Granger causality is significant in both directions. The case in which Granger causality is significant in both directions can be resolved using the equivalence of transfer entropy and the F-statistics obtained from Granger causality tests under the multivariate Gaussian framework, as previously discussed in Section 4.3 of this paper and in more detail in Barnett et al. [2009]. More specifically, in order to make inference regarding the net Granger causality direction or the net information flow, we compare the magnitude

of the F-statistic associated with Granger causality test in one direction to that of the reverse direction for each of the three regional spillover pairs.

Our results in Table 5.12 show that all values of $F_{NA \to EU}$ are greater than those of $F_{EU \to NA}$, suggesting that net information flows from the NA spillover to the EU spillover and the NA spillover Granger-causes the EU spillover on a net basis. Comparing the values of $F_{NA \to ASEAN}$ and those of $F_{ASEAN \to NA}$, we find that net information flows from the NA spillover to the ASEAN spillover and the NA spillover Granger-causes the ASEAN spillover on a net basis. Similarly, we compare the values of $F_{EU \to ASEAN}$ and those of $F_{ASEAN \to EU}$ and find that net information flows from the EU spillover to the ASEAN spillover and the EU spillover Granger-causes the ASEAN spillover on a net basis. Our results in Table 5.12 align with the findings of Rapach et al. [2013] who observed that lagged U.S. returns are significant predictors of numerous non-U.S. industrialized countries, but lagged non-U.S. returns have limited predictive ability with respect to the U.S. returns.

For robustness, we perform Granger causality tests on total spillovers of the three regions over the three 800-day sub-periods: (1) March 28, 2006 to June 10, 2009, (2) June 11, 2009 to August 10, 2012, and (3) August 18, 2012 to November 2, 2015. The results are illustrated in Table 5.13.

The first period of March 28, 2006 to June 10, 2009 covers the Global Financial Crisis of 2007-2009. In this period we find that the NA spillover Granger-causes the EU spillover for 2-30 day forecast horizons but not for 1-day forecast horizon and in the reverse direction, the EU spillover does not Granger-cause the NA spillover for any forecast horizons. This suggests that the net Granger causality direction is from the NA to EU. The NA spillover Granger-causes the ASEAN spillover for forecast horizons of 2-30 days but not for forecast horizon of 1 day and in the reverse direction, the ASEAN spillover also Granger-causes the NA spillover for 2-30 day forecast horizons but not for 1-day forecast horizon. Because all significant values of $F_{NA \to ASEAN}$ are greater than those of $F_{ASEAN \to NA}$, the net Granger causality direction is from NA to ASEAN. The EU spillover Granger-causes the ASEAN spillover for 2-30 forecast horizons but not for 1-day forecast horizon while in the reverse direction, the ASEAN spillover does not Granger-cause the EU spillover for all forecast horizons.

The second period of June 11, 2009 to August 10, 2012 covers most of the euro-

Table 5.12: Tests for Granger causality between regional spillovers: March 28, 2006-November 2, 2015 (full sample).

Hypothesis	F-statistic	$F_{0.05}$	$F_{0.01}$
H_0: NA Granger-causes EU			
lag = 1 day	0.43	3.85	6.65
lag = 2 days	11.95***	3.85	6.65
lag = 3 days	17.49***	3.85	6.65
lag = 4 days	18.19***	3.85	6.65
lag = 5-30 days	18.26***	3.85	6.65
H_0: EU Granger-causes NA			
lag = 1-2 days	3.57	3.85	6.65
lag = 3-30 days	4.26**	3.85	6.65
H_0: NA Granger-causes ASEAN			
lag = 1 day	1.04	3.85	6.65
lag = 2 days	43.61***	3.85	6.65
lag = 3 days	36.23***	3.85	6.65
lag = 4-30 days	36.61***	3.85	6.65
H_0: ASEAN Granger-causes NA			
lag = 1 day	3.68	3.85	6.65
lag = 2 days	23.06***	3.85	6.65
lag = 3-30 days	18.28***	3.85	6.65
H_0: EU Granger-causes ASEAN			
lag = 1 day	2.14	3.85	6.65
lag = 2 days	14.85***	3.85	6.65
lag = 3 days	12.28***	3.85	6.65
lag = 4-30 days	11.35***	3.85	6.65
H_0: ASEAN Granger-causes EU			
lag = 1 day	0.16	3.85	6.65
lag = 2 days	9.20***	3.85	6.65
lag = 3 days	7.75***	3.85	6.65
lag = 4 days	7.98***	3.85	6.65
lag = 5-30 days	5.98***	3.85	6.65

Table 5.13: Tests for Granger causality between regional spillovers. Each period covers 800 days, i.e., (1) 28/03/2006 -10/06/2009, (2) 11/06/2009-10/08/2012, (3) 18/08/2012-02/11/2015. The critical F-statistic are 3.86 at 5% significance level and 6.69 at 1% significance level

Hypothesis	F (1)	F (2)	F (3)
H_0: NA Granger-causes EU			
lag = 1 day	3.29	3.19	1.80
lag = 2 days	10.67***	1.77	2.01
lag = 3 days	11.00***	15.23***	2.01
lag = 4 days	12.75***	15.23***	2.01
lag = 5-30 days	11.22***	14.94***	2.01
H_0: EU Granger-causes NA			
lag = 1 day	0.27	8.43***	1.78
lag = 2 days	0.27	7.05***	1.78
lag = 3 days	0.27	5.70**	1.78
lag = 4-30 days	0.27	5.70**	1.78
H_0: NA Granger-causes ASEAN			
lag = 1 day	0.37	0.70	0.19
lag = 2 days	13.36***	38.83***	0.31
lag = 3 days	11.29***	28.16***	0.08
lag = 4-30 days	12.30***	28.16***	0.17
H_0: ASEAN Granger-causes NA			
lag = 1 day	2.27	1.75	0.53
lag = 2 days	7.80***	27.82***	0.53
lag = 3 days	7.80***	15.77***	0.53
lag = 4-30 days	7.80***	15.77***	0.53
H_0: EU Granger-causes ASEAN			
lag = 1 day	0.37	13.53***	1.09
lag = 2 days	8.78***	12.74***	0.84
lag = 3 days	7.83***	9.55***	0.34
lag = 4 days	6.80***	9.55***	0.21
lag = 5-30 days	8.88***	9.55***	0.21
H_0: ASEAN Granger-causes EU			
lag = 1 day	2.76	5.48**	0.80
lag = 2 days	2.37	7.97***	3.80
lag = 3 days	2.07	5.14**	3.80
lag = 4 days	1.93	7.56***	3.80
lag = 5-30 days	1.22	6.34**	3.80

zone crisis. In this period we find that the NA spillover Granger-causes the EU spillover for 3-30 day forecast horizons but not for 1-2 day forecast horizons while in the reverse direction, the EU spillover Granger-causes the NA spillover for all forecast horizons. Comparing the values of $F_{NA \to EU}$ and those of $F_{EU \to NA}$ for 3-30 day forecast horizons, we find that the 3 to 30-day lagged values of NA spillover have predictive power over the EU spillover but the 1 to 2-day lagged values of the EU spillover have predictive power over the NA spillover. This suggests that over 1 and 2-day windows, information flows from EU to NA but over 3 to 30-day windows, information flows from NA to EU on a net basis. The NA spillover Granger-causes the ASEAN spillover for 2-30 day forecast horizons but not for 1-day forecast horizon and in the reverse direction, the ASEAN spillover also Granger-causes the NA spillover for 2-30 forecast horizons but not for 1-2 day forecast horizon. Because all significant values of $F_{NA \to ASEAN}$ are greater than those of $F_{ASEAN \to NA}$, the net Granger causality direction is from NA to ASEAN. The EU spillover Granger-causes the ASEAN spillover for all forecast horizons and in the reverse direction, the ASEAN spillover Granger-cause the EU spillover for all forecast horizons. The net Granger causality direction is from the EU to ASEAN because all values of $F_{EU \to ASEAN}$ are greater than those of $F_{ASEAN \to EU}$.

The third period of August 18, 2012 to November 2, 2015 covers some of the Greek crisis. In this period, none of the values of the F-statistics is significant, suggesting no Granger causality in any of the regional spillover pairs.

In sum, our Granger causality results in Table 5.13 suggest that total connectedness in NA dominated those from other regions during the Global Financial Crisis while total connectedness in the EU became more dominant during the eurozone crisis. In other words, net information flowed from NA to EU and ASEAN during the Global Financial Crisis while net information flowed from the EU to NA (for shorter horizons) and ASEAN (for all horizons) during the eurozone debt crisis.

5.5.2.2 Transfer entropy tests

In this section we compute transfer entropy and information flow using changes of total connectedness (one and five-day changes) in the three regions—the NA, EU, and ASEAN banking systems—in order to quantify the lead-lag relationships among them. We estimate transfer entropy using both a linear and non-linear approaches.

The linear approach computes transfer entropy $T_{Y\to X}$ using the relationship with Granger causality in Equations 4.23, 4.20 and 4.21. The non-linear approach taken from Tungsong et al. [2018] estimates entropies by first discretizing the signal, i.e. variable A with mean μ_A and standard deviation σ_A, into three states respectively associated with a central band of values within $\mu_A \pm \delta\sigma_A$ and two external bands associated with values smaller than $\mu_A - \delta\sigma_A$ and larger than $\mu_A + \delta\sigma_A$. Denote respectively p_A^0, p_A^- and p_A^+ the relative frequencies of the observations in the three bands, we estimate entropy as $H(A) = -p_A^- \log p_A^- - p_A^0 \log p_A^0 - p_A^+ \log p_A^+$. The joint entropy of two variables is equivalently defined by the combination of values of the two variables in the three bands obtaining 9 combined states $p_{A,B}^{-,-}$, $p_{A,B}^{-,+}$, $p_{A,B}^{+,-}$, $p_{A,B}^{+,+}$, $p_{A,B}^{-,0}$, $p_{A,B}^{+,0}$, $p_{A,B}^{0,-}$, $p_{A,B}^{0,+}$, $p_{A,B}^{0,0}$ from which joint entropy can be estimated as $H(A,B) = -\sum_{r,s=\{0,+,-\}} p_{A,B}^{r,s} \log p_{A,B}^{r,s}$. If $T_{Y\to X} > T_{X\to Y}$, then the direction of the information transfer goes from Y to X. Conversely, if $T_{X\to Y} > T_{Y\to X}$, then the direction of the information transfer goes from X to Y. The net information flow between X and Y is quantified as $T_{X\to Y} - T_{Y\to X}$.

The results for the daily differences in total connectivities and one-day lag are reported in Table 5.14. Statistical significance was estimated with respect to a null hypothesis via permutation test using 10,000 permutations for each measure. We recall that the linear measure is equivalent to Granger causality where a significant transfer entropy corresponds to a validated Granger causality. The non-linear measure was computed for fluctuation bands at $\delta = 1, 2, 3$ standard deviations. We observe that there is a significant information transfer between NA and EU, NA and ASEAN and the EU and ASEAN which prevails the opposite direction. For the linear case, this implies NA Granger causes the EU, NA Granger causes ASEAN and the EU Granger causes ASEAN. We observe that the non-linear test provides consistent results with those from the linear test for all values of δ, demonstrating robustness of the result.

We also observe that there are significant causal relations in the opposite directions. Given the extended temporal lags between the three regions it is fair to question whether one-day lag and one-day time horizon will asymmetrically affect markets depending on their relative opening hours. We therefore compute transfer entropy and information flow across regions for time-horizon and lag of 5 days instead of one day. Transfer entropies and information flows, computed from non-overlapping five-day returns for the entire period, are reported in Table 5.15. We find that the results are

Table 5.14: Transfer entropy between regional spillovers: March 28, 2006-November 2, 2015 (full sample), computed from one-day changes in the total spillover.

Method	$TE_{NA\to EU}$	$TE_{EU\to NA}$	Net Information Flow
linear	0.004722**	0.001354*	0.003369
non-linear treshold σ	0.005251***	0.006711**	-0.001460
non-linear treshold 2σ	0.003980***	0.002012*	0.001968
non-linear treshold 3σ	0.004939***	0.000561	0.004378
Method	$TE_{NA\to AS}$	$TE_{AS\to NA}$	Net Information Flow
linear	0.017336***	0.008931***	0.008405
non-linear treshold σ	0.008789***	0.005837**	0.002953
non-linear treshold 2σ	0.005348***	0.002305*	0.003042
non-linear treshold 3σ	0.003150**	0.002803***	0.000348
Method	$TE_{EU\to AS}$	$TE_{AS\to EU}$	Net Information Flow
linear	0.005659**	0.003633**	0.002026
non-linear treshold σ	0.005553**	0.001262	0.004291
non-linear treshold 2σ	00.005960***	0.000228	0.005732
non-linear treshold 3σ	0.004238***	0.002118***	0.002120

* p-value < 0.05, ** p-value < 0.01, *** p-value < 0.001.

Table 5.15: Transfer entropy between regional spillovers: March 28, 2006-November 2, 2015 (full sample), computed from weekly changes (5 days) in the total spillover.

Method	$TE_{NA\to EU}$	$TE_{EU\to NA}$	Net Information Flow
linear	0.008003*	0.001255	0.006747
non-linear threshold σ	0.009204	0.009474	-0.000271
non-linear threshold 2σ	0.017228***	0.003196	0.014032
non-linear threshold 3σ	0.024087***	0.002335*	0.021752
Method	$TE_{NA\to AS}$	$TE_{AS\to NA}$	Net Information Flow
linear	0.017200**	0.003703	0.013497
non-linear threshold σ	0.010598*	0.004354	0.006244
non-linear threshold 2σ	0.006509	0.006475	0.000034
non-linear threshold 3σ	0.002107	0.006805***	-0.004698
Method	$TE_{EU\to AS}$	$TE_{AS\to EU}$	Net Information Flow
linear	0.022020**	0.000619	0.021401
non-linear threshold σ	0.021641***	0.002374	0.019267
non-linear threshold 2σ	0.022964***	0.002900	0.020063
non-linear threshold 3σ	0.007488**	0.000405	0.007083

* p-value < 0.05, ** p-value < 0.01, *** p-value < 0.001.

consistent with those for one-day time horizon and lag reported in Table 5.14 with the main difference being lower statistical significance, most likely because the time series for the five-day changes are five times shorter than the time series for daily changes.

5.6 Full vs. sparse network connectedness

In this section we illustrate network connectedness of the three banking systems computed from transfer entropy in the context of sparse modeling discussed in Chapter 6. As the data used to produce Figure 5.10 are the same as those used to produce Figure 5.9, we can look at Figure 5.10 and Figure 5.9 analogously.

While the total connectedness metric computed from FEVDs of the full network and that computed from transfer entropy of the sparse network can identify major crises correctly, the total connectedness derived from the sparse network demonstrates much clearer peaks during the crises. For example, the NA total connectedness computed from the sparse network allows us to distinguish major crises e.g. the Global Financial Crisis, the European sovereign debt crisis, the US credit downgrade, and the LIBOR scandal, from smaller crisis events. The NA total connectedness surrounding those major crises are much higher than that surrounding smaller crises. This confirms that the sparse network has higher signal-to-noise ratio which improves the interpretability of the connectedness measure, allowing for better inference and identification of crises. On the contrary, the connectedness measure computed based on the full network, which has lower signal-to-noise ratio, does not provide clear visibility of peaks associated with extreme events.

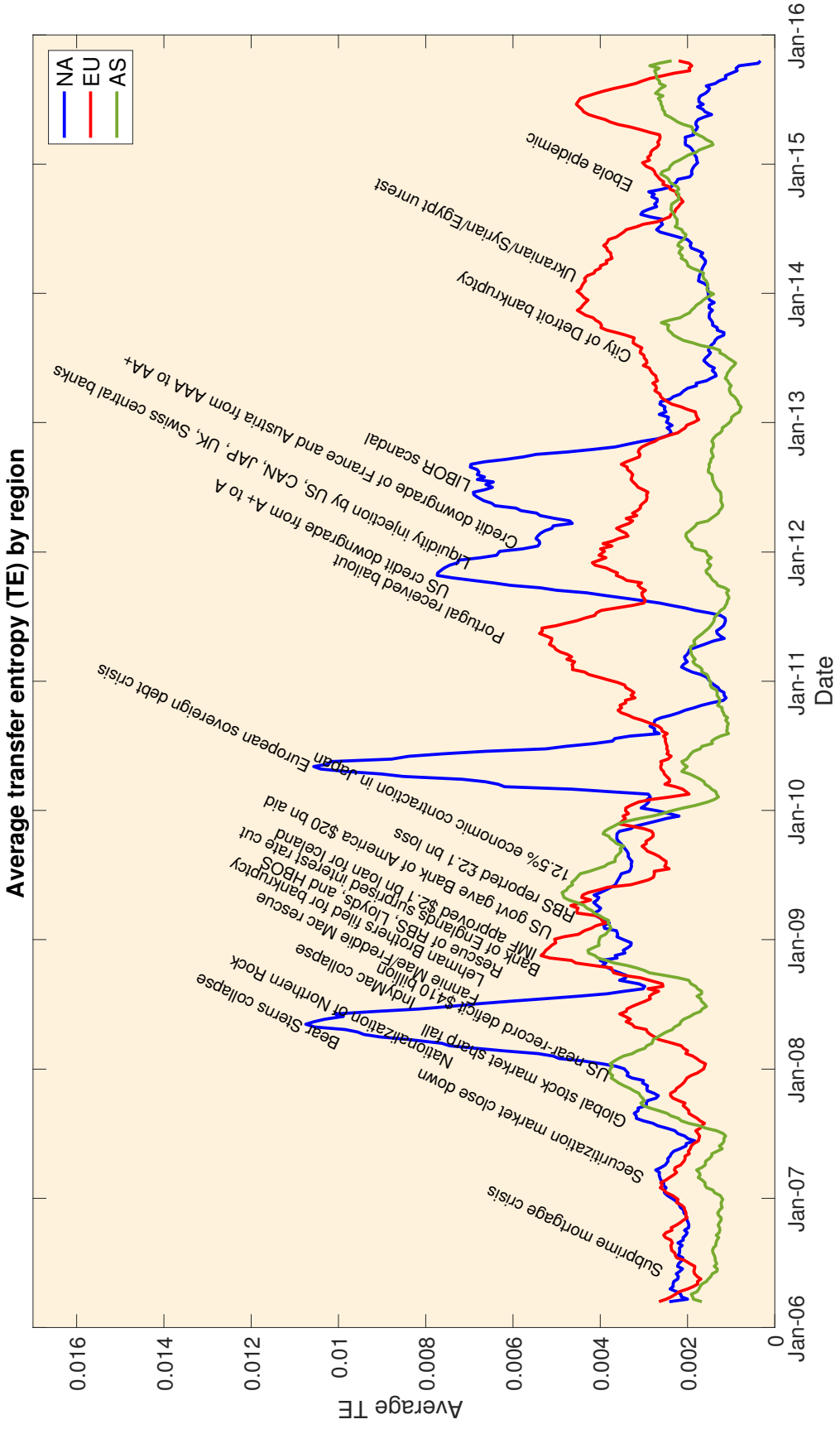

Figure 5.10: Average transfer entropy, a measure of total connectedness, computed from sparse inverse covariance matrix estimated using the LoGo-TMFG algorithm.

5.7 Conclusion

In this chapter we quantify pairwise and system-wide connectedness in the NA, EU, and ASEAN banking systems using our improved VAR-FEVD methodology on banks' stock returns from 2005 to 2015 and demonstrate that the results from the improved VAR-FEVD framework are superior to those from the classical VAR framework proposed by Diebold and Yilmaz [2009, 2012, 2014]. Our proposed VAR-FEVD improves the classical VAR-FEVD method in two ways. First, the problems of unreliability of forecasts and high variance due to increased dimensionality are addressed through the use of ridge regression. Second, we mitigate the sensitivity to outliers in remote observations by assigning exponential weights to data points, with more recent data points receiving larger weights. In this way, we obtain visible connectedness peaks which enable us to identify crises that took place in the three banking systems—NA, EU, and ASEAN.

Our time-varying total connectedness metric for each banking system indicates temporal changes in the systemic risk, with peaks during major crisis events and troughs during normal periods, which are similar to those observed in other financial systems (Diebold and Yilmaz [2009, 2012, 2014], Chau and Deesomsak [2014], Alter and Beyer [2014], Fengler and Gisler [2015], and Demirer et al. [2017]. In general, the level of total connectedness in the NA banking system is the highest, followed by those of the EU, and ASEAN banking systems respectively.

We test for Granger causality over the full sample and three subsamples covering the period from 2006 to 2015 and find that there is causality in both directions e.g. NA to EU vs. EU to NA, NA to ASEAN vs. ASEAN to NA, and EU to ASEAN vs. ASEAN to EU. The F-statistics associated with NA to EU, NA to ASEAN, and EU to ASEAN are higher than the opposite directions, suggesting that net information flows from NA to EU and EU to ASEAN. Our results support the findings in research such as Rapach et al. [2013] which provides evidence that lagged U.S. returns are significant predictors of numerous non-U.S. industrialized countries but lagged non-U.S. returns have limited predictive ability with respect to the U.S. returns.

For robustness, we perform nonlinear causality tests based on transfer entropies and information flows computed on the changes of total connectedness in the three banking systems. We find that there is a significant information flow from NA to EU,

NA to ASEAN and EU to ASEAN, consistent with the results from our Granger causality tests.

The contributions of our research are three folds. First, we provide technical improvements including the assignment of exponential weights to the data and the application of ridge regression on the VAR estimation, which mitigates the sensitivity to outliers problem and the curse of dimensionality and eventually leads to better identification of crisis events and more insightful interpretation of the results. Second, we study the structures of total spillover in the three banking systems—NA, EU, and ASEAN. While other studies such as Diebold and Yilmaz [2009] and Demirer et al. [2017] analyze a global network composed of financial institutions from many regions, we investigate individually the NA, EU and ASEAN banking systems and show that, despite the regions' geographical distances, they are affected in various degrees by major financial crisis events originated in dominant regions such as the NA and EU banking systems. Third, we perform a Granger causality and transfer entropy test on the connectedness time series generated by the improved VAR-FEVD method. This is to investigate the causal relationships among the spillover structures of the aforementioned three banking systems. To the best of our knowledge, this causality study is the first of its kind.

The intuition for using VAR framework in our analysis is that we view a banking system as an endogenous system composed of banks, each of which is subject to external shocks to itself as well as transmission of risk from the others within the system. The VAR methodology also allows for inference of systemic risk using market data such as stock returns of banks, which are available to the public. This differentiates our study from previous studies such as Furfine [2003], Upper and Worms [2004], Degryse and Nguyen [2004] which use interbank lending data which are proprietary information and inaccessible to the public. Using stock returns to infer systemic risk enables us to capture both direct and indirect connections between the banks, which we cannot achieve using interbank data as they reflect only direct connections between them.

Chapter 6

Background: Sparse models for connectedness estimation

Summary: In this chapter we provide a summary of the sparsity modeling framework called LoGo-TMFG, which is implemented in this research, and related concepts including graphical models and Gaussian Markov Random Field (GMRF). We also discuss the well-known graphical lasso algorithm and its drawbacks, which motivate us to use the LoGo-TMFG.

Common issues when dealing with large datasets are non-invertible covariance matrices and overparameterization which leads to other issues such as overfitting and unreliable estimates and forecasts. It is often the case that a model with fewer parameters has stronger predictive power and can better describe the statistical variability of data than overparameterized models. One way to obtain such a parsimonious model is to use sparsity modeling.

The idea of sparsity modeling is to keep the significant non-zero patterns (representing signal) and discard insignificant patterns (representing noise) in the full information set, whereby increasing the signal to noise ratio. In the context of our research, such patterns are the links between two nodes in a high dimensional network.

The point of departure for sparsity modeling in this research is to formulate the links or relationships between the nodes as a graphical model, specifically a GMRF. An important feature of a GMRF is the precision matrix, which describes conditional dependence of the nodes. The elements of the precision matrix are non-zero only for neighbors, i.e., nodes that are conditionally dependent, and diagonal elements. Non-neighbors or nodes that are conditionally independent are represented by zeros in the

precision matrix.

At the end of this chapter, we discuss relationships between the precision matrix and conditional covariance which will be useful for computing conditional entropy, mutual information, and transfer entropy.

6.1 Graphical models

In this section we summarize from existing literature probabilistic graphical model concepts that we use to understand the joint distribution of the random variables in our network and to measure connectedness between the variables. Connectedness in the context of this research is defined as conditional dependence between two variables, given all other variables in the network.

In graphical models, each of the variables is represented by a node (vertex), a set of nodes with certain connectedness structure is called a network (graph), and a connection between two nodes is referred to as a link (edge). The presence of a link between two variables in a graphical model means they are conditionally dependent while the absence of a link between two variables means they are conditionally independent given the other variables [Bishop, 2006].

When discussing conditional independence, we have to bear in mind that conditional independence does not equate unconditional independence. For example, if two nodes A and B are not directly linked to each other but they are linked via another node C, we can say that A and B are unconditionally dependent but are conditionally independent given C. In other words, A and B are conditionally independent given C as there is no path between A and B that does not pass through C. This conditional independence feature is a variation on the Markov property, that is, the state of a node, e.g., A, is a function only of the states of its neighbors, e.g. C, since all other nodes, e.g., B, in the graph are conditionally independent of A given the neighbors of A.

Our aim is to use graphs to represent the conditional dependence structure that best describes the relationship between variables which are the log returns of the global financial institutions. We will focus primarily on undirected graphs, which has conditional independence as described above; these graphs are commonly referred to as Markov Random Fields. More specifically, the type of Markov Random Fields that is of interest to us is the Gaussian Markov Random Field (GMRFs) which are used to

encode multivariate Gaussian distributions. The GMRFs have well-understood mathematical properties, leading to tractable analysis, simpler interpretation of results, as well as computationally efficient learning algorithms [Barfuss et al., 2016]. As a result, GMRFs are often used for modeling continuous variables in practical applications including finance, computer vision, sparse sensing, gene expression, biological neural networks, climate networks, geostatistics, and spatial statistics [Barfuss et al., 2016].

As autoregressive processes are GMRFs, the VAR-FEVD for connectedness framework described in Section 3.1 is related to the analysis of conditional dependence using sparsity modeling on a GMRF construct described in this section.

6.1.1 Gaussian Markov Random Fields (GMRFs)

A Gaussian Markov Random Fields (GMRF) or Gaussian graphical model (GGM) is a simple and widely-used construct of jointly normally distributed random variables $\boldsymbol{y} = (y_1, ..., y_p)'$ with the Markov property $y_i \perp y_j | y \setminus \{y_i, y_j\}$, that is, y_i and y_j are independent conditionally on all other variables $\{y_k, k \neq i, j\}$. The GMRF has the property that all conditional distributions are also Gaussian.

A GMRF is a major class of graphical model representing dependencies in an undirected network (i.e., the links do not carry arrows), which may be cyclic [1] [Bishop, 2006]. Given a random vector $\boldsymbol{y} = (y_1, ..., y_p)'$ with mean $\boldsymbol{\mu}$ and precision matrix $\boldsymbol{Q} > \boldsymbol{0}$ whose graph is $G = (V = \{1, ..., K\}, E)$, where V is a set of vertices $1, ...K$ and E is a set of edges $\{i, j\}$ in the graph G. The random vector $\boldsymbol{y}$ is called a GMRF if its density has the forms

$$f(\boldsymbol{y}) = (2\pi)^{-p/2} \det(\boldsymbol{Q})^{1/2} \exp\left(-\frac{1}{2}(\boldsymbol{y} - \boldsymbol{\mu})' \boldsymbol{Q} (\boldsymbol{y} - \boldsymbol{\mu})\right), \tag{6.1}$$

and $Q_{ij} \neq 0$ if and only if $\{i, j\} \in E$. In other words, y_i and y_j are conditionally independent if and only if the (i, j)th element of $\boldsymbol{Q}$ is zero [Rue and Held, 2005].

[1] This is in contrast to another major class of graphical model, the Bayesian network, which is directed and acyclic.

Elements of the precision matrix $\boldsymbol{Q}$ have the following conditional interpretations.

$$\mathbb{E}(y_i|y \setminus y_i) = \mu_i - \frac{1}{Q_{ii}} \sum_{j,j\neq i} Q_{ij}(y_j - \mu_j), \tag{6.2}$$

$$\text{Prec}(y_i|y \setminus y_i) = Q_{ii}, \tag{6.3}$$

$$\text{Corr}(y_i, y_j|y \setminus y_i) = -\frac{Q_{ij}}{\sqrt{Q_{ii}Q_{jj}}}, i \neq j \tag{6.4}$$

6.2 Sparse precision matrix estimation

Given a data matrix $\boldsymbol{Y}_{n\times p}$, which is a sample of n realizations from a p-dimensional Gaussian distribution with zero mean and positive definite covariance matrix $\boldsymbol{\Sigma}$, the traditional way to estimate a precision matrix $\boldsymbol{Q} = \boldsymbol{\Sigma}^{-1}$ under the Gaussian model is to maximize the log-likelihood of the data with respect to $\boldsymbol{Q}$,

$$l(\boldsymbol{Q}) = \log\det\boldsymbol{Q} - \text{tr}(\boldsymbol{S}\boldsymbol{Q}), \tag{6.5}$$

where $\boldsymbol{S}$ is the sample covariance matrix. This results in the maximum-likelihood estimate of $\boldsymbol{Q}$,

$$\hat{\boldsymbol{Q}} = \boldsymbol{S}^{-1} = \frac{1}{n}\left[\sum_{i=1}^{n}(\boldsymbol{y}_i - \bar{\boldsymbol{y}})(\boldsymbol{y}_i - \bar{\boldsymbol{y}})'\right]^{-1}. \tag{6.6}$$

In general, the sample covariance matrix $\boldsymbol{S}$ is a reliable estimate of the true covariance matrix when $p << n$, but when $p > n$, $\boldsymbol{S}$ is singular [Ledoit and Wolf, 2012], which means the maximum-likelihood estimate $\hat{\boldsymbol{Q}}$ cannot be computed. In the case where p is close to n, there is still a large number of parameters, i.e., $\frac{p(p+3)}{2}$ to estimate, which often results in overfitting and the sample covariance matrix $\boldsymbol{S}$ being estimated with a lot of errors [Ledoit and Wolf, 2012].

It is often the case that a model with fewer parameters has stronger predictive power and can better describe the statistical variability of data than overparameterized models. Thus, it is desirable to use a parsimonious model to describe high dimensional datasets, and in the GMRF context, one can arrive at such model by constraining a selected number of second moments. The unconstrained moments are then associated with zeros in the sparse inverse covariance matrix $\boldsymbol{Q}$.

According to Barfuss et al. [2016], there are four main approaches to learn the sparse structure of a GMRF: (1) the constraint based approach, (2) score based approach, (3) constrained optimization based approach, and (4) information filtering networks based approach. In Sections 6.2.1 and 6.2.3 below, we discuss the widely-used algorithm graphical lasso, which is a constrained optimization based approach and the novel LoGo-TMFG algorithm which is based on information-filtering networks.

6.2.1 Graphical lasso

The graphical lasso or Glasso, introduced by [Friedman et al., 2008] is arguably the most widely-used approach to estimate a sparse precision and covariance matrix. In order to understand the Glasso algorithm, we start by considering a data matrix $\boldsymbol{Y}_{n\times p}$, which is a sample of n realizations from a p-dimensional Gaussian distribution with zero mean and positive definite covariance matrix $\boldsymbol{\Sigma}$.

As previously mentioned, the task of estimating $\boldsymbol{\Sigma}$ based on the n samples when $p > n$ is not a trivial task because in the case where $p > n$, the sample covariance matrix $\boldsymbol{S}$ will be singular and the ML estimate $\hat{\boldsymbol{Q}}$ does not exist. In the case where $p \leq n$ when $\boldsymbol{S}$ is positive definite and the ordinary MLE does exist, the $\boldsymbol{Q}$ is not sparse and often poorly behaved. By trading off maximality of the log-likelihood for parsimony, the Glasso algorithm aims to find as sparse a solution as possible that still adequately explains the data [Banerjee et al., 2008].

Rather than maximizing the log-likelihood in Equation (6.5), the Glasso algorithm maximizes the ℓ_1-penalized log-likelihood,

$$l(\boldsymbol{Q}) = \log\det\boldsymbol{Q} - \operatorname{tr}(\boldsymbol{S}\boldsymbol{Q}) - \lambda\|\boldsymbol{Q}\|_1, \tag{6.7}$$

where $\boldsymbol{S} = \frac{1}{n}\sum_{i=1}^{n}(\boldsymbol{y}_i - \bar{\boldsymbol{y}})(\boldsymbol{y}_i - \bar{\boldsymbol{y}})'$ is the sample covariance matrix of $\boldsymbol{Y}$, $\bar{\boldsymbol{y}}$ is the sample mean vector, $\|\boldsymbol{Q}\|_1$ is the ℓ_1 norm, the sum of the absolute values of the elements of $\boldsymbol{Q}$. The Glasso problem is to maximize the ℓ_1-penalized log-likelihood subject to the non-negative definite precision matrix $\boldsymbol{Q}$.

In learning the structure of the GMRF $\boldsymbol{Y}$, the Glasso uses the ℓ_1 regularization to control the number of zeros (i.e., sparsity) in the precision matrix. That is, if λ is sufficiently large, the estimate $\hat{\boldsymbol{Q}}$ will be sparse due to the lasso-type penalty ℓ_1 on the elements of $\boldsymbol{Q}$. A larger value of λ corresponds to a sparser solution that fits the data

less well while a smaller λ corresponds to a solution that fits the data well but is less sparse. In addition, the ℓ_1 regularization ensures that the estimated covariance matrix is always invertible, no matter how small the ratio of sample size n to number of variables p is.

The Glasso treats the estimation of the sparse precision matrix as a constrained optimization problem and exploits the fact that there is a one-to-one correspondence between zeros in the precision matrix and absent edges in the graph. The Glasso can be solved using several optimization algorithms, however, the simplest and most widely-used one proposed by Friedman et al. [2008] is based on coordinate descent algorithm. Glasso operates on the sample covariance matrix $\boldsymbol{S}$ via block coordinate descent which maintains a positive definite covariance matrix at every row and column update. However, the estimated precision matrix is not the exact inverse of $\boldsymbol{S}$ and as a result, it is not always positive definite. Algorithms (1) and (2) [Friedman et al., 2008] illustrate the Glasso method.

Algorithm 1 Graphical lasso

1. Initialize $W = S + \lambda I$. The diagonal of W remains unchanged in what follows.
2. Repeat for $j = 1, 2, \ldots p, 1, 2, \ldots p, \ldots$ until convergence:
   i. Partition the matrix W into part 1: all but the j-th row and column, and part 2: the j-th row and column,
   ii. Solve the estimating equations $W_{11}\beta - s_{12} + \lambda.\text{Sign}(\beta) = 0$ using the pathwise coordinate-descent algorithm for the modified lasso defined in Algorithm (2),
   iii. Update $w_{12} = W_{11}\hat{\beta}$.
3. In the final cycle (for each j), solve for $\hat{q}_{12} = -\hat{\beta}.\hat{q}_{22}$, with $\frac{1}{\hat{q}_{22}} = w_{22} - w'_{12}\hat{\beta}$.

Algorithm 2 Pathwise coordinate descent for graphical lasso

1. Let $V = W_{11}$, the update has the form
2. For $j = 1, 2, \ldots, p-1, 1, 2, \ldots, p-1, \ldots,$

$$\hat{\beta}_j \leftarrow \frac{\tau\left(s_{12j} - \sum_{k \neq j} V_{kj}\hat{\beta}_k, \lambda\right)}{V_{jj}} \tag{6.8}$$

where τ is the soft-threshold operator $\tau(x,t) = \text{sign}(x)(|x| - t)_+$.

6.2.2 Critiques of graphical lasso

Despite being the most well-known sparsity algorithm, the Glasso share similar drawbacks with other ℓ_1-based methods. Relevant to this research is the fact that the Glasso is generally unreliable with respect to larger networks and tends to yield overly sparsified or disconnected graphs. Heinavaara et al. [2016] analyzed real gene expression data and showed that (1) all ℓ_1-based methods fail dramatically for models with nearly linear dependencies between the variables and (2) all ℓ_1-based methods become unreliable for larger networks. Zhao and Yu [2006] concluded that ℓ_1 penalization shrinks the estimates for non-zero values too heavily such that true non-zero values are often wrongly pushed toward zero.

In addition, Glasso is less computationally efficient than information filtering network-based algorithms such as LoGo-TMFG Barfuss et al. [2016] described in the next section. This is due to the fact that Glasso constructs the global sparse network from a full covariance matrix while LoGo-TMFG does so from summing the local sparse precision matrices.

6.2.3 Novel sparsity algorithm: LoGo-TMFG

An alternative approach to estimate inference models, proposed by Barfuss et al. [2016], is called LoGo (Local Global). The LoGo combines information filtering networks such as triangulated maximally planar graphs (TMFG) or minimum spanning trees (MST) with GMRFs in order to estimate the global sparse inverse covariance from a simple sum of local inverse covariances computed on small sub-parts of the network. The fact that the LoGo algorithm breaks down a large problem involving a large matrix into small problems involving much smaller matrices makes it particularly suitable to analyze high dimensional datasets whose correlation matrices are not invertible.

The LoGo algorithm is statistically robust and computationally efficient as it is based on local, low-dimensional inversions, allowing parallel computations and partial updating when the properties of some variables change without having to recompute the entire model. Compared to the Glasso, the LoGo is much less computationally intensive and yields comparable or better maximum likelihood results [Barfuss et al., 2016].

Barfuss et al. [2016] discuss two variants of the LoGo algorithm, namely the

LoGo-TMFG and the LoGo-MST. Both the LoGo-TMFG and LoGo-MST are sparsity structure estimation algorithms which constructs a global sparse network from the sums of small, local networks; however, the difference is that the LoGo-TMFG builds a network from triangulated planar graphs (TMFG) while the LoGo-MST does so from minimum spanning trees (MSTs). The following section summarizes the LoGo-TMFG algorithm which is a main methodology used in the experiments in Chapters 7 and 8.

6.2.3.1 Triangulated maximally planar graph (TMFG)

In the LoGo-TMFG algorithm, a network is represented by a triangulated graph (or chordal graph) which is a type of planar graph [2], in which every cycle of length four and greater has a cycle chord. The network is made up of four-node cliques (4-cliques) and separators which are three-node cliques (3-cliques). By representing a network as a system comprising 4-cliques and 3-cliques, we reduce the inversion of a high dimensional matrix into a sum of inversions of matrices corresponding to the 4-cliques and 3-clique separators [Barfuss et al., 2016].

Given the triangulated graph as our network, we can write the joint probability density function for our data, which are the set of p variables $\boldsymbol{Y} = (\boldsymbol{y}_1, ..., \boldsymbol{y}_p)'$, in terms of the following factorization into cliques and separators,

$$f(\boldsymbol{Y}) = \frac{\prod_{m=1}^{M} f_{\mathscr{C}_m}(\boldsymbol{Y}_{\mathscr{C}_m})}{\prod_{n=1}^{M-1} f_{\mathscr{S}_n}(\boldsymbol{Y}_{\mathscr{S}_n})^{k(\mathscr{S}_n)-1}}. \tag{6.9}$$

where $f_{\mathscr{C}_m}(\boldsymbol{Y}_{\mathscr{C}_m})$ and $f_{\mathscr{S}_n}(\boldsymbol{Y}_{\mathscr{S}_n})$ are the marginal probability density functions of the variables constituting the clique $\mathscr{C}_m$ and the separator $\mathscr{S}_n$. $k(\mathscr{S}_n)$ counts the number of disconnected components produced by removing the separator $\mathscr{S}_n$ and is therefore equal to the degree of the separator in the clique tree.

In the context of LoGo-TMFG, we start by computing a triangulated graph from a tetrahedron and inserting recursively vertices inside existing triangles (T2 move) in order to approximate a maximal planar graph with the largest total weight. Then we use the local inversion formula in Equation 6.10 to estimate the sparse inverse covariance

[2] A planar graph is a graph that can be embedded in the plane in such a way that its edges do not cross one another but intersect only at their endpoints.

matrix J using as inputs cliques and separators from the triangulated planar graph.

$$J_{i,j} = \sum_{\mathscr{C}\,\text{s.t.}\,\{i,j\}\in\mathscr{C}} \left(\boldsymbol{S}_{\mathscr{C}}^{-1}\right)_{i,j} - \sum_{\mathscr{S}\,\text{s.t.}\,\{i,j\}\in\mathscr{S}} (k(\mathscr{S})-1)\left(\boldsymbol{S}_{\mathscr{S}}^{-1}\right)_{i,j}, \tag{6.10}$$

where S is sample covariance matrix and $J_{i,j} = 0$ if $\{i, j\}$ are both not a part of a common clique. Equation (6.10) is a simple formula that reduces the global problem of a $p \times p$ matrix inversion to a sum of local inversions of matrices whose dimensions are the sizes of the cliques $\mathscr{C}_m$ and separators $\mathscr{S}_n$. In other words, only four observations are enough to produce a non-singular global estimate of the inverse covariance using triangulated maximally planar graph (TMFG).

In order to construct a model that is closest to what is observed, we search for the set of parameters, $\boldsymbol{J}$, associated with the largest likelihood of observing the observations $\{y_{11},...,y_{1q}\},\{y_{21},...,y_{2q}\}....,\{y_{p1},...,y_{pq}\}$. The log-likelihood of the model distribution function, $f(\boldsymbol{Y})$, with parameters $\boldsymbol{J}$, is associated with the empirical estimate of the covariance matrix $\boldsymbol{S}$ as follows.

$$\log l(\boldsymbol{J}) = \frac{n}{2}\left(\log\det(\boldsymbol{J}) - \operatorname{tr}(\boldsymbol{SJ}) - p\log(2\pi)\right) \tag{6.11}$$

One can show that for all decomposable graphs, following Equation (6.10), $\operatorname{tr}(\boldsymbol{SJ}) = p$. This makes maximizing Equation (6.11) simpler as the maximization problem reduces to maximizing $\log\det(\boldsymbol{J})$,

$$\log\det(\boldsymbol{J}) = \sum_{n=1}^{M-1} (k(\mathscr{S})-1)\log\det(\boldsymbol{S}_{\mathscr{S}_n}) - \sum_{m=1}^{M} \log\det(\boldsymbol{S}_{\mathscr{C}_m}) \tag{6.12}$$

From Algorithm (3) [Barfuss et al., 2016] we see that the algorithm constructs a triangulated graph initially with a tetrahedron, $\mathscr{C}_1 = \{v_1, v_2, v_3, v_4\}$ whose correlation determinant $\det(\boldsymbol{R}_{\mathscr{C}_1})$ is the smallest. Then we iteratively introduce inside existing triangular faces the vertex that maximizes $\log\det(\boldsymbol{R}_{\mathscr{S}})\log\det(\boldsymbol{R}_{\mathscr{C}})$ where $\mathscr{C}$ and $\mathscr{S}$ are the new clique and separator created by the vertex insertion. The LoGo-TMFG algorithm produces a $3(p-2)$-edged decomposable graph, which is a clique-tree comprising four-cliques which are connected by three-clique separators. For LoGo-TMFG, $k(\mathscr{S}_n)$ always equals 2.

Algorithm 3 LoGo-TMFG

Input: A sample covariance matrix $\boldsymbol{S} \in \mathbb{R}^{p\times p}$ and the associated correlation matrix $\boldsymbol{R} \in \mathbb{R}^{p\times p}$

Output: $\boldsymbol{J}$ a sparse estimation of the inverse covariance matrix

1. $\boldsymbol{J} \leftarrow 0$ Initialize $\boldsymbol{J}$ with zero elements.
2. $\mathscr{C}_1 \leftarrow$ Tetrahedron, $\{v_1, v_2, v_3, v_4\}$, with the smallest $\det\left(\boldsymbol{R}_{\mathscr{C}_1}\right)$
3. $\mathscr{T} \leftarrow$ Assign to $\mathscr{T}$ the four triangular faces in $\mathscr{C}_1 : \{v_1, v_2, v_3\}, \{v_1, v_2, v_4\}, \{v_1, v_4, v_3\}, \{v_4, v_2, v_3\}$.
4. $\mathscr{V} \leftarrow$ Assign to $\mathscr{V}$ the remaining $p-4$ vertices not in $\mathscr{C}_1$.
5. While $\mathscr{V}$ is not empty, do:

   i. Find the combination of $\{v_a, v_b, v_c\} \in \mathscr{T}$ and $v_d \in \mathscr{V}$ with the largest $\frac{\det\left(\boldsymbol{R}_{\{v_a,v_b,v_c\}}\right)}{\det\left(\boldsymbol{R}_{\{v_a,v_b,v_c,v_d\}}\right)}$. Note that $\{v_a, v_b, v_c, v_d\}$ is a new 4-clique $\mathscr{C}$, $\{v_a, v_b, v_c\}$ becomes a separator $\mathscr{S}$, three new triangular faces, $\{v_a, v_b, v_d\}$, $\{v_a, v_c, v_d\}$, and $\{v_b, v_c, v_d\}$ are created.

   ii. Remove v_d from $\mathscr{V}$.

   iii. Remove $\{v_a, v_b, v_c\}$ from $\mathscr{T}$.

   iv. Add $\{v_a, v_b, v_d\}, \{v_a, v_c, v_d\}, \{v_b, v_c, v_d\}$ to $\mathscr{T}$.

   v. Compute $J_{i,j} = J_{i,j} + \left(S^{-1}_{\{v_a,v_b,v_c,v_d\}}\right)_{i,j} - \left(S^{-1}_{\{v_a,v_b,v_c\}}\right)_{i,j}$.

6.3 Inverse covariance matrix & conditional covariance

The precision matrix has elements that are conditional dependencies of the variables. If variables X_i and X_j are from multivariate normal distribution, and the (i, j)th element in the precision matrix is zero, we then have that X_i and X_j are conditionally independent given all other variables [Friedman et al., 2008].

Via Schur complement, the inverse of a block within the precision matrix provides conditional covariances of the variables in the block given all other variables. The joint covariance matrix of two multivariate random variables $\boldsymbol{X} \in \mathbb{R}^n$ and $\boldsymbol{Y} \in \mathbb{R}^m$ is $\boldsymbol{\Sigma}_{X,Y} = \begin{bmatrix} \boldsymbol{\Sigma}_{XX} & \boldsymbol{\Sigma}_{XY} \\ \boldsymbol{\Sigma}_{YX} & \boldsymbol{\Sigma}_{YY} \end{bmatrix}$. The block $\boldsymbol{\Sigma}_{XX} \in \mathbb{R}^{n\times n}$ is the variance matrix of $\boldsymbol{X}$, $\boldsymbol{\Sigma}_{YY} \in \mathbb{R}^{m\times m}$ is the variance matrix of $\boldsymbol{Y}$, $\boldsymbol{\Sigma}_{XY} \in \mathbb{R}^{n\times m}$ is the covariance matrix between $\boldsymbol{X}$ and $\boldsymbol{Y}$, and $\boldsymbol{\Sigma}_{YX} \in \mathbb{R}^{m\times n}$ is the covariance matrix between $\boldsymbol{Y}$ and $\boldsymbol{X}$, which is equal to the transpose of $\boldsymbol{\Sigma}_{XY}$.

The conditional covariance of $\boldsymbol{Y}$ given $\boldsymbol{X}$ is the Schur complement of $\boldsymbol{\Sigma}_{XX}$ in $\boldsymbol{\Sigma}_{X,Y}$,

$$\boldsymbol{\Sigma}_{Y|X} = \boldsymbol{\Sigma}_{YY} - \boldsymbol{\Sigma}_{YX}\boldsymbol{\Sigma}_{XX}^{-1}\boldsymbol{\Sigma}_{XY}. \tag{6.13}$$

Similarly, the conditional covariance of $\boldsymbol{X}$ given $\boldsymbol{Y}$ is the Schur complement of $\boldsymbol{\Sigma}_{YY}$ in $\boldsymbol{\Sigma}_{X,Y}$, $\boldsymbol{\Sigma}_{X|Y} = \boldsymbol{\Sigma}_{XX} - \boldsymbol{\Sigma}_{XY}\boldsymbol{\Sigma}_{YY}^{-1}\boldsymbol{\Sigma}_{YX}$. Given a precision matrix $\boldsymbol{J}$ and its counterpart covariance matrix $\boldsymbol{\Sigma}_{X,Y}$, both of which can be partitioned into block matrices. Using block matrix inversion, the relationship between $\boldsymbol{J}$ and $\boldsymbol{\Sigma}_{X,Y}$ is as follow.

$$\boldsymbol{\Sigma}_{X,Y} = \boldsymbol{J}^{-1} = \begin{bmatrix} J_{11} & J_{12} \\ J_{21} & J_{22} \end{bmatrix}^{-1} = \begin{bmatrix} (J_{11} - J_{12}J_{22}^{-1}J_{21})^{-1} & -J_{11}^{-1}J_{12}(J_{22} - J_{21}J_{11}^{-1}J_{12})^{-1} \\ -(J_{22} - J_{21}J_{11}^{-1}J_{12})^{-1}J_{21}J_{11}^{-1} & (J_{22} - J_{21}J_{11}^{-1}J_{12})^{-1} \end{bmatrix}. \tag{6.14}$$

$$J = \boldsymbol{\Sigma}_{X,Y}^{-1} = \begin{bmatrix} \boldsymbol{\Sigma}_{XX} & \boldsymbol{\Sigma}_{XY} \\ \boldsymbol{\Sigma}_{YX} & \boldsymbol{\Sigma}_{YY} \end{bmatrix}^{-1} = \begin{bmatrix} (\Sigma_{XX} - \Sigma_{XY}\Sigma_{YY}^{-1}\Sigma_{YX})^{-1} & -\Sigma_{XX}^{-1}\Sigma_{XY}(\Sigma_{YY} - \Sigma_{YX}\Sigma_{XX}^{-1}\Sigma_{XY})^{-1} \\ -(\Sigma_{YY} - \Sigma_{YX}\Sigma_{XX}^{-1}\Sigma_{XY})^{-1}\Sigma_{YX}\Sigma_{XX}^{-1} & (\Sigma_{YY} - \Sigma_{YX}\Sigma_{XX}^{-1}\Sigma_{XY})^{-1} \end{bmatrix}. \tag{6.15}$$

Putting together Equation (6.14) and Equation (6.15), we can see that

$$\Sigma_{Y|X} = (J_{22})^{-1} = \Sigma_{YY} - \Sigma_{YX}\Sigma_{XX}^{-1}\Sigma_{XY}. \tag{6.16}$$

The unconditional covariance of Y can be computed from either the large matrix J^{-1}, $\Sigma_{YY} = (J^{-1})_{22}$, or via Schur complement using blocks of J^{-1}, $\Sigma_{YY} = (J_{22} - J_{21}J_{11}^{-1}J_{12})^{-1}$. We can use the equality between conditional covariances and inverses of blocks within a precision matrix in computing mutual information and transfer entropy. The mutual information $I(X;Y)$ in Equation (4.16) can be computed from the determinants of $\Sigma_{Y|X}$ and Σ_Y, via the identity $|M^{-1}| = \frac{1}{|M|}$:

$$I(X;Y) = \frac{1}{2}(\log|(J_{22} - J_{21}J_{11}^{-1}J_{12})^{-1}| - \log|(J_{22})^{-1}|), \tag{6.17}$$

$$= \frac{1}{2}\left(\log|J_{22}| - \log|J_{22} - J_{21}J_{11}^{-1}J_{12}|\right). \tag{6.18}$$

The transfer entropy $TE(X \to Y) = \frac{1}{2}(\log|\Sigma_{Y|Y^-}| - \log|\Sigma_{Y|Y^-,X^-}|)$ in Equation (4.17) can

be computed by applying Schur's complement on the joint covariance matrix $\Sigma_{X^-,Y^-,Y}$ and its corresponding precision matrix J,

$$\Sigma_{X^-,Y^-,Y} = \begin{bmatrix} \Sigma_{X^-,X^-} & \Sigma_{X^-,Y^-} & \Sigma_{X^-,Y} \\ \Sigma_{Y^-,X^-} & \Sigma_{Y^-,Y^-} & \Sigma_{Y^-,Y} \\ \Sigma_{Y,X^-} & \Sigma_{Y,Y^-} & \Sigma_{Y,Y} \end{bmatrix} = J^{-1} = \begin{bmatrix} J_{11} & J_{12} & J_{13} \\ J_{21} & J_{22} & J_{23} \\ J_{31} & J_{32} & J_{33} \end{bmatrix}^{-1}. \tag{6.19}$$

The covariance matrix of Y conditional on the past values of Y and X is:

$$\Sigma_{Y|X^-,Y^-} = J_{33}^{-1}. \tag{6.20}$$

The joint covariance matrix of Y and the past of and X, conditional on the past of Y is:

$$\Sigma_{X^-,Y|Y^-} = \begin{bmatrix} J_{11} & J_{13} \\ J_{31} & J_{33} \end{bmatrix}^{-1}. \tag{6.21}$$

The covariance matrix of Y conditional on the past of Y is the following

$$\Sigma_{Y|Y^-} = \left(J_{33} - J_{3,1} J_{1,1}^{-1} J_{1,3}\right)^{-1} \tag{6.22}$$

Chapter 7

Empirical analysis: Sparse regional network construction using LoGo-TMFG

Summary: In this chapter we use a novel sparsity algorithm called LoGo-TMFG, proposed by Barfuss et al. [2016], to quantify connectedness in the global financial network comprising all publicly listed financial institutions in ten economic regions of the world. The necessity for sparsification arises from the fact that our global financial network datasets are wide, i.e., the sample size is much smaller than the number of variables.

Combining sparsity modeling with well-known information theoretic measures such as mutual information and transfer entropy, we learn about the global financial network and analyze the interactions between them. In addition, we propose two metrics based on transfer entropy called "impact" and "vulnerability," which measure, respectively, how much one region affects another and how much one region is affected by another.

Our global financial network comprises financial institutions in the financial sector in ten economic regions of the world. We perform both full-sample and rolling-window analyses. Our two full-sample datasets cover the period from 1990 to 1999 and from 2000 to 2016, containing respectively 914 and 1,127 financial companies that were active throughout the respective sample periods. Our rolling-window datasets comprise twenty five rolling windows, each of which comprises three years of daily returns for

a large number of financial companies, i.e., from 1,680 companies in the 1990-1992 window to 4,310 companies in the 2014-2016 window.

For comparison, we use graphical lasso which is the well-known sparsity algorithm on our datasets, yielding disconnected graphs in which none of the financial institutions is connected to the others, which we believe is unrealistic. The underperformance of graphical lasso when used on our datasets supports the findings in Zhao and Yu [2006] and Heinavaara et al. [2016] who conclude that ℓ_1-based methods generally become unreliable for larger networks and graphical lasso often wrongly pushes true non-zero elements toward zero.

7.1 Methodology

7.1.1 The LoGo-TMFG algorithm

The LoGo-TMFG proposed by Barfuss et al. [2016] combines the triangulated maximally planar graphs (TMFG), which is an information filtering network, with a Gaussian graphical model (GGM) and estimates the global sparse inverse covariance by simply summing up the local inverse covariances computed on small sub-parts of the network. In the LoGo-TMFG algorithm, a high-dimensional network is broken down into four-node cliques (4-cliques) and three-node cliques (3-cliques) which are called separators. By representing a network as a system comprising 4-cliques and 3-cliques, our high-dimensional matrix inversion problem is reduced into a sum of inversions of small matrices corresponding to the 4-cliques and 3-cliques. In other words, our global network is obtained from computing the sum of local networks, hence the name LoGo. The implementation of the LoGo-TMFG algorithm is outlined in Algorithm 3 in Chapter 6. After the sparse inverse covariance matrix J is estimated using LoGo-TMFG, we use it as input to compute conditional mutual information and conditional transfer entropy for each economic region of the global network.

7.1.2 Conditional mutual information and conditional transfer entropy

We analyze a network which comprises three sets of variables $\{X, Y, W\}$, where X can be viewed as stock returns of companies in Region X, Y as stock returns of companies in Region Y, and W as stock returns of companies in Region W, respectively. The

entropy of X conditioned on Y is given by

$$H(X|Y) = \frac{1}{2} log(2\pi e)^m |\Sigma_{X|Y}|, \tag{7.1}$$

where m is the dimension of $\Sigma_{X|Y}$. The precision matrix or inverse of the covariance matrix of X conditioned on Y is given by

$$\Sigma^{-1}_{X|Y} = J(X,X) - J(X,W)J(W,W)^{-1}J(W,X), \tag{7.2}$$

where $J(i,j)$ is the precision matrix associated with Region i and Region j. The mutual information between X and Y conditioned on W is given by

$$I(X,Y|W) = H(X|W) - H(X|Y,W), \tag{7.3}$$

where $H(X|W)$ and $H(X|Y,W)$ are conditional entropies. The transfer entropy from X to Y conditioned on the rest of the variables in the system W, denoted $TE(X \to Y|W)$ is the mutual information between the past of X and present of Y conditioned on the past of Y and present of W,

$$TE(X \to Y|W) = I(X-,Y|W,Y-) = H(Y|W,Y-) - H(Y|W,Y-,X-). \tag{7.4}$$

Conditional mutual information and conditional transfer entropy allows us to estimate, respectively, the contemporaneous and temporal links between two variables with the effect from a third variable removed. In this way we can truly focus on measuring the link that reflects direct relationship between the two variables of interest, which is not driven by another variable being present in the system.

7.2 Economic regions of the world

In this section we provide a description of the data used in estimation of the sparse global financial network over the period from 1990 to 2016 which covers many major crisis episodes including the Mexican economic crisis of 1994, the Asian financial crisis of 1997-1998, the Russian financial crisis of 1998, the Dotcom bubble of 1999-2000, the global financial crisis of 2007-2008, and the eurozone crisis of 2009-2014.

From Compustat North America and Compustat Global databases, we obtained daily prices from 1990 to 2016 for companies in the financial sector from 117 countries globally. We then adjusted the closing prices for events such as stock splits using the total adjustment factor provided by Compustat and computed log returns for each stock. We take as a guideline the World Bank's categorization of economic regions to divide the countries into economic regions, however with two modifications. First, we split the World Bank's "Asia and Pacific" region into three regions, namely East Asia, Southeast Asia, and Australia to better reflect the regions' economic diversity. For the same reason as above, we divide the World Bank's "Europe and Central Asia" into Europe and West Asia. Table 7.1 provides the list of economic regions, number of countries and the names of the countries in each economic region in our sample.

In our research we analyzed the full-sample datasets as well as rolling-window datasets where each window covers a period of three years (750 trading days). While our two full-sample datasets allow us to look at connectedness over the corresponding sample periods in aggregate, our rolling-window datasets provide an opportunity to analyze the time-varying dynamic of connectedness. In several ways the rolling-window datasets make up for the limitations associated with the longer full-sample datasets. That is, the full-sample datasets include only companies that are alive for decades but exclude companies that are new, short-lived or bankrupt, which most likely have had significant contributions to connectedness and systemic risk. As such, analyzing datasets which contain only companies that are active over a long time period often leads to a survival bias, which in turn leads to false conclusions in several ways.

Our two full-sample datasets cover the periods from 1990 to 1999 and from 2000 to 2016, containing 914 and 1,127 financial companies that are active throughout the respective sample periods. Our rolling-window datasets comprise twenty five rolling windows, each of which features three years of daily returns for a large number of financial companies, i.e., between 1,680 companies in the 1990-1992 window to 4,310 in the 2014-2016 window. The rich datasets in our study are one of the key features of our research that make our contribution unique; to the best of our knowledge, published research to date that empirically measures financial connectedness has not used datasets of this size.

Table 7.1: List of countries in each economic region

	Code	Region	Number of countries	Country
1.	NA	North America	3	Bermuda, Canada, United States
2.	SA	South America	17	Argentina, Bahamas, Barbados, Brazil, Belize, Cayman Islands, Chile, Colombia, Ecuador, Jamaica, Mexico, Panama, Peru, Peuto Rico, Trinidad and Tobago, Venezuela, Virgin Islands
3.	AF	Africa	14	Boswana, Cote d'Ivoire, Ghana, Kenya, Malawi, Mauritius, Namibia, Nigeria, Senegal, South Africa, Tanzania, Uganda, Zambia, Zimbabwe
4.	EU	Europe	35	Austria, Belgium, Bulgaria, Switzerland, Cyprus, Czech Republic, Germany, Denmark, Spain, Estonia, Finland, France, Great Britain, Guernsey, Greece, Greenland, Croatia, Hungary, Ireland, Italy, Jersey, Liechtenstein, Lithuania, Luxembourg, Monaco, Malta, Netherlands, Norway, Poland, Portugal, Romania, Serbia, Slovakia, Slovenia, Sweden
5.	ASW	West Asia	5	Georgia, Kazakhstan, Russia, Turkey, Ukraine
6.	ME	Middle East	16	Algeria, Bahrain, Egypt, Iran, Iraq, Israel, Jordan, Kuwait, Lebanon, Morocco, Oman, Palestine, Qatar, Saudi Arabia, Tunisia, United Arab Emirates
7.	ASS	South Asia	8	Afghanistan, Bangladesh, Bhutan, India, Maldives, Nepal, Pakistan, Sri Lanka
8.	ASE	East Asia	6	China, Hong Kong, Japan, Korea, Macau, Taiwan
9.	ASSE	Southeast Asia	10	Brunei, Burma, Cambodia, Indonesia, Laos, Malaysia, Philippines, Singapore, Thailand, Vietnam
10.	AU	Australia	3	Australia, New Zealand, Papua New Guinea

7.3 Full-sample analysis

Table 7.2 shows the number of financial companies in each of the ten economic regions of the world for the the 1990-1999 and 2000-2016 full-sample periods. In 1990-1999, North America had the largest number of financial companies (530), followed by East Asia (173), and Europe (150) and the bottom three with respect to number of financial companies were West Asia (2), the Middle East (1) and South Asia (2). In 2000-2016, North America had the largest number of financial companies (586), followed by Europe (233), and East Asia (176) and the bottom three with respect to number of financial companies were the Middle East (2), West Asia (14), South America (15),

Table 7.2: Number of financial companies in each of the ten economic regions of the world for the 1990-1999 and 2000-2016 full-sample datasets

	Region	1990-1999	2000-2016
1.	North America	530	586
2.	South America	4	15
3.	Africa	5	15
4.	Europe	150	233
5.	West Asia	2	14
6.	Middle East	1	2
7.	South Asia	2	24
8.	East Asia	173	176
9.	Southeast Asia	36	47
10.	Australia	11	15
	Total	914	1127

Africa (15), and Australia (15).

It is worth mentioning that the full samples exclude companies that were alive for less than the durations of the sample periods. Hence, the full samples exclude companies that were bankrupt which may have had significant contribution to volatility, connectedness and systemic risk.

Figure 7.1(a) and Figure 7.1(b) illustrate the topology graphs of the financial companies that were active in 1990-1999 and in 2000-2016 full-sample periods, respectively. The links in the graph correspond to non-zero values in the sparse inverse covariance matrices for the corresponding periods, estimated using the LoGo-TMFG algorithm, implying the existence of conditional dependence between pairs of variables. In other words, the presence of a link indicates contemporaneous relationship between a pair of nodes, conditioned on all other nodes. In both figures, clusters of companies with strong relationship are represented by groups of nodes that are pulled in closer to one another. It appears that as the number of financial companies increased from 914 companies in 1990-1999 to 1,127 companies in 2000-2016, so did the number and size of clusters.

Figure 7.2(a) and Figure 7.2(b) illustrate the **conditional mutual informations** of the ten economic regions in 1990-1999 and in 2000-2016 respectively. We grouped 914 financial companies in 1990-1999 and 1,127 financial companies in 2000-2016 by economic regions and computed conditional mutual information between a pair of

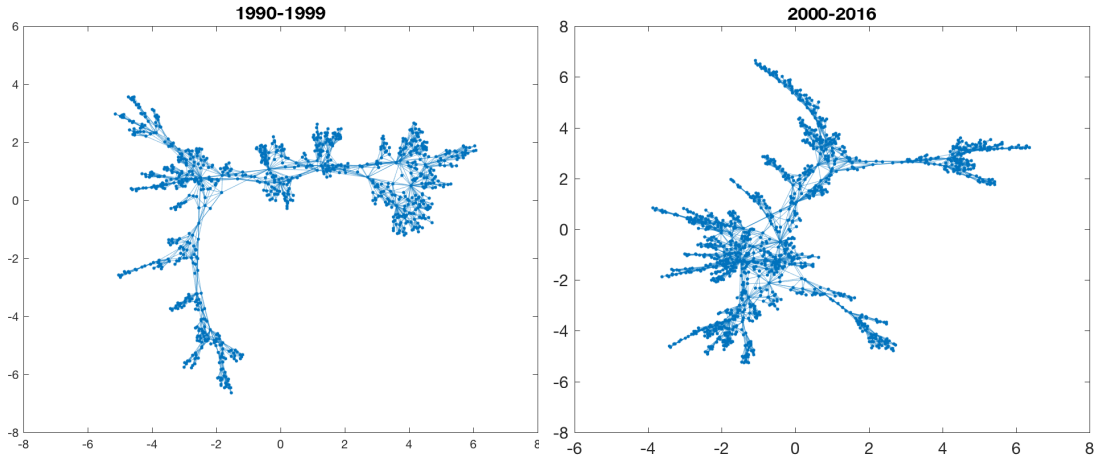

(a) Sparse network of 914 financial companies in 1990-1999

(b) Sparse network of 1,127 financial companies in 2000-2016

Figure 7.1: Sparse network of global financial companies in 1990-1999 and 2000-2016, constructed from the non-zero entries in the sparse inverse covariance matrix estimated using the LoGo-TMFG algorithm.

economic regions conditioned on all other regions, using as input the sparse inverse covariance matrix, which had been estimated using the LoGo-TMFG algorithm on weekly log returns of the financial companies.

North America and Europe had the strongest link because the conditional mutual information between the two regions was the highest followed by that between Europe and East Asia, both in 1990-1999 and in 2000-2016. The link between North America and Europe weakened overtime, provided that the mutual information between the two regions decreased to 1.48 in 2000-2016 from 4.96 in 1990-1999. Similarly, the link between Europe and East Asia weakened over time (0.86 in 1990-1999 and 0.33 in 2000-2016). On the contrary, North America and South America became more interconnected over time (0.01 in 1990-1999 and 0.27 in 2000-2016).

Figure 7.3(a) and Figure 7.3(b) plot the **conditional transfer entropies** for the ten economic regions of the world in 1990-1999 and in 2000-2016 respectively. The conditional transfer entropy was computed using as input the sparse inverse covariance matrix, which had been estimated using the LoGo-TMFG algorithm on weekly log returns of the financial companies. The thickness of the line corresponds to the magnitude of the link between the regions. In general, the economic regions were more interconnected in the 2000-2016 period than in the the 1990-1999 period, provided

that the magnitudes and number of the links between regions in the 2000-2016 sample are greater than those in the 1990-1999 sample. It is worth nothing that mutual information represents **contemporaneous** connectedness while transfer entropy represents **temporal** connectedness.

Table 7.3 and Table 7.4 summarize the transfer entropies from an economic region to the rest and vice versa for the periods of 1990-1999 and 2000-2016 respectively. In 1990-1999, the three most impactful economic regions are North America, East Asia, and Europe and the three most vulnerable economic regions are Europe, East Asia, and North America. In 2000-2016, the three most impactful economic regions are North America, Europe, and South America and the three most vulnerable economic regions are Europe, North America, and South America. The emergence of South America, despite having a small number of financial companies (15), reflects the new economic era of the region in the 2000s which is characterized by steady and high economic growth. According to Garry and Carlos Moreno-Brid [2015], Real GDP growth of South America grew on average 1.8 percent in the 1980s, climbed to 3.1 percent in the 1990s and further expanded to 3.6 percent over the period from 2000-08. In the wake of the global financial crisis, South America's quick recovery in 2010, with a real GDP growth of 6.3 percent, was evidence of the region's solid macroeconomic foundations. As mentioned previously, the full samples include only companies that were alive for the entire durations of the sample periods and exclude companies that were bankrupt which may have had significant contribution to connectedness and systemic risk. As a consequence, the results are subject to the survival bias and one should interpret them with caution.

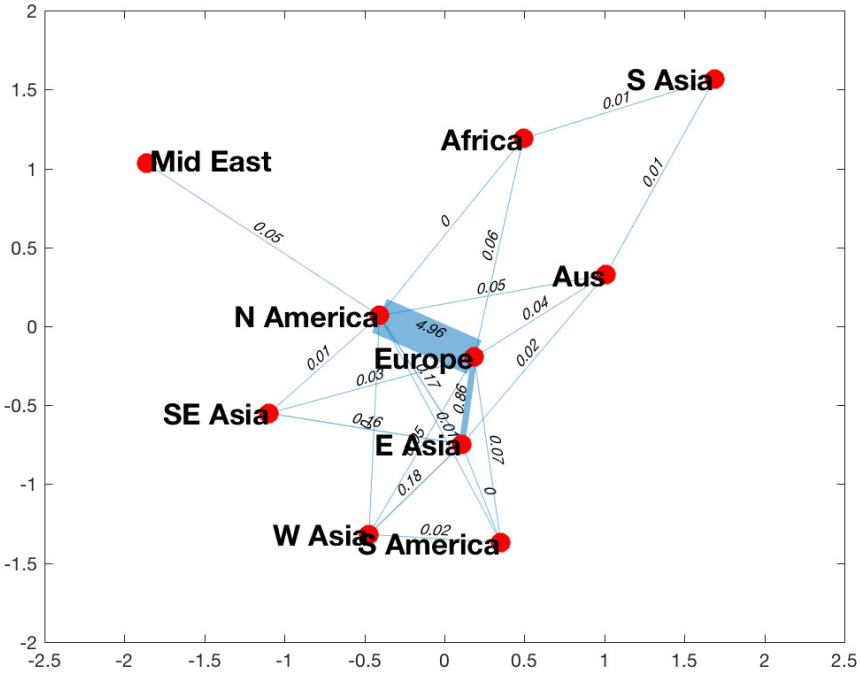

(a) Mutual information between economic regions of the world in 1990-1999

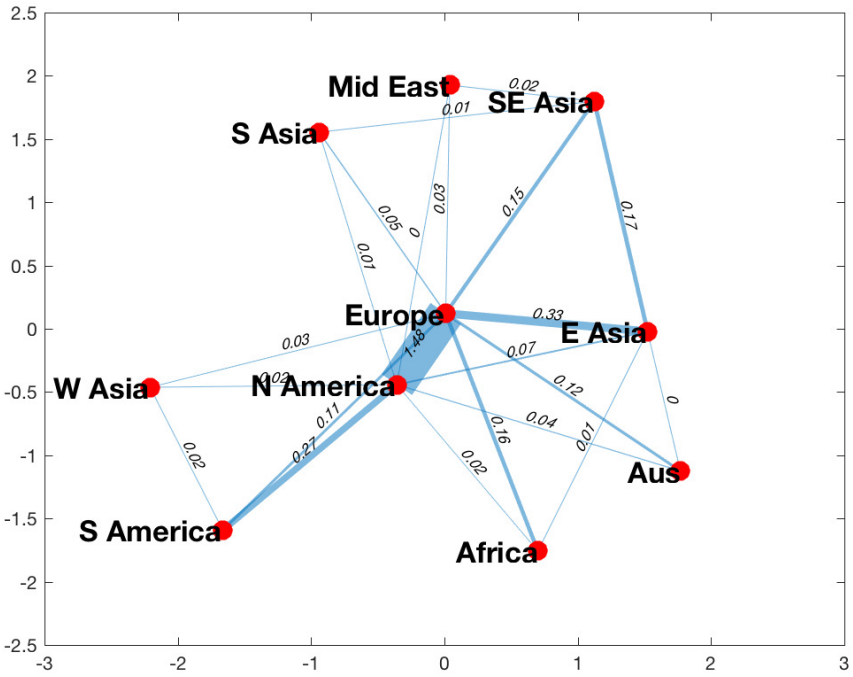

(b) Mutual information between economic regions of the world in 2000-2016

Figure 7.2: Mutual information between the ten economic regions between in 1990-1999 and 2000-2016. We grouped 914 financial companies in 1990-1999 and 1,127 financial companies in 2000-2016 by economic regions and computed conditional mutual information between a pair of economic regions using as input the sparse inverse covariance matrix, which had been estimated via the LoGo-TMFG algorithm.

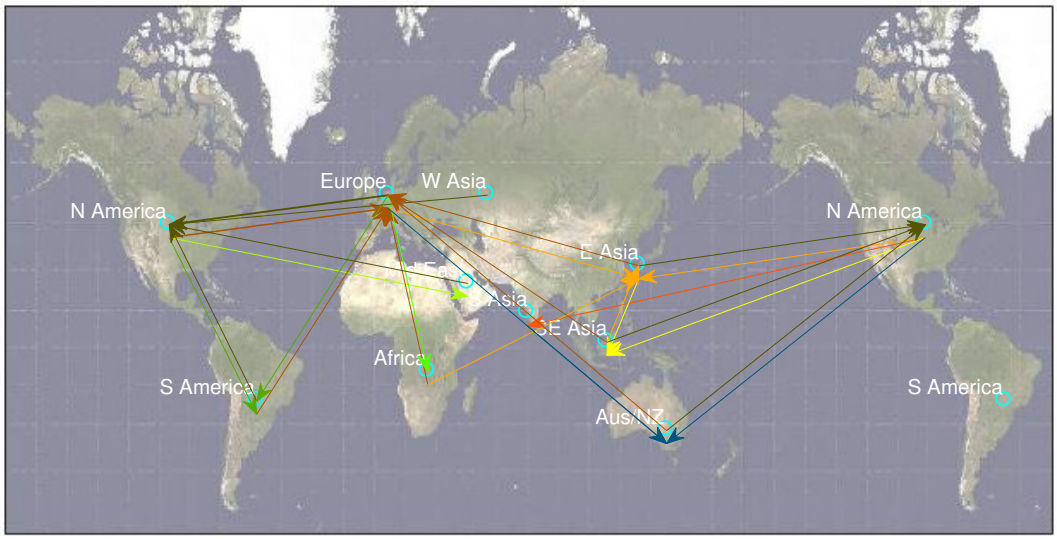

(a) Conditional transfer entropy in 1990-1999

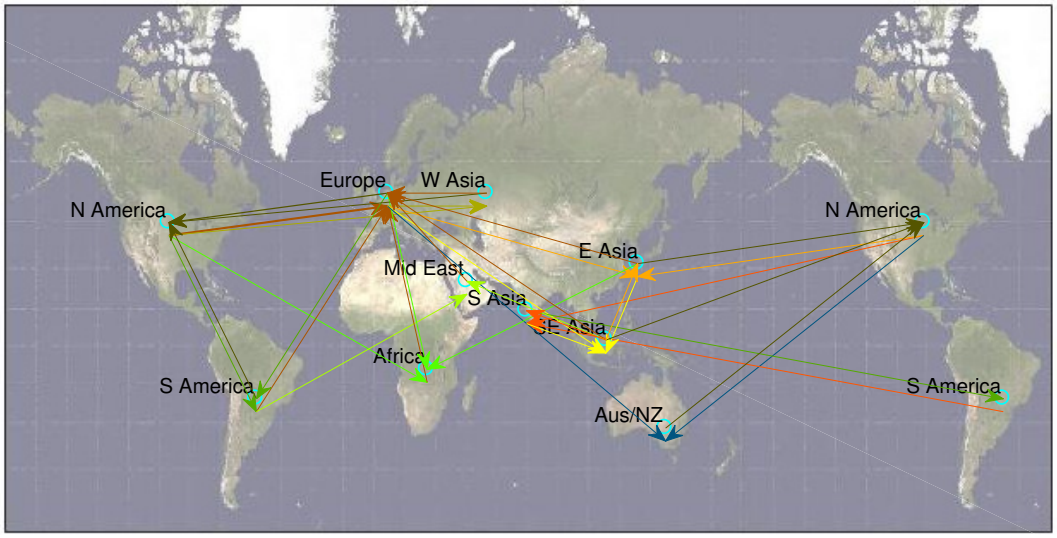

(b) Conditional transfer entropy in 2000-2016

Figure 7.3: Conditional transfer entropy between the ten economic regions during the full-sample periods of 1990-1999 and 2000-2016, using as input the sparse inverse covariance matrix, which had been estimated via the LoGo-TMFG algorithm.

Table 7.3: Transfer entropy from each region to the rest and from the rest to each region during the 1990-1999 period computed from the sparse inverse covariance matrix estimated using LoGo-TMFG algorithm.

	region → rest	**TE**	**rest → region**	**TE**
1.	N America → rest	0.123	rest → N America	0.139
2.	S America → rest	0.003	rest → S America	0.003
3.	Africa → rest	0.010	rest → Africa	0.015
4.	Europe → rest	0.146	rest → Europe	0.133
5.	W Asia → rest	0.001	rest → W Asia	0.000
6.	Mid East → rest	0.001	rest → Mid East	0.000
7.	S Asia → rest	0.001	rest → S Asia	0.003
8.	E Asia → rest	0.046	rest → E Asia	0.076
9.	SE Asia → rest	0.064	rest → SE Asia	0.031
10.	Australia → rest	0.015	rest → Australia	0.009

Table 7.4: Transfer entropy from each region to the rest and from the rest to each region during the 2000-2016 period computed from the sparse inverse covariance matrix estimated using LoGo-TMFG algorithm.

	region → rest	**TE**	**rest→ region**	**TE**
1.	N America → rest	0.325	rest → N America	0.255
2.	S America → rest	0.096	rest → S America	0.099
3.	Africa → rest	0.034	rest → Africa	0.016
4.	Europe → rest	0.230	rest → Europe	0.439
5.	W Asia → rest	0.023	rest → W Asia	0.031
6.	Mid East → rest	0.007	rest → Mid East	0.028
7.	S Asia → rest	0.027	rest → S Asia	0.030
8.	E Asia → rest	0.036	rest → E Asia	0.059
9.	SE Asia → rest	0.014	rest → SE Asia	0.040
10.	Australia → rest	0.002	rest → Australia	0.027

7.4 Sparse network estimation using graphical lasso

We implemented graphical lasso with both least angle regression (LARS) and coordinate descent (CD) solvers using `graph_lasso` function from Python's `scikit-learn` library, with regularization parameter $\lambda = \{0.001, 0.005, 0.01, 0.05, 0.1, 0.2, 0.3, 0.4, 0.5, 0.6, 0.7, 0.8, 0.9\}$. Despite the fact that all covariance matrices (full and rolling-window) have eigenvalues between -1 and 1, during estimation we encountered the two following errors especially for lower regularization, e.g., $\lambda = \{0.001, 0.005, 0.01, 0.05, 0.1\}$:

- FloatingPointError: Non SPD result: the system is too ill-conditioned for this

solver. The system is too ill-conditioned for this solver. For some windows, this error disappears as we increase regularization to, e.g., $\lambda = 0.4, 0.5$, for other windows, this error disappears only with very high regularization, e.g., $\lambda = 0.9$.

- OverflowError: int too large to convert to float. This error disappears as we increase regularization to $\lambda \geq 0.1$.

None of the rolling windows can be estimated with $\lambda < 0.1$. Different windows (full and rolling) can be estimated without error with different minimum λ but the results are unrealistically too sparse graphs for all windows—all graphs have **no** non-zero edges which means none of the firm is connected to the others.

Computational time depends on the type of solver (CD or LARS) and the dataset size. In general, the CD solver takes longer than LARS for a given dataset and the larger the dataset, the longer it takes to complete a run. For a dataset whose number of observations $n = 748$ and dimension $p = 2,578$, graphical lasso with LARS takes approximately 1.8 times longer than LoGo-TMFG (298 vs 166 seconds). For another dataset that is twice as large ($n = 748$, $p = 5,156$), graphical lasso with LARS takes approximately 6.2 times longer than LoGo-TMFG (7,050 vs 1,145 seconds).

The underperformance of graphical lasso when used on our datasets is due to the algorithm's tendency to over-sparsify larger networks which leads to unreliable graph estimates. This is because graphical lasso constructs the global network "top-down" by sparsifying the large global covariance matrix, contrary to LoGo-TMFG which constructs a global network "bottom-up" by summing small local precision matrices. Our findings supports [Zhao and Yu, 2006] who conclude that ℓ_1-based methods generally become unreliable for larger networks and Heinavaara et al. [2016] who conclude that graphical lasso shrinks the estimates for the non-zero elements too heavily and often wrongly pushes true non-zero elements toward zero.

7.5 Rolling-window analysis

We analyze twenty five rolling-window periods, each of which comprises three years of log returns of financial companies that were active throughout the period. In aggregate, our rolling-window samples cover the period from 1990 to 2016. Table 7.5 summarizes the total number of companies in each of the ten economic regions for each three-year window from 1990 to 2016.

Table 7.5: Number of financial companies in each economic region for all twenty five three-year periods between 1990-2016

Year	NA	SA	AF	EU	ASW	ME	ASS	ASE	ASSE	AUS	Total
1990-92	1163	4	7	225	1	2	5	195	60	18	1680
1991-93	1203	5	8	267	2	3	8	205	67	20	1788
1992-94	1247	6	12	286	2	2	10	210	79	27	1881
1993-95	1311	22	14	310	2	3	9	241	123	40	2075
1994-96	1412	25	19	392	2	6	12	265	166	51	2350
1995-97	1378	31	36	436	10	6	33	301	154	56	2441
1996-98	1347	33	47	518	13	13	45	343	158	61	2578
1997-99	1402	40	44	544	18	15	50	355	158	61	2687
1998-00	1492	46	49	594	19	21	50	361	159	53	2844
1999-01	1688	39	49	581	35	22	53	360	152	53	3032
2000-02	1690	34	43	606	39	22	53	351	146	55	3039
2001-03	1710	36	64	657	38	29	57	400	145	66	3202
2002-04	1676	40	68	664	80	46	68	419	157	71	3289
2003-05	1720	45	74	660	108	47	87	427	178	79	3425
2004-06	1742	48	72	694	141	47	112	446	180	94	3576
2005-07	1769	49	63	680	89	52	119	440	164	95	3520
2006-08	1715	55	71	696	121	55	124	450	158	98	3543
2007-09	1652	64	96	771	169	62	161	457	166	94	3692
2008-10	1636	75	100	800	224	63	195	458	162	98	3811
2009-11	1530	126	143	989	363	71	322	468	242	142	4396
2010-12	1468	121	136	935	374	77	375	464	263	127	4340
2011-13	1404	123	138	885	374	82	427	467	266	123	4289
2012-14	1336	126	143	848	390	83	564	479	262	118	4349
2013-15	1305	132	149	817	385	85	623	475	260	112	4343
2014-16	1251	125	144	803	377	88	661	477	269	115	4310

Measured by total number of companies, the global financial network grew every year from 1990 to 2011, was the largest in the period from 2009 to 2011 with 4,396 companies, from which point it declined every year with 4,310 companies in 2016. North America has the greatest number of financial companies, followed by Europe, East Asia, and South Asia. The number of financial companies in North America increased gradually from 1990, with a plateau between 1999 and 2010 and a peak in the period from 2005 to 2007 (1,769 companies); it contracted from 2007 onward, ending at 1,251 companies in 2016. Similarly, the number of financial companies in Europe increased gradually from 1990, peaked in the period from 2009 to 2011 (989 companies), after which it declined every year with 803 companies in 2016.

It is worth noting that the number of financial companies in North America and

Europe were the highest during the financial bubble preceded a crisis. More specifically, the birth rate of companies in North America reached its plateau just before the Dotcom bubble, after which it declined and became negative after the Global Financial Crisis. In Europe, the number of financial companies peaked prior to the eurozone crisis in 2009, after which it dropped sharply. However, the number of financial companies in each of the other eight regions which are generally less economically developed than North America and Europe increased overtime, with that of South Asia growing the most rapidly.

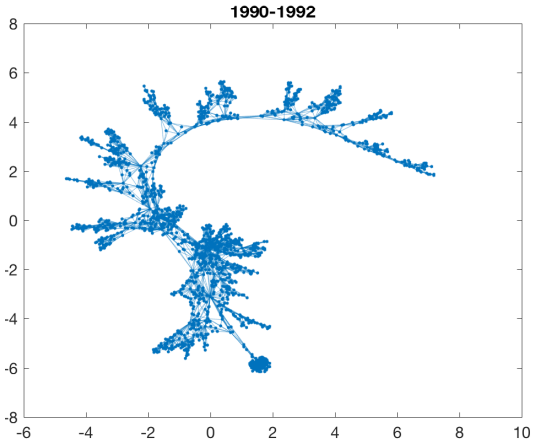

(a) Sparse network topology of 1,680 financial companies in 1990-1992

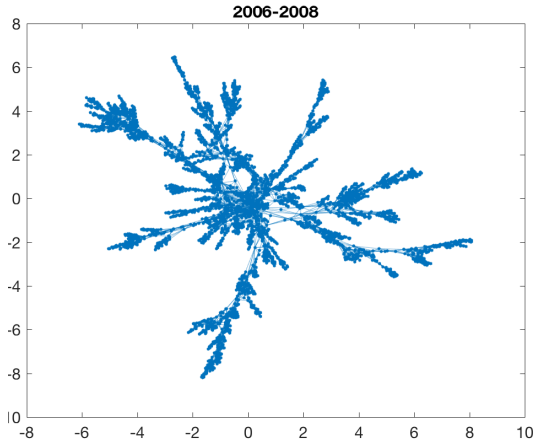

(b) Sparse network topology of 3,543 financial companies in 2006-2008

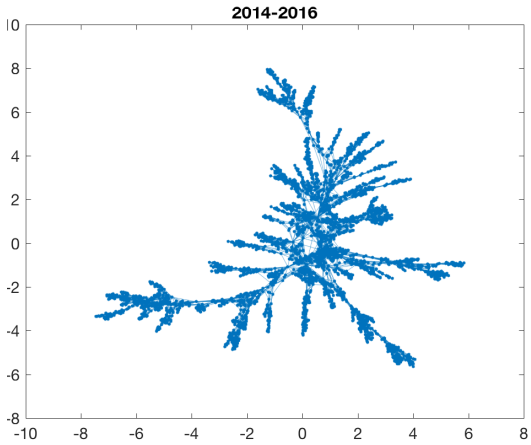

(c) Sparse network topology of 4,310 financial companies in 2014-2016

Figure 7.4: Sparse network of global financial companies in 1990-1992, 2006-2008, and 2014-2016 rolling windows, constructed from the non-zero entries in the sparse inverse covariance matrix estimated using the LoGo-TMFG algorithm.

Figure 7.4(a), Figure 7.4(b), and Figure 7.4(c) illustrate the topology graphs of financial companies that were active in the 1990-1992, 2006-2008, and 2014-2016 rolling windows, respectively. The links in the graphs correspond to non-zero values in the sparse inverse covariance matrices for the respective windows, estimated using the LoGo-TMFG algorithm on weekly returns. Similar to the full-sample results, we see that the number and size of clusters increased with the number of financial companies.

7.5.1 Transfer entropy

Figures 7.5, 7.6, 7.7, and 7.8 report the conditional transfer entropies for the ten economic regions of the world in 1990-1992, 1997-1999, 2006-2008, and 2014-2016 respectively. Both daily and weekly returns incorporate information regarding interdependencies between the economic regions. While conditional transfer entropies in Figure 7.5(a), Figure 7.6(a), Figure 7.7(a), and Figure 7.8(a) were computed from sparse inverse covariance matrices estimated using daily log-returns, those in Figure 7.5(b), Figure 7.6(b), Figure 7.7(b), and Figure 7.8(b) were computed from sparse inverse covariance matrices estimated using weekly log-returns.

The thickness of the line corresponds to the magnitude of the link between the regions and the number of lines corresponds to the number of links between the regions. For the same rolling windows, using weekly returns as input results in stronger links than using daily returns because weekly returns are generally of greater magnitudes than daily returns.

In general, the ten economic regions of the world were more interconnected during crises, e.g., the Asian crisis in 1997-1999, and the subprime crisis and global financial crisis in 2006-2008 than during normal periods, e.g., 1990-1992. The effect of globalization also leads to more interconnections between economic regions in more recent periods than in those further in the past as evidenced by the increase in the number of pairwise links between the ten economic regions, e.g., in 2014-2016 compared to 1990-1992. For example, South Asia connected with many more economic regions in 2006-2008 and 2014-2016 than in 1990-1992 and 1997-1999.

North America and Europe were connected to all other economic regions of the world in all 25 rolling windows. This is not surprising because North America and Europe have always been the most dominating regions. The pairwise links between North

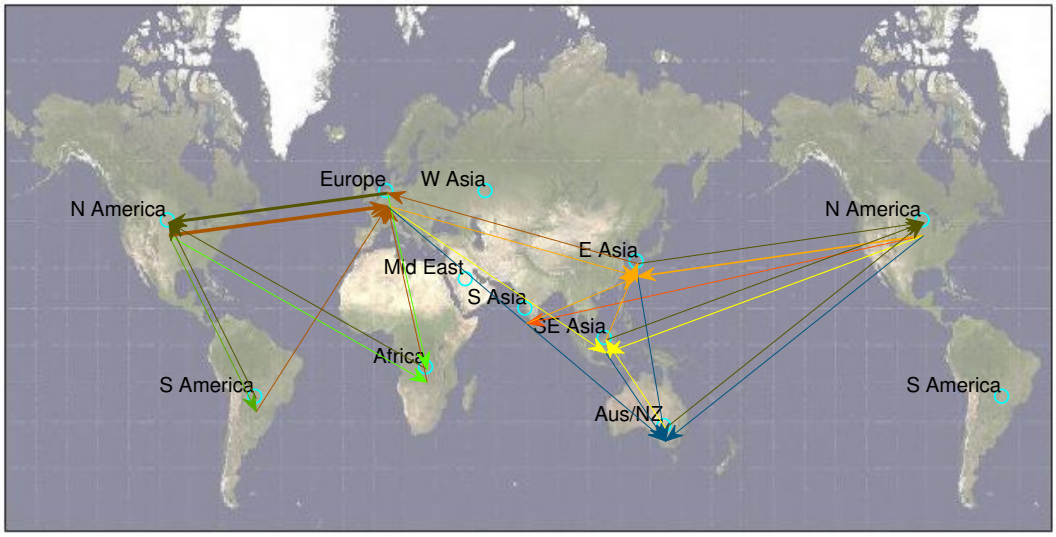

(a) Conditional transfer entropy from daily returns 1990-1992

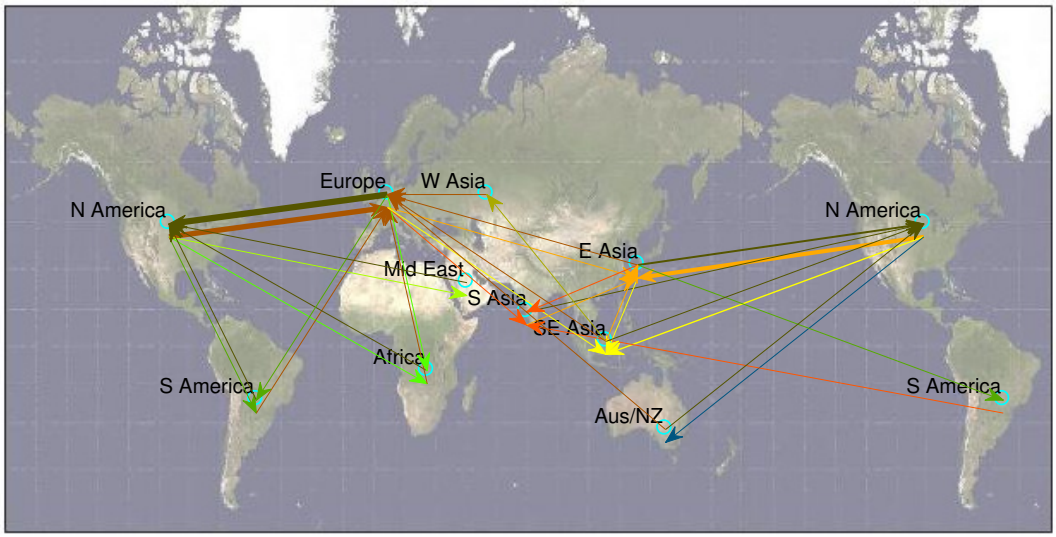

(b) Conditional transfer entropy from weekly returns 1990-1992

Figure 7.5: Conditional transfer entropy between the ten economic regions of the world during the period of 1990-1992, using as input the sparse inverse covariance matrix, which had been estimated via the LoGo-TMFG algorithm.

America and Europe were the strongest in all rolling windows, suggesting that the two regions were the most connected economic regions than any other pair of regions, with their interconnectedness reaching the highest point in 2006-2008 during the subprime crisis and the Global Financial Crisis.

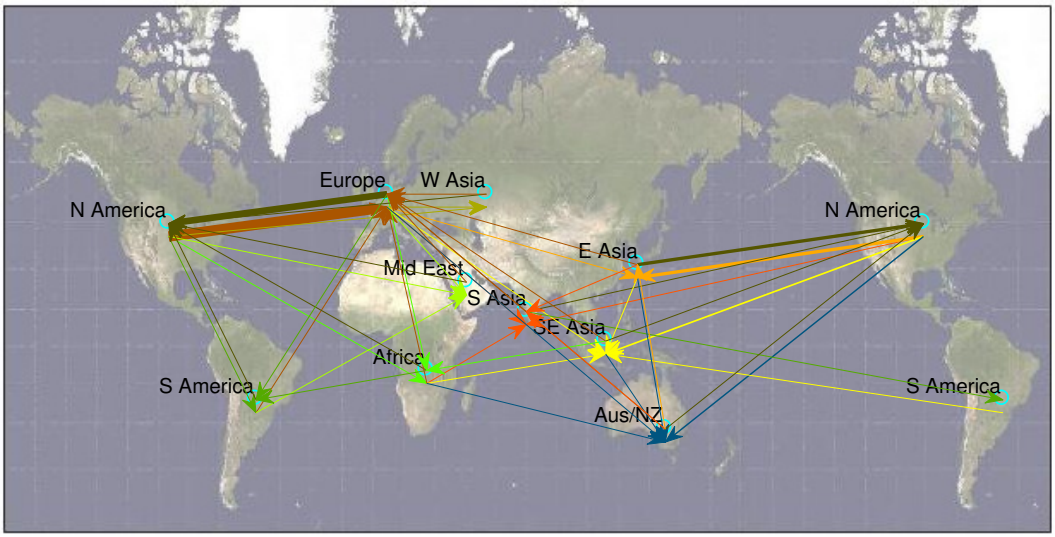

(a) Conditional transfer entropy from daily returns 1997-1999

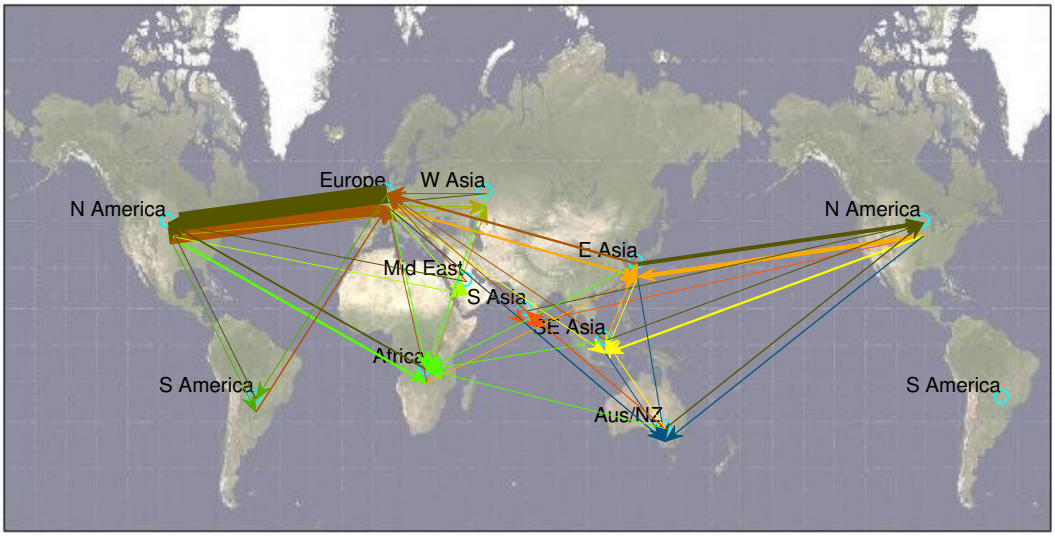

(b) Conditional transfer entropy from weekly returns 1997-1999

Figure 7.6: Conditional transfer entropy between the ten economic regions of the world during the period of 1997-1999, using as input the sparse inverse covariance matrix, which had been estimated via the LoGo-TMFG algorithm.

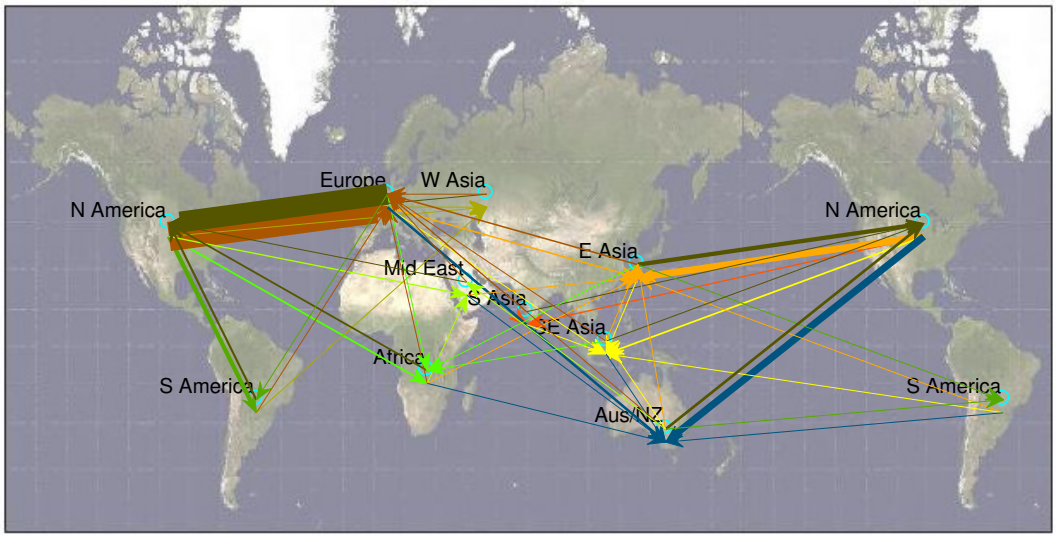

(a) Conditional transfer entropy from daily returns 2006-2008

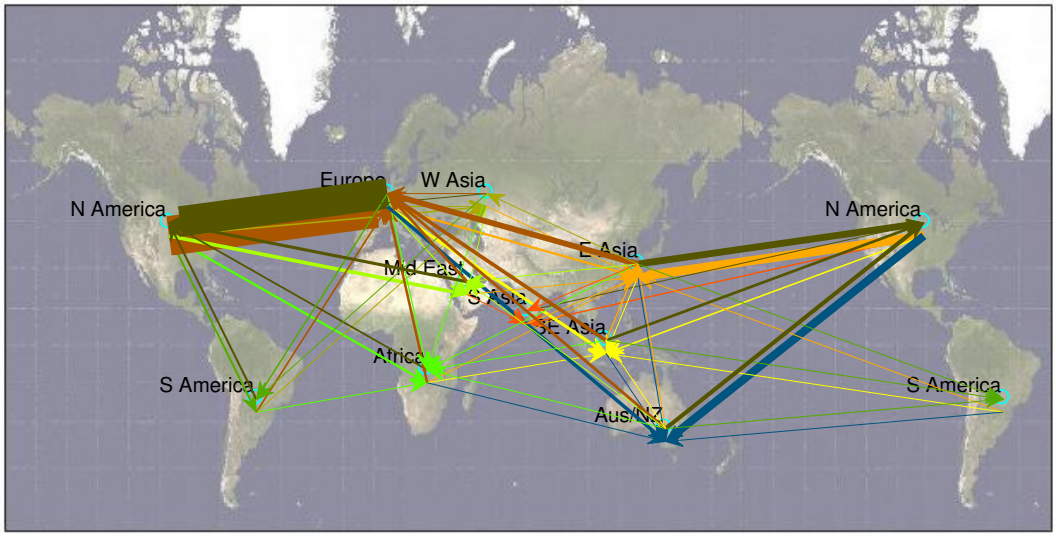

(b) Conditional transfer entropy from weekly returns 2006-2008

Figure 7.7: Conditional transfer entropy between the ten economic regions of the world during the period of 2006-2008, using as input the sparse inverse covariance matrix, which had been estimated via the LoGo-TMFG algorithm.

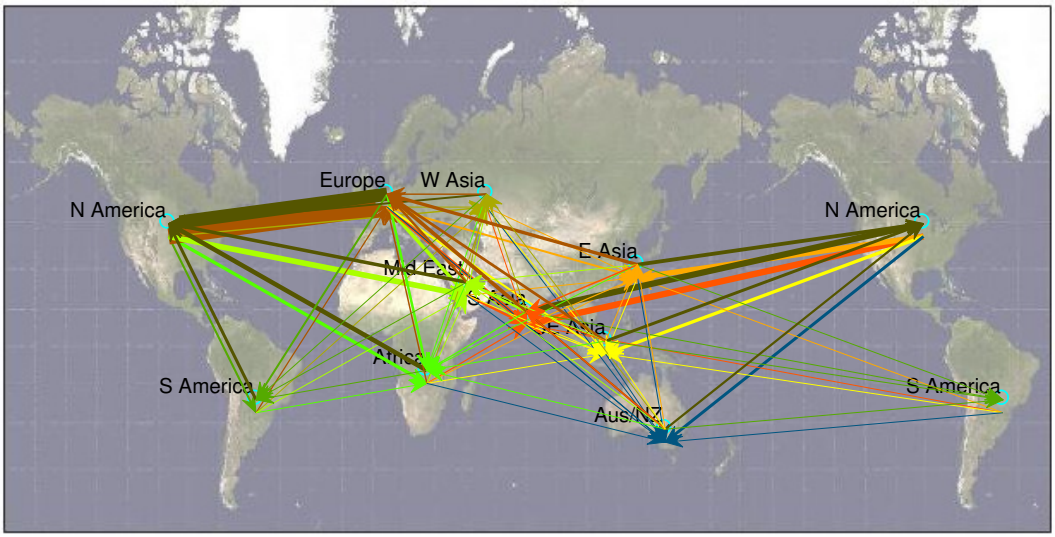

(a) Conditional transfer entropy from daily returns 2014-2016

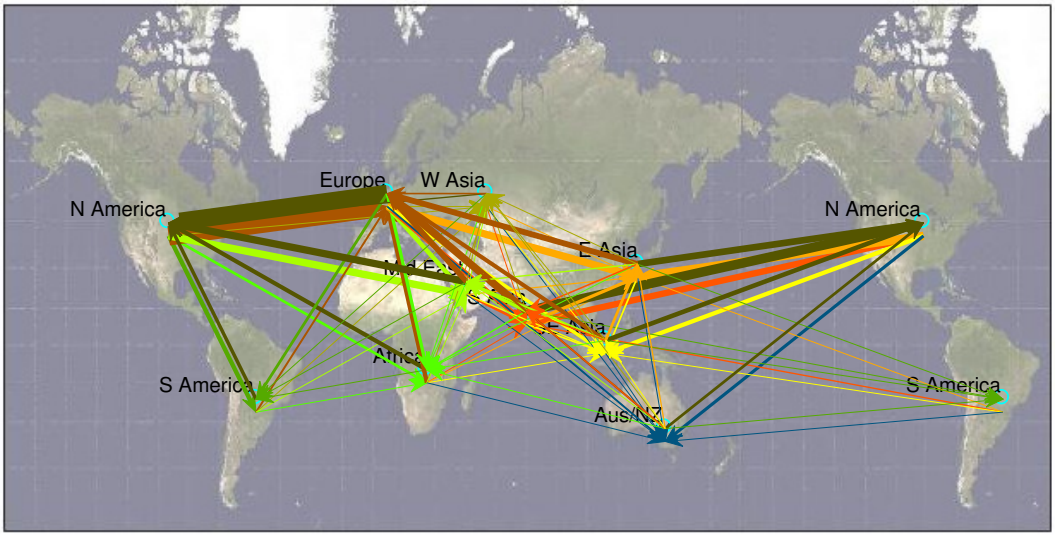

(b) Conditional transfer entropy from weekly returns 2014-2016

Figure 7.8: Conditional transfer entropy between the ten economic regions of the world during the period of 2014-2016, using as input the sparse inverse covariance matrix, which had been estimated via the LoGo-TMFG algorithm.

7.5.2 Impact and vulnerability

We measure the impact of a region by computing transfer entropy from the region to the rest of the world. Similarly, we measure vulnerability of a region by computing transfer entropy to the region from the rest of the world. We observe that North America and Europe have been the most dominating regions, having significantly higher impact and vulnerability than the other economic regions of the world. The impact and vulnerability measures are computed using the elements from the sparse inverse covariance matrix obtained from using the LoGo-TMFG on weekly returns. In Figure 7.9, the impacts and vulnerabilities of North America and Europe are approximately twice as high as those in the other regions. East Asia and Southeast Asia were the third and fourth most impactful and vulnerable regions from 1992 to 2007, after which the Middle East, South Asia and Australia took over.

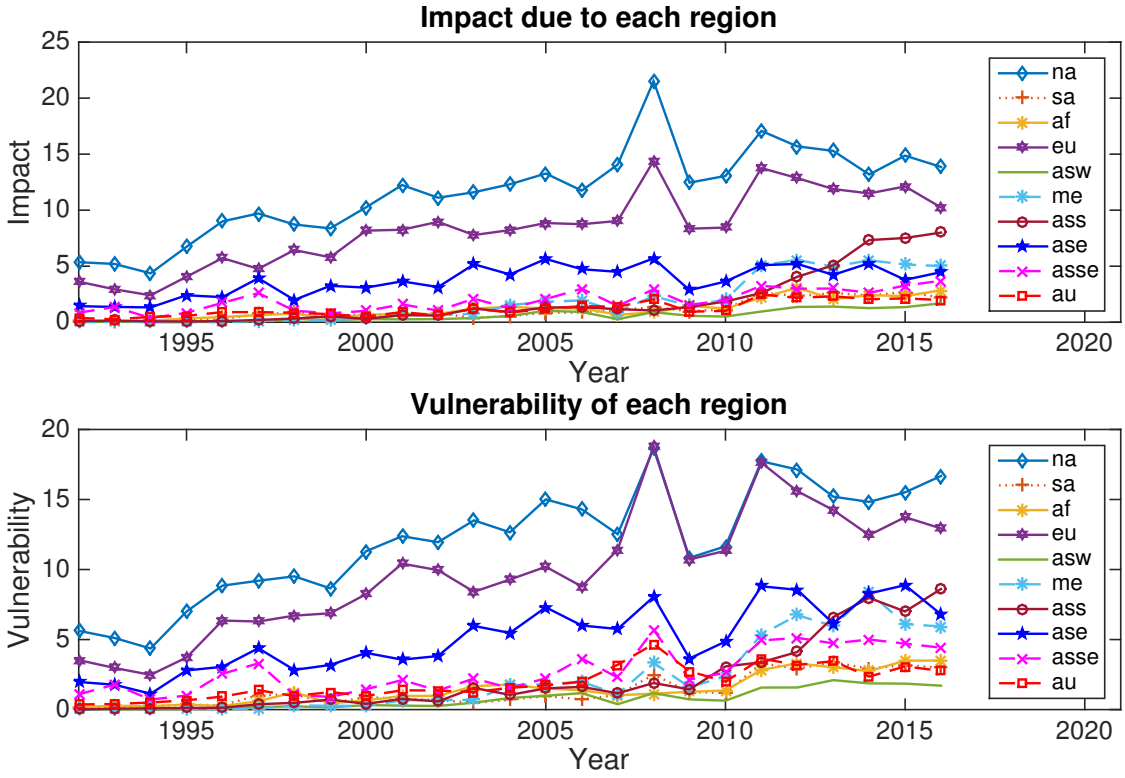

Figure 7.9: Impact and vulnerability of each economic region of the global financial network. Impact of each region is the sum of weekly transfer entropy from that region to the rest. Vulnerability of each region is the sum of weekly transfer entropy to that region from the rest.

According to Figure 7.10 North America was a net impacter in 1996, 2008-2011 and 2013-2014, Europe was a net impacter in 1992-1995, East Asia was a net impacter

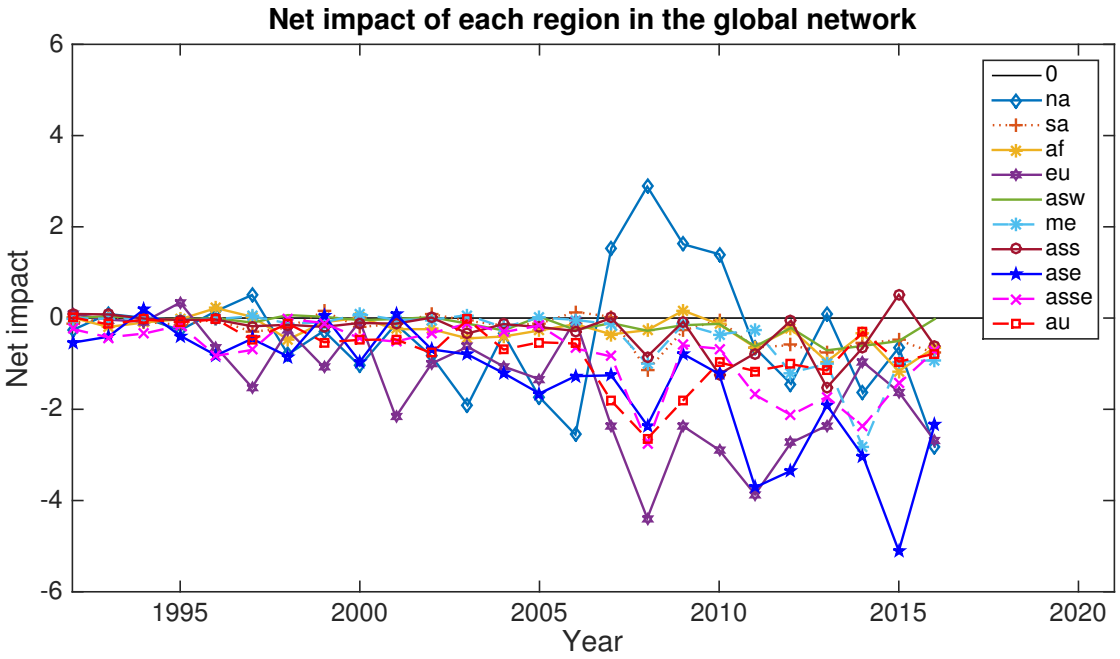

Figure 7.10: Net impact of each region of the global network, computed from subtracting a region's vulnerability from its impact.

in 1997, 2000 and 2005, and South Asia was a net impacter in 2001-2004, 2006-2007, and 2013-2016. When North America was the largest net impacter in 2008-2011, Europe was the largest net receiver, followed by Australia, East Asia and Southeast Asia. Europe was the biggest net receiver in 1996-2001 and 2005-2016 and a net receiver throughout the 20-year period from 1996-2016. North America was a net receiver throughout the ten-year period from 1997-2007. Despite a small positive impact it had in 1993-1994, Australia was a net receiver throughout the entire sample period from 1990-2016.

7.5.3 Inter-regional and intra-regional links

Figures 7.11 and 7.12 illustrate the *pairwise* time-varying number of links from and to North America and Europe, respectively. For South America, Africa, West Asia, the Middle East, South Asia, East Asia, Southeast Asia and Australia refer to Figures B.1, B.2, B.3, B.4, B.5, B.6, B.7, and B.8 in Appendix B.1.

The number of links, which is equal to the number of non-zero conditional transfer entropies, indicates how many financial institutions from each region are connected to financial institutions from the other economic regions. That is, if conditional transfer entropy from a North American company, say, NA1 to a European company EU1 is

different from zero, that counts as one link. Furthermore, if conditional transfer entropy in the reverse direction—from EU1 to NA1—is different from zero, that counts as one more link and we have in total two links.

Focusing on the graphs that illustrate the number of intra-regional links or the links between financial companies within the same region, one finds that the number of links between North American financial institutions decreased over time, suggesting that fewer North American financial companies stayed connected over time. In 1990 there were 1,163 financial companies in North America with roughly 3,600 intra-regional links (on average 3.10 links for every one company) but in 2016 there were 1,251 financial companies with roughly 2,500 intra-regional links (on average 2.00 links for every one company). The number of links between European financial institutions increased steadily from 1990 to 2000, plateaued between 2000 and 2005, then increased slightly and peaked in 2011 before dropping from 2011 onward. For other regions which are smaller than North America and Europe, the number of intra-regional links generally increased overtime.

The number of inter-regional links or links between financial companies from two different regions increased over time for each pair of regions, except between North America and Europe which generally increased until 2011 but decreased thereafter.

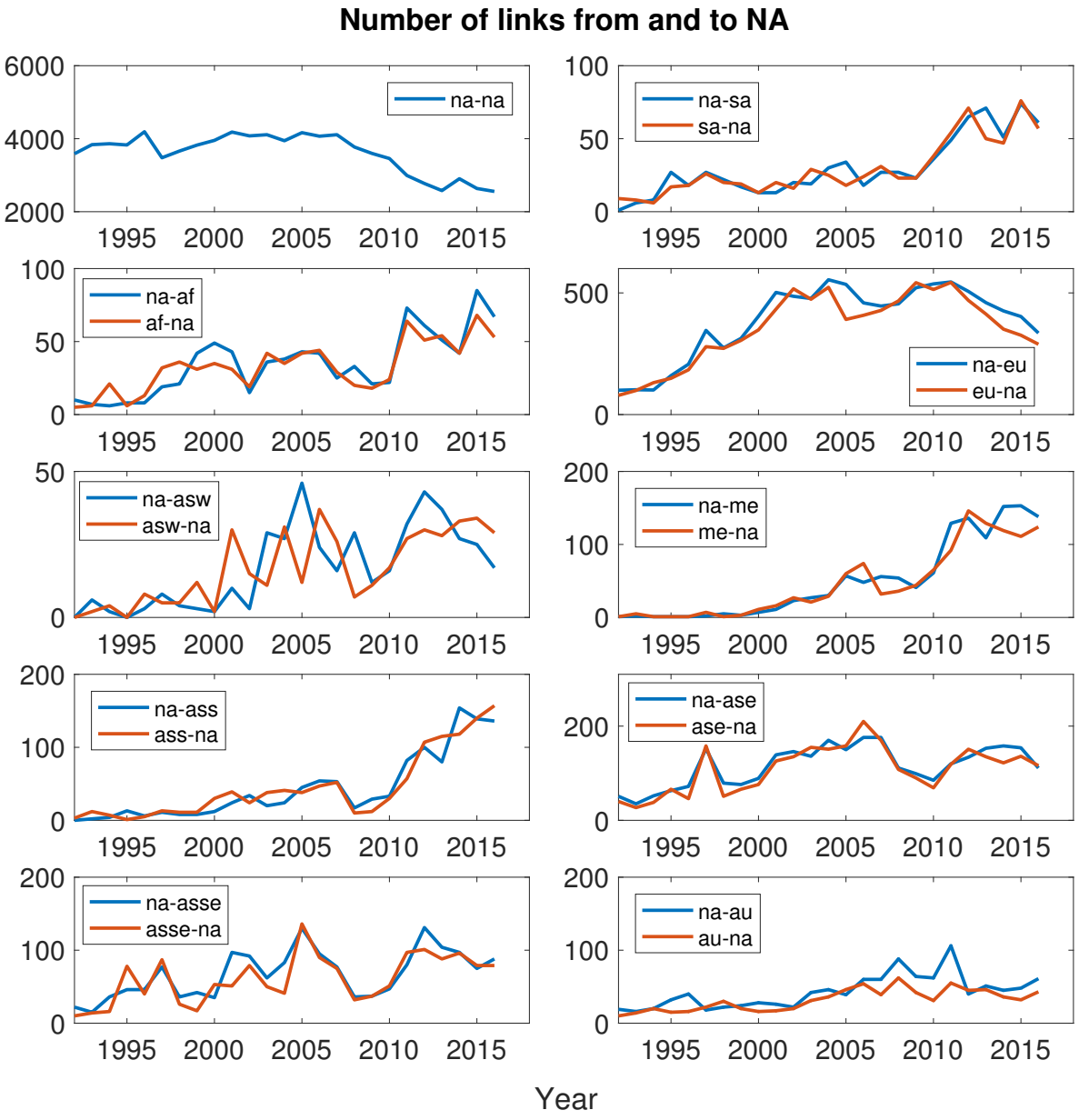

Figure 7.11: Number of links from North America to the other economic regions and from the other economic regions to North America, computed based on conditional transfer entropy for the period from 1990 to 2016. The conditional transfer entropy was computed using sparse inverse covariance matrix estimated via LoGo-TMFG algorithm. Over time, the number of links between financial companies in North America and those in the other regions increased but the number of links between financial companies within North America decreased, suggesting increasing inter-regional links but decreasing intra-regional links. North America is connected with Europe the most, followed by East Asia, Southeast Asia, South Asia, and the Middle East.

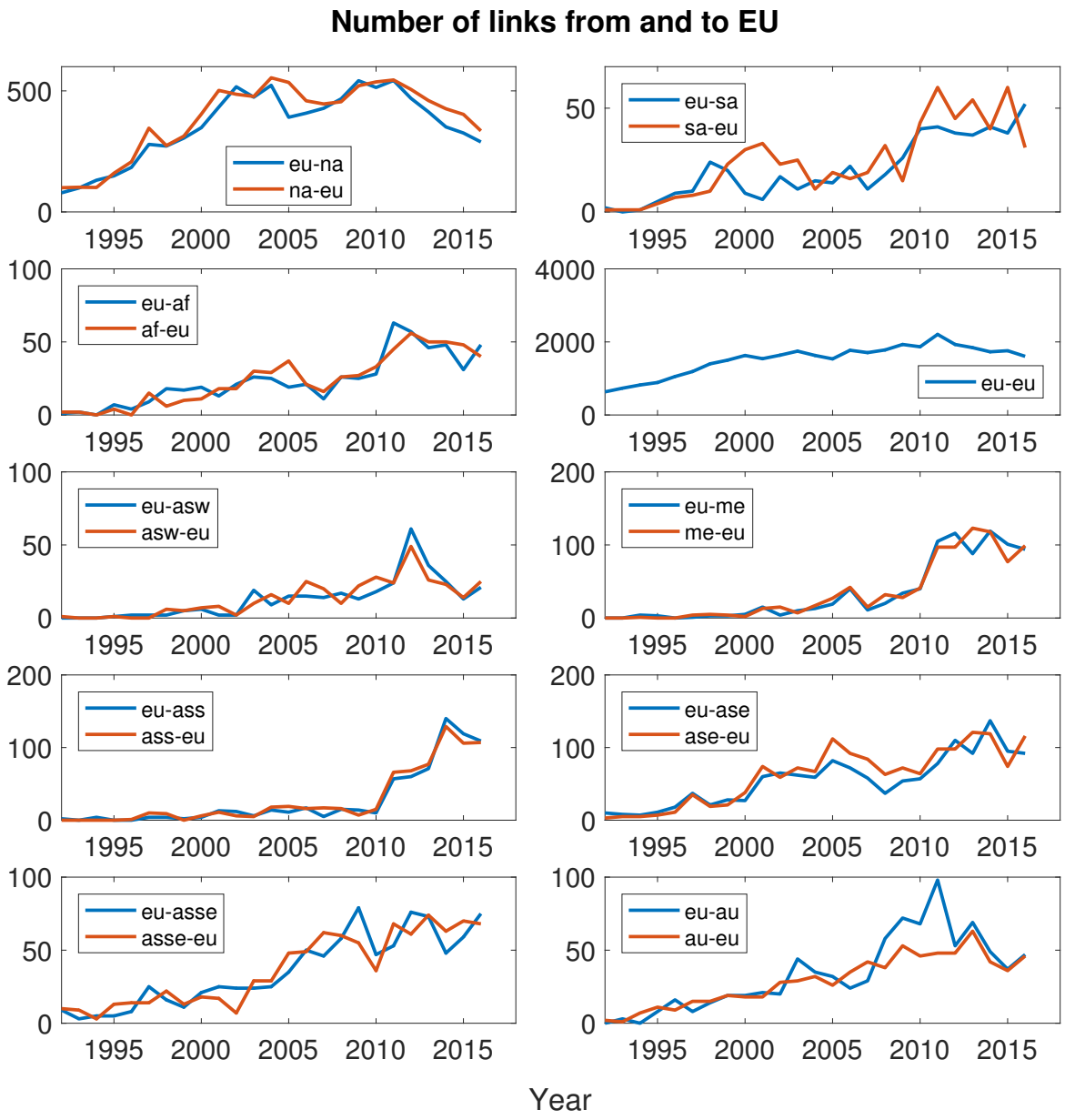

Figure 7.12: Number of links from Europe to the other economic regions and from the other economic regions to Europe, computed based on conditional transfer entropy for the period from 1990 to 2016. The conditional transfer entropy was computed using sparse inverse covariance matrix estimated via LoGo-TMFG algorithm. Europe was connected with North America the most, followed by East Asia, Southeast Asia, the Middle East and South Asia. The number of links between European companies and those in the Middle East and South Asia increased significantly in 2010. The number of intra-regional links between European companies increased steadily and peaked in 2011 before declining slightly thereafter.

7.6 Conclusion

In this chapter we address the curse of dimensionality using a novel sparsity modeling technique called LoGo-TMFG to measure interdependency between financial companies in ten economic regions of the world, namely North America, South America, Africa, Europe, West Asia, the Middle East, South Asia, East Asia, Southeast Asia and Australia. We analyzed daily and weekly stock returns over two full samples covering the periods from 1990-1999 and 2000-2016 and 25 rolling-window samples covering 3-year periods from 1990 to 2016. Six interdependency metrics are computed in this chapter including the number of links, magnitude of links, conditional mutual information, conditional transfer entropy, impact, and vulnerability.

With regards to number of companies, the global financial network grew every year between 1990 and 2011 with the largest number of companies in the window covering 2009-2011, after which it declined slightly and ended with 4,310 companies in the window covering 2014-2016. The number of companies in North America grew steadily from 1,163 companies in 1990-1992 to 1,769 in 2005-2007, but declined gradually thereafter, ending with 1,251 companies in 2014-2016. That is, the number of financial companies in North America peaked during a financial bubble which preceded the Global Financial Crisis. The size of the European financial sector grew steadily with 225 companies in 1990-1992 to 989 companies in 2009-2011, after which it contracted, ending with 803 companies in 2014-2016. Similar to North America, the size of the European financial sector was the largest during the financial bubble which preceded the eurozone crisis. For other regions, the number of companies grew over time, with the most rapid growth occurring in South Asia, from 5 companies in 1990-1992 to 661 companies in 2014-2016.

The number of *intra-regional* pairwise links, computed based on conditional transfer entropies, between North American financial institutions decreased over time, suggesting that fewer North American financial companies stayed connected over time. Similarly, the number of *intra-regional* pairwise links between European financial institutions increased steadily from 1990 to 2000, plateaued between 2000 and 2005, then increased slightly and peaked in 2011 before dropping from 2011 onward. For other regions which are smaller than North America and Europe, the number of *intra-regional* pairwise links generally increased overtime. The number of *inter-regional* pairwise

links between financial companies from two different regions increased over time for each pair of regions, except for North America vs. Europe which generally increased until 2011 but decreased thereafter.

The regionally aggregated conditional mutual informations and conditional transfer entropies in both the full and rolling-window samples suggest that the ten economic regions of the world became more interconnected over time—the number and magnitude of the two interconnectedness metrics generally increased over time. In all samples the conditional transfer entropy between Europe and North America was the largest, with significantly larger magnitude than that of the next strongest link. During the 2006-2008 period which covers the subprime crisis and the Global Financial Crisis, the conditional transfer entropy between Europe and North America was the highest, and much higher than those in the other time periods, suggesting that the two regions were the most interconnected during the crises.

Impact and vulnerability of a region are conditional transfer entropies from that region to the rest of the world and to that region from the rest of the world, respectively. Our impact and vulnerability metrics suggest that North America and Europe were the two most impactful and vulnerable regions over time, with East Asia coming third having impact and vulnerability below a third of those of North America and Europe.

We also demonstrate that graphical lasso which is the most popular sparsity algorithm underperforms LoGo-TMFG. This is due to the fact that graphical lasso constructs a global network "top-down", i.e., by sparsifying the global covariance matrix but LoGo-TMFG constructs a global network "bottom-up", i.e., from sums of small local networks. When used to analyze our extremely large datasets, graphical lasso yields unrealistically disconnected graphs with all off-diagonals equal zero. This corresponds with Zhao and Yu [2006] and Heinavaara et al. [2016] who conclude that ℓ_1-based methods generally become unreliable for larger networks and graphical lasso often wrongly forces true non-zero elements toward zero.

Chapter 8

Empirical analysis: Sparse industrial network construction using LoGo-TMFG

Summary: This chapter provides an insight that complements what we know about the global financial network put forward in Chapter 7. While in Chapter 7 we look at the global financial network as an aggregate of ten economic regions of the world, in this chapter we look at the global financial network as comprising four industries, namely banks, diversified financials, insurance, and real estate. Using the same datasets and metrics as in Chapter 7, e.g., number of links, conditional mutual informations, conditional transfer entropies, impact, and vulnerability, we analyze the interactions between the four industries on the global scale. In addition, we perform a more granular analysis by zooming in on each economic region and analyzing the connectivities between the four industries within it. The empirical results of this chapter help us understand the importance of each industry in the global network as well as in each of the 10 economic regions.

8.1 Four industries within the financial sector

The financial sector, whose GICS [1] code is 40 comprises four industries including banks (4010), diversified financials (4020), insurance (4030), and real estate (4040).

[1]The Global Industry Classification Standard (GICS), as previously mentioned in Section 5.3 is a standardized classification system for equities developed jointly by Morgan Stanley Capital International (MSCI) and Standard and Poor's.

Banks (4010) encompass commercial banks (diversified banks, regional banks) and thrifts & mortgage finance. Diversified financials (4020) encompass diversified financial services (multisector holdings, specialized finance), consumer finance, and capital markets (asset management & custody banks, investment banking & brokerage, diversified capital markets). Insurance (4030) comprises insurance brokers, life & health insurance, multi-line insurance, property & casualty insurance and reinsurance. Real estate (4040) comprises Real Estate Investment Trusts (diversified REITs, industrial REITs, mortgage REITs, office REITs, residential REITs, retail REITs, specialized REITs) and real estate management & development. Table 8.1 provides further information on industry classification for the financial sector.

There are extensive business ties between the four industries of the financial sector, although some have emerged more recently than others. The ties between insurance companies and commercial banks and those between insurance companies and diversified financial companies came about as insurance companies moved away from their core activities into insuring financial products, issuing credit-default swaps, derivatives trading, and investment management [Billio et al., 2012]. Large insurance companies such as AIG were a significant player in the derivatives market prior to and during the global financial crisis. AIG was bailed out by the US government during the crisis mostly due to concerns about the effects on other financial institutions which have derivative exposures to AIG [Liu et al., 2015].

As a result of regulatory changes and financial innovations, the banking industry has been transformed over the past decade. The repeal of Glass-Steagall Act means commercial banks can now engage in investment banking activities. Financial innovations such as securitization have increased the complexities of financial products, narrowing the distinction between loans, bank deposits, securities, and trading strategies. The types of business relationships between banks, investment management firms, and insurance companies have also changed. While banks and insurance companies provide credit to investment management firms, they also compete against them through their own proprietary trading desks. Similarly, investment management firms use insurers to provide principal protection on their funds and compete with them by offering insurance products such as catastrophe-linked bonds [Billio et al., 2012].

Billio et al. [2012] analyzed the returns of financial institutions and found that

Table 8.1: Industry classification

Industry Group Code	Industry Group	Industry Code	Industry	Subindustry Code	Subindustry
4010	Banks	401010	Commercial Banks	40101010	Diversified Banks
				40101015	Regional Banks
		401020	Thrifts & Mortgage Finance	40102010	Thrifts & Mortgage Finance
4020	Diversified Financials	402010	Diversified Financial Services	40201010	Consumer Finance (discontinued in 2003)
				40201020	Other diversified Financial Services
				40201030	Multi-Sector Holdings
				40201040	Specialized Finance
		402020	Consumer Finance	40202010	Consumer Finance
		402030	Capital Markets	40203010	Asset Management & Custody Banks
				40203010	Investment Banking & Brokerage
				40203010	Diversified Capital Markets
4030	Insurance	403010		40301010	Insurance Brokers
				40301020	Life & Health Insurance
				40301030	Multi-Line Insurance
				40301040	Property & Casualty Insurance
				40301050	Reinsurance
4040	Real Estate	404010	Real Estate (discontinued in 2006)	40401010	Real Estate Investment Trusts (discontinued in 2006)
					Real Estate Management & Development (discontinued in 2006)
		404020	Real Estate Investment Trusts (REITs)	40402010	Diversified REITs
				40402020	Industrial REITs
				40402030	Mortgage REITs
				40402040	Office REITs
				40402050	Residential REITs
				40402060	Retail REITs
				40402070	Specialized REITs
		404030	Real Estate Management & Development	40403010	Real Estate Management & Development

banks and insurers seem to have more significant impact on hedge funds and brokers than vice versa, and the pattern was more significant prior to the Global Financial Crisis. Banks were found to be more central to systemic risk than hedge funds which constitute the so-called shadow banking system. The authors attributed the asymmetry of impacts to the nature of business ties between the financial institutions, i.e., banks lend capital to hedge funds and insurers but not the other way around. In addition, banks and insurers may have taken on risks from other activities, which are typically core businesses of hedge funds, beyond lending and deposit taking. As a result, banks and insurers constitute the "shadow hedge-fund system" which traditional banking regulations are unable to handle.

8.2 US vs. European financial institutions

It is common knowledge that business environments and organizational cultures vary from country to country and from firm to firm. The US capital markets are less regulated, significantly larger, and much more developed than any other global markets. Despite the fact that European policy makers have been advocating for an economy less reliant on bank but more reliant on capital markets, Europe in aggregate is a bank-based economy. In other words, corporates in general raise capital for their operations in the form of bank loans. According to a report by the Chicago Mercantile Exchange (CME), approximately 80 percent of corporate debt in Europe is in the form of bank lending, with the rest coming from the corporate bond markets; on the other hand, 80 percent of corporate debt in the U.S. are bonds [Brecht, 2015].

8.2.1 Commercial banks

One of the main factors contributing to the difference between US and European commercial banks are accounting standards. As of 2017, US banks adhere to a combination of FASB and Basel I, II and III regulations while delaying the changeover to International Accounting Standards (IAS) and Basel III.

The FASB permits US banks to understate their derivative positions and keep most mortgage-linked bonds off their balance sheets [Weigand, 2015], which encourages US banks to securitize or sell on many of their loans into the much more developed institutional loan market, whereas a far larger proportion of European bank loans remain on

bank balance sheets [Brecht, 2015]. As securitization allows banks to swiftly transfer part of their credit risk to the markets (including institutional investors such as hedge funds, insurance companies and pension funds), US banks transmit more risks to the other industries in the US financial sector than European banks do [Carbo-Valverde et al., 2011]. As a result, regulatory requirements on US bank capital can be significantly underestimated.

According to Onaran [2013], if US banks followed the International Accounting Standards regarding disclosure of derivatives and consolidated mortgage securitizations, the capital ratios for JP Morgan and Bank of America, the two largest US lenders, would fall below the required level of 4 percent. The capital ratios for Citigroup and Wells Fargo would fall to just above 4 percent, from 7 and 9.5 percent respectively. The FASB accounting rules allow US banks to net their derivative positions and as a result, erase about USD 4 trillion in assets. By packaging most mortgages into securities, US banks can trim an additional USD 3 trillion in assets. On the contrary, the International Accounting Standards does not allow European banks that sell covered bonds to finance mortgage originations to move off their balance sheets the mortgages that back the covered bonds. Similarly, Canadian banks, which use international standards, are not allowed to move mortgages off their balance sheets, even though about 75 percent are insured by the government.

The leverage ratio, which limits the amount banks can borrow in order to make loans, adversely punishes holding relatively safe assets such as mortgages or government bonds which are what the majority of European banks holds. On the contrary, American banks are not as affected by the leverage ratio as they hold relatively few mortgages on their balance-sheets with the help of government agencies like Fannie Mae and Freddie Mac who buy mortgages from banks for securitization.

Another important characteristic of the US banking market is the presence of a large number of localized US commercial banks. The lack of full nationwide branching for commercial banks is a result of the restriction on inter-state expansion of US banks which was lifted in late 1990s. Today only a few banks have an extensive network of branch locations, notably Bank of America, JP Morgan Chase, and Wells Fargo. In addition, with the US Federal Reserve restriction on how much a bank can lend to a customer, many US companies have several, or in some cases tens or even hundreds of,

banking relationships while companies in other developed economies such as Canada have only one primary commercial bank relationship [Masson, 2007].

8.2.2 Investment banks and brokerage firms

Large European investment banks are generally more indecisive and less efficient relative to large American banks, which was evident in the American banks' quicker restructuring during crisis events. In addition, American investment banks are significantly larger than their European counterparts. As size matters in banking, the American bigger firms gain higher market shares and as a result, half of all global investment-banking revenues are generated in the US [banks, 2017].

8.3 Full-sample analysis

Table 8.2 illustrates conditional transfer entropies between the four industries namely banks, diversified financials, insurance, and real estate, for the full sample covering 1990-1999. Transfer entropies represent *temporal* interdependency between the industries and the transfer entropy from A to B does not have to equal the transfer entropy from B to A. In our analysis we estimated the sparse inverse covariance matrix using the LoGo-TMFG algorithm on weekly returns, then computed conditional transfer entropies corresponding to each pair of industries using the elements of the inverse covariance matrix. Similarly, Table 8.3 illustrates conditional transfer entropies between the four industries for the full sample covering 2000-2016.

Figures 8.1(a) and 8.1(b) illustrate conditional mutual information between the four industries of the global financial sector. Mutual informations represent *contemporaneous* interconnectedness and the mutual information from A to B must equal that from B to A. Banks vs. diversified financials had the highest mutual information followed by banks vs. insurance and diversified financials vs. insurance.

Table 8.2: Transfer entropy between the four industries in the period from 1990 to 1999 computed from the sparse inverse covariance matrix estimated using LoGo-TMFG algorithm.

	4010	4020	4030	4040
4010	0	1.0569	0.6621	0.3297
4020	0.9637	0	0.3929	0.1203
4030	0.3892	0.3080	0	0.0576
4040	0.2995	0.1314	0.0660	0

Table 8.3: Transfer entropy between the four industries in the period from 2000 to 2016 computed from the sparse inverse covariance matrix estimated using LoGo-TMFG algorithm.

	4010	4020	4030	4040
4010	0	0.6440	0.3101	0.0168
4020	0.3760	0	0.0513	0.0108
4030	0.1607	0.1355	0	0.0005
4040	0.0378	0.0013	0.0005	0

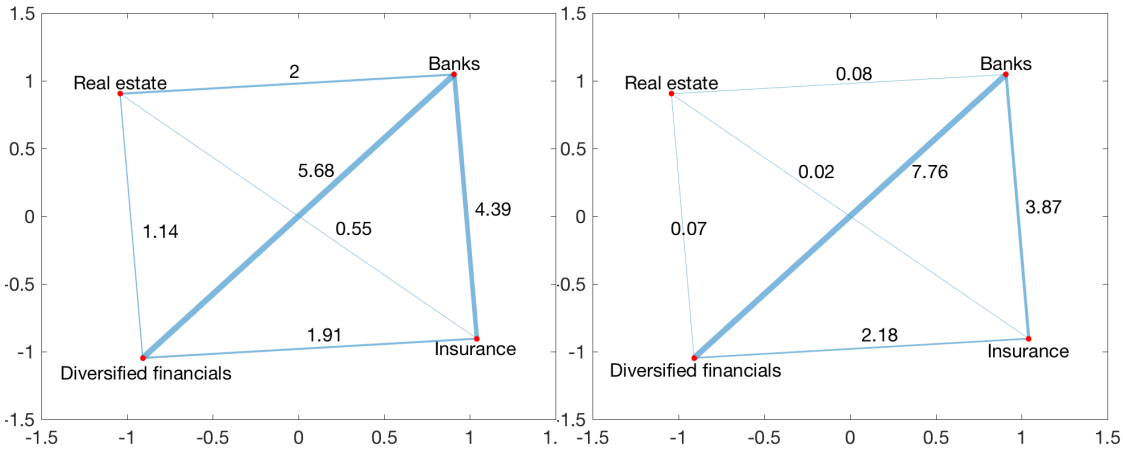

(a) Mutual information between the four industries in 1990-1999

(b) Mutual information between the four industries in 2000-2016

Figure 8.1: Mutual information between the four industries between in 1990-1999 and 2000-2016. We grouped 914 financial companies in 1990-1999 and 1,127 financial companies in 2000-2016 by industry and computed conditional mutual information between a pair of industries using as input the sparse inverse covariance matrix, which had been estimated via the LoGo-TMFG algorithm.

8.4 Rolling-window analysis

Similar to Section 7.5, we analyze twenty five rolling-window periods, each of which comprises three years of log returns of financial companies that were active throughout the three-year period. In total we cover the 27 years of daily financial stock data from 1990 to 2016. Figure 8.2 provides annual global breakdown indicating the total number of companies in each of the four industries—commercial banks (4010), diversified financials (4020), insurance (4030), and real estate (4040) for each three-year window from 1990 to 2016. Refer to Table B.1 in Section B.2 for the numbers corresponding to Figure 8.2. Overall, the number of banks increased from 1990 to 2011 but declined

thereafter, ending in 2016 with 1,593 banks. The number of diversified financial companies increased the most rapidly throughout the entire rolling window samples, and in 2016 nearly half (2,159 out of 4,310) of the companies belonged in this industry. The number of insurance companies increased rather slowly over the rolling samples while the number of real estate companies increased from 1990 to 2000 but declined thereafter, ending in 2016 with 16 companies.

Figure 8.3 plots the total number of companies in each industry for each economic region over 25 three-year rolling windows from 1990 to 2016. North America, South America, and Africa are the regions in which banks outnumbered companies in the other industries. However, for the rest of the regions, diversified financial companies outnumbered companies in the other industries.

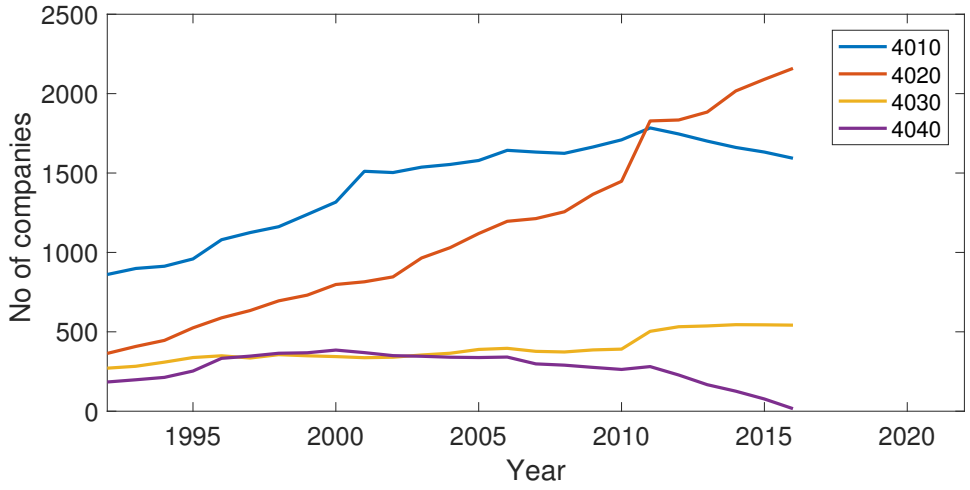

Figure 8.2: Annual breakdown indicating the total number of companies in each of the four industries of the global financial network.

Figure B.9 and Figure B.10 in Section B.2 plot respectively the average annualized log returns and the average annualized standard deviations by industry for all ten economic regions of the world between 1990 and 2016. In general, the returns of all financial industries were low but volatilities were high during crises, e.g., the Asian financial crisis 1997-1999, the Global Financial Crisis 2007-2009, the Eurozone crisis 2009-2012. Except for South America, banks in all regions have lower volatility than those of the other industries.

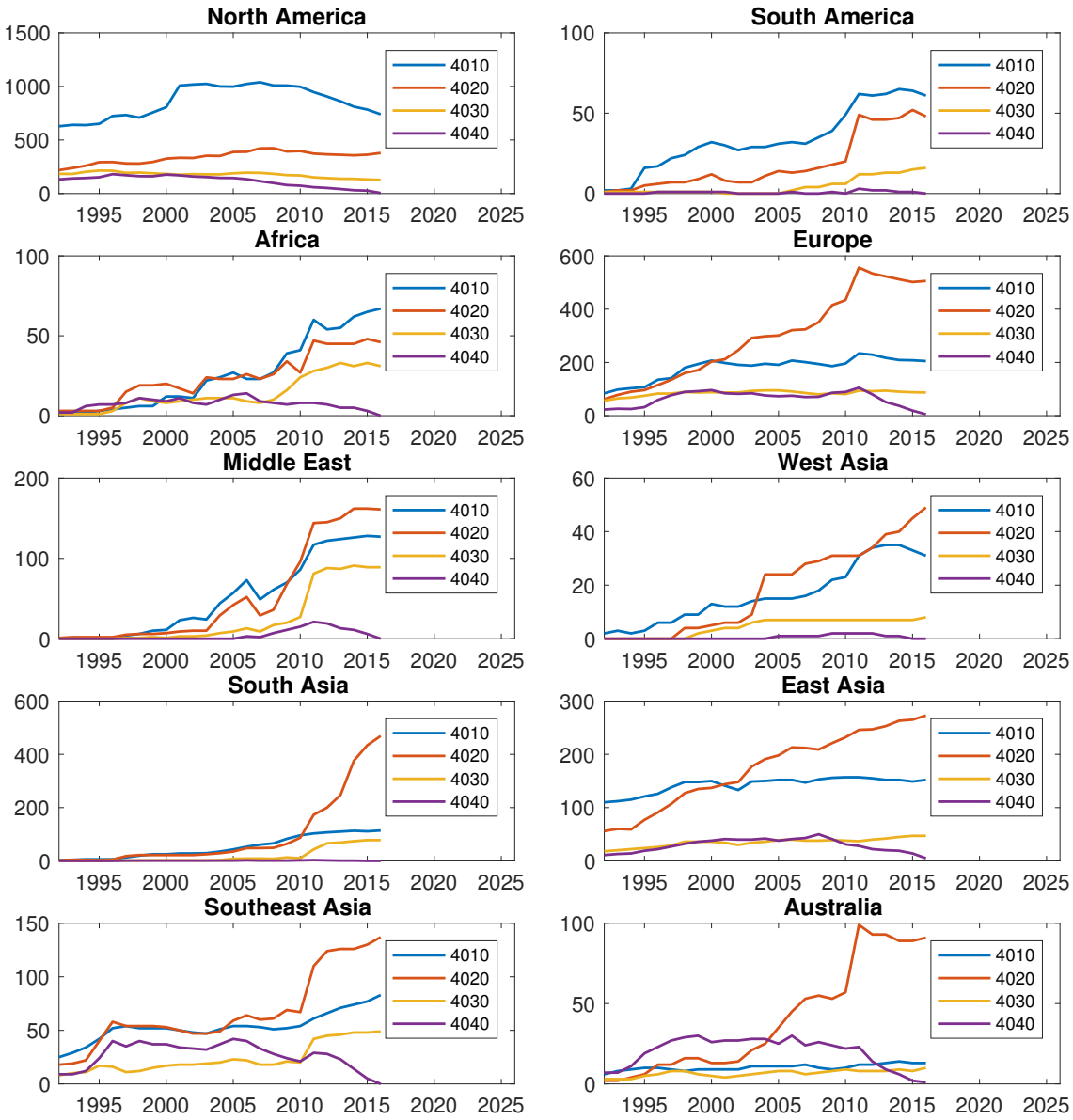

Figure 8.3: Annual breakdown indicating the total number of companies in each of the four industries—commercial banks (4010), diversified financials (4020), insurance (4030), and real estate (4040)—for ten economic regions of the global network.

8.4.1 Inter-industry links

Figures 8.4, 8.5, and 8.6 illustrate the *pairwise* time-varying number of links from and to each of the four industries in the global network, the US, and Europe, respectively. The number of links equals the number of non-zero conditional transfer entropies, which were computed using the sparse inverse covariance matrix obtained from the LoGo-TMFG algorithm. The time-varying number of links indicates how many finan-

cial institutions from each industry are connected to financial institutions from the other industries for the period from 1990 to 2016. It is a way to keep track of inter-industrial connectivities over time.

For the global network, the number of links between real-estate firms (4040) and those in the other industries decreased over the entire sample period from 1990 to 2016, suggesting a gradual decline in connectivity between real-estate and the other industries. This reflects the fact that the number of real-estate firms globally declined over time. The number of links between banks (4010) and diversified financials (4020) companies, those between banks (4010) and insurance (4030), and those between diversified financials (4020) and insurance (4030) increased over time.

For the US, the number of inter-industry links between all pairs of industries decreased over time. For Europe, the number of links between banks (4010) and diversified financials (4020) and those between diversified financials (4020) and insurance (4030) increased, while the number of all other inter-industry links decreased over time.

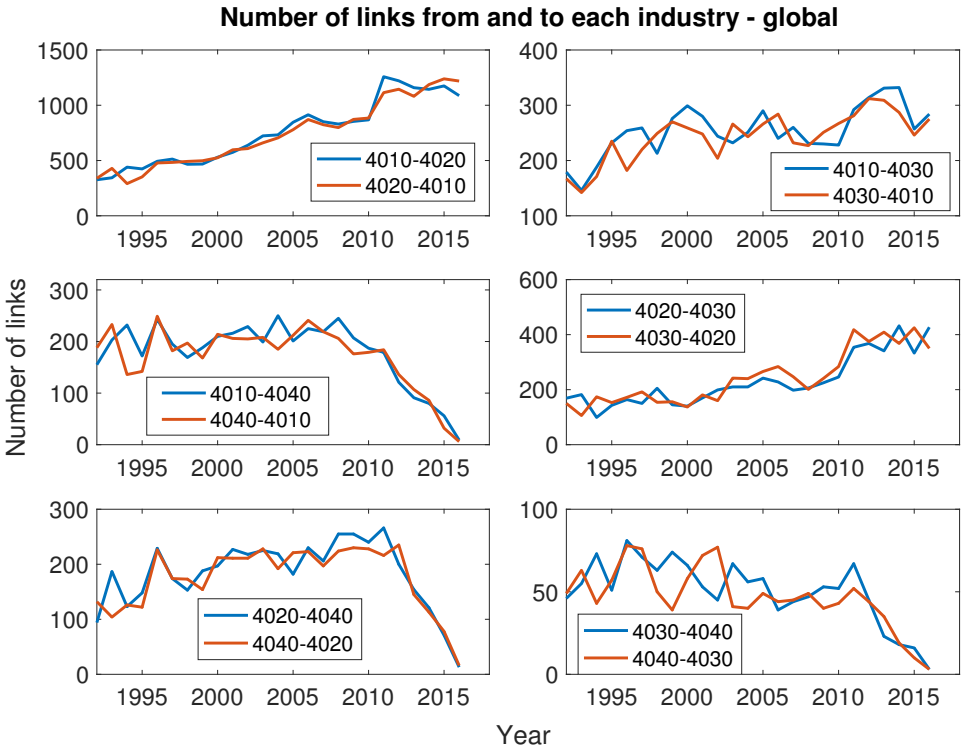

Figure 8.4: Global network: Number of links from each industry to the others and vice versa.

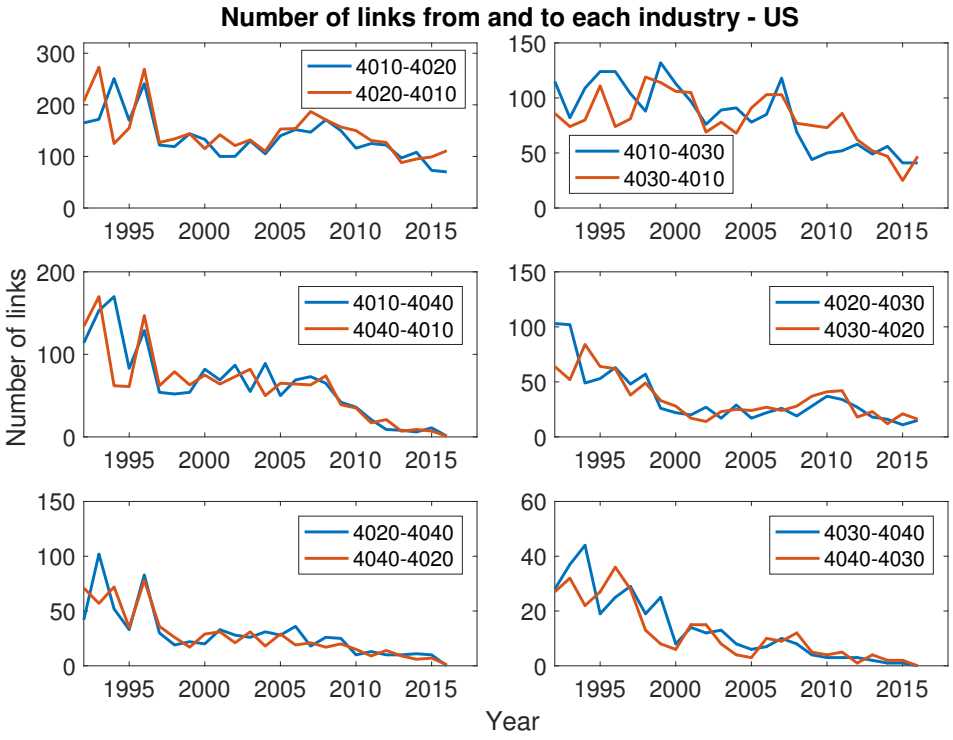

Figure 8.5: US: Number of links from each industry to the others and vice versa.

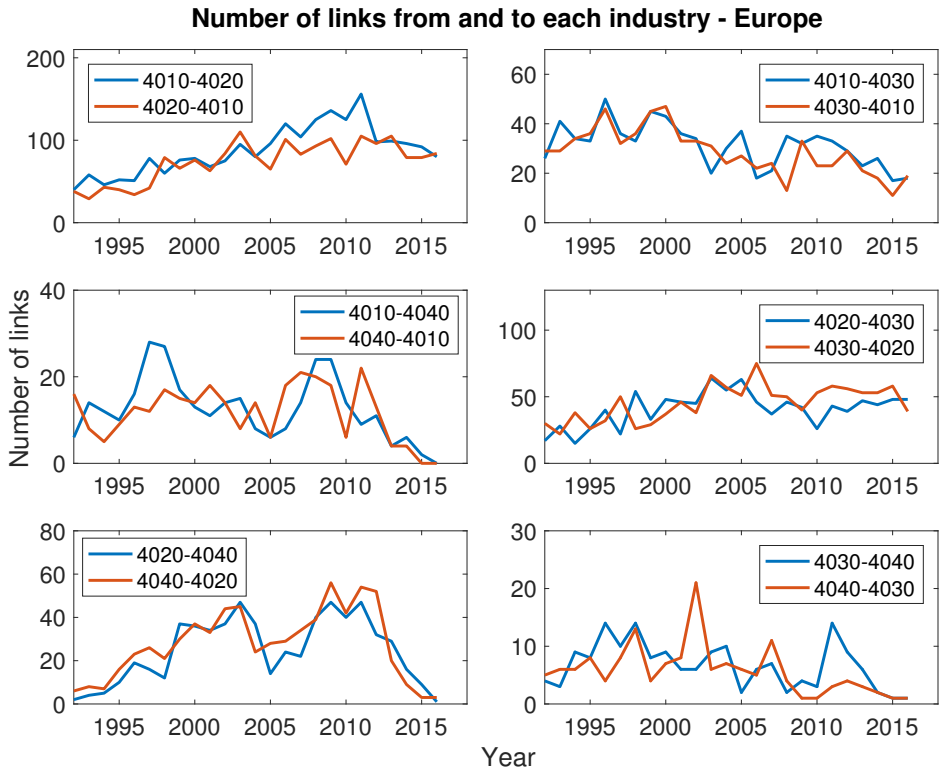

Figure 8.6: Europe: Number of links from each industry to the others and vice versa.

8.4.2 Impact and vulnerability by industry

Similar to Section 7.5.2, we compute impact from an industry to the rest and vulnerability of an industry due to fluctuations in the other industries. Impact of an industry is the sum of transfer entropies from that industry to the rest of the industries and vulnerability is the sum of transfer entropies from the rest of the industries to that industry. Transfer entropies are computed using the elements from the sparse inverse covariance matrix which is obtain from using the LoGo-TMFG algorithm on weekly returns.

The top panels in Figure 8.7, Figure 8.8, Figure 8.9, Figure 8.10, Figure 8.11, Figure 8.12, Figure 8.13, Figure 8.14, Figure 8.15, Figure 8.16, Figure 8.17, and Figure 8.18 illustrate the time-varying impact due to each of the four industries to the remaining three industries during the period between 1990 to 2016 within the global network, North America, the US, South America, Africa, Europe, West Asia, the Middle East, South Asia, East Asia, Southeast Asia, and Australia respectively. The corresponding bottom panels illustrate the time-varying vulnerability of each of the four industries to fluctuations from the remaining three industries for the aforementioned regions.

For the global network, commercial banks (4010) had the highest impact in all years from 1992 to 2010 but diversified financials (4020) became the highest impactful industry from 2011-2016. Commercial banks (4010) had the highest impact in 2008, after which their impact declined until 2011 when it picked up again. The two most vulnerable industries in the global financial network were commercial banks (4010) and diversified financials (4020). While the difference in vulnerabilities of commercial banks (4010) and diversified financials (4020) were insignificant prior to 2005, it became evident from 2005 to 2016, with diversified financials (4020) being the most vulnerable during the subprime crisis in 2005-2006, the Global Financial Crisis in 2008-2009 and the eurozone crisis in 2010-2013. However, commercial banks (4010) became the most vulnerable industry in 2014-2016. Insurance (4030) and real estate (4040) were the second least and the least impactful and vulnerable industries in the global network. It is worth noting that the difference between the impacts and vulnerabilities due to each of the four industries were small from 1992 to 1996 but became significantly larger from 1997 onwards, with the impact and vulnerability of real estate (4040) peaking in 2008 and plunging thereafter to almost zero.

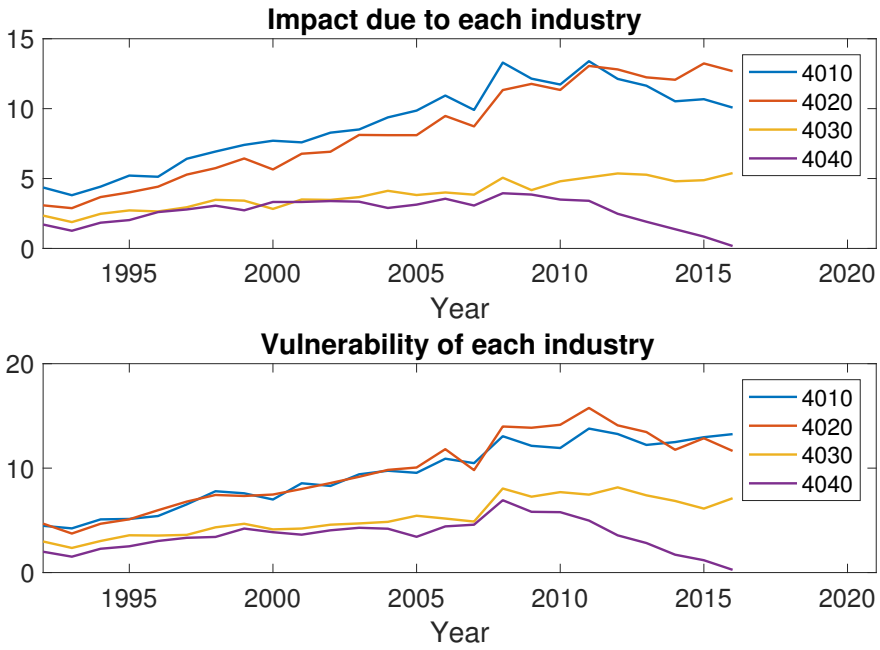

Figure 8.7: Global Network: Time-varying impact due to each industry and vulnerability of each industry for the global network.

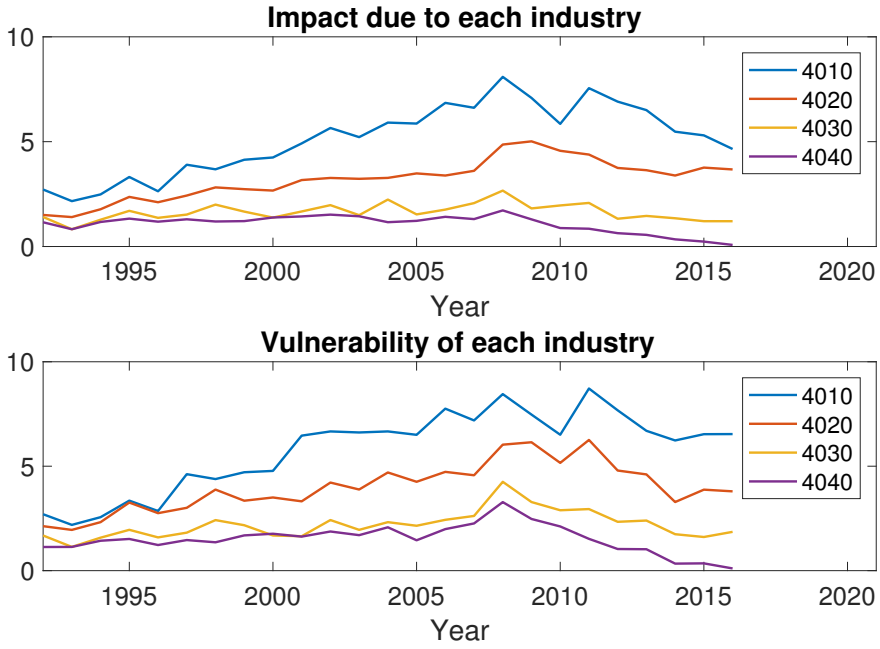

Figure 8.8: North America: Time-varying impact due to each industry and vulnerability of each industry for North America.

North America which comprises three countries including Bermuda, Canada, and the US was tremendously dominated by the US. As a result, the patterns of impacts and vulnerabilities of the four industries of North America are similar to those of the

US. Commercial banks (4010) was the most impactful and the most vulnerable industry, followed by diversified financials (4020), insurance (4030) and real estate (4040) in North America and in the US over the entire sample period from 1990 to 2016. The impact of commercial banks (4010) gradually increased from the beginning of the sample period in 1992, peaking in 2008 and declining thereafter. Similar pattern is observed for vulnerability of commercial banks (4010), except its peak occurred in 2011. The US is predominantly dominated by commercial banks (4010) whose impact and vulnerability are significantly larger than those of other industries.

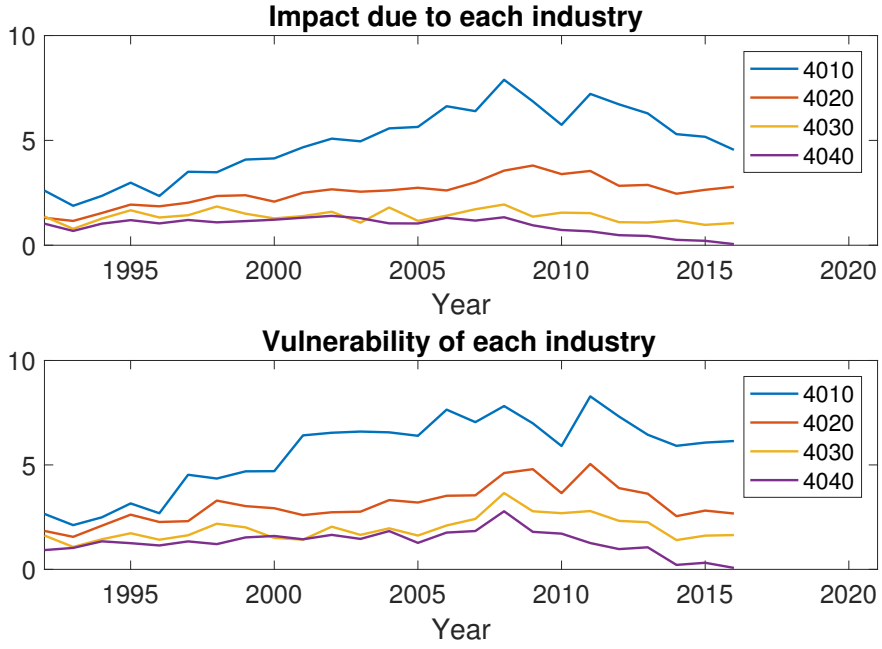

Figure 8.9: US: Time-varying impact due to each industry and vulnerability of each industry for the U.S.

For South America, commercial banks (4010) was generally the most impactful industry from 1992 to 2013, after which diversified financials (4020) became the most impactful. The most vulnerable industry for South America in 1992-2002, 2004, and 2007-2013 was commercial banks (4010), while in the remaining years of the sample diversified financials (4020) was the most vulnerable. This makes sense as the majority of financial companies in South America over the entire sample period were commercial banks. The number of companies in diversified financials (4020) were half of that in commercial banks (4010), until 2011 where the number of companies in diversified financials (4020) increased more rapidly to 75 percent of that in commercial banks

(4010). There were virtually no insurance companies until 2005, after which a handful of them emerged, while real estate companies were almost non-existent over the entire sample period. As a consequence, insurance (4030) had close to zero impact and vulnerability prior to 2005 but their impact and vulnerability increased steadily from then on. The impact and vulnerability of real estate (4040) remained close to zero over the entire sample period.

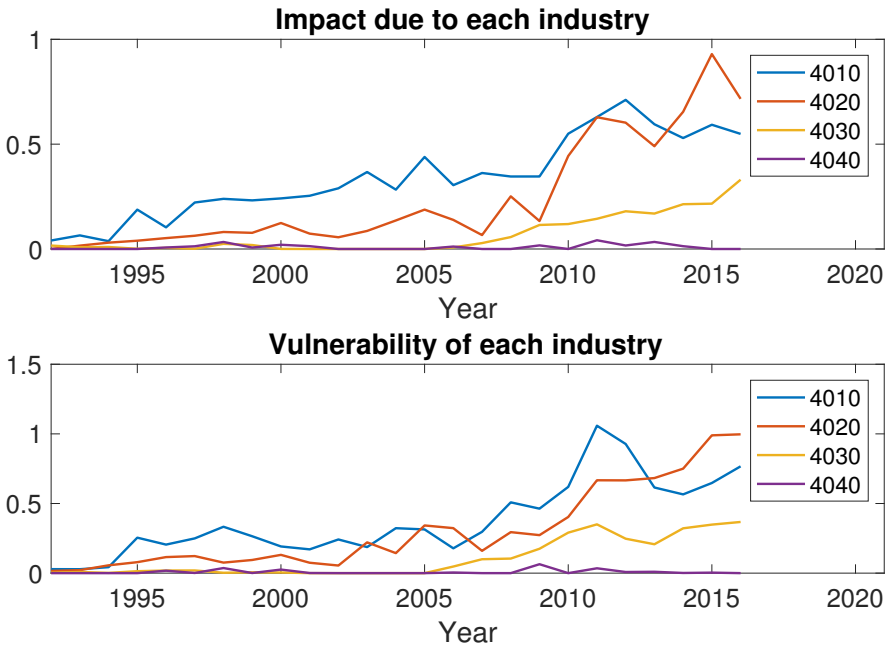

Figure 8.10: South America: Time-varying impact due to each industry and vulnerability of each industry for South America.

From 2008 onward, Africa had more commercial banks than any other financial institutions. In 2016, the number of commercials is roughly 1.5 times that of diversified financial companies and twice as many of that in insurance, while there were close to zero real estate companies. In 2003-2006 and 2012-2016 commercial banks (4010) was the most impactful industry in Africa but for the majority of the remaining years diversified financials (4020) was the most impactful. Diversified financials (4020) was the most vulnerable in most years over the sample period except in 1998-2001 where insurance was the most vulnerable and in 2013-2016 where commercial banks (4010) was most vulnerable.

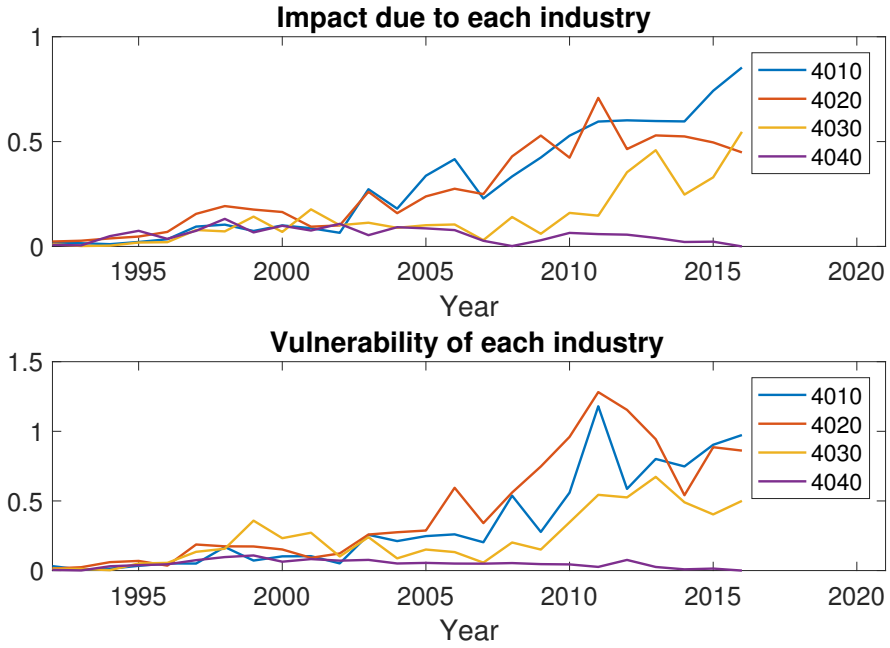

Figure 8.11: Africa: Time-varying impact due to each industry and vulnerability of each industry for Africa.

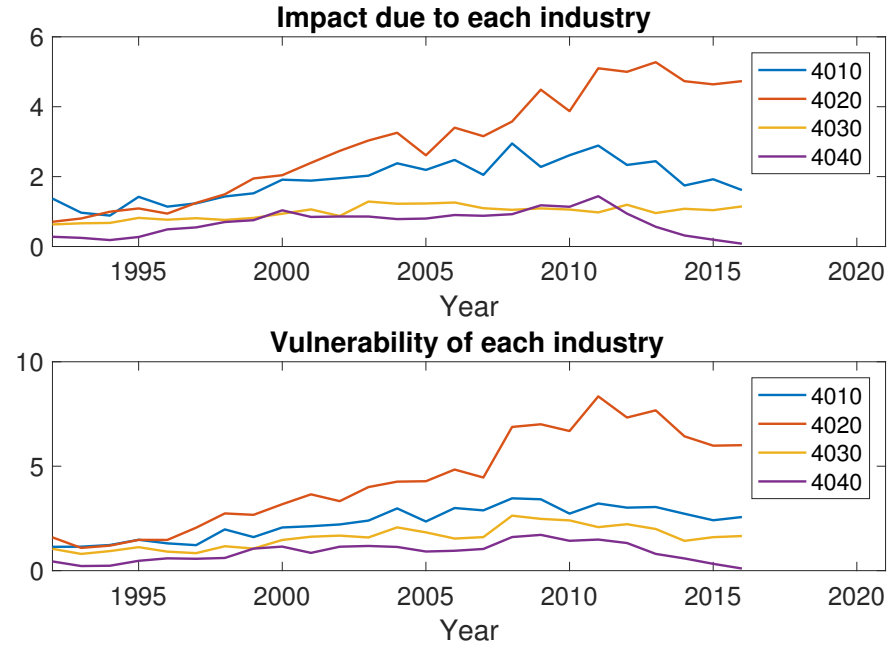

Figure 8.12: Europe: Time-varying impact due to each industry and vulnerability of each industry for Europe.

For Europe, commercial banks (4010) was the most impactful industry in 1992-1996 but in 1997-2016, the most impactful industry was diversified financials (4020). The impact of diversified financials (4020) peaked in 2009, 2011, and 2013, after which

time it started to decline. The impact of commercial banks (4010) peaked in 2008 and declined thereafter. The most vulnerable industry in Europe over the entire sample period was diversified financials (4020), followed by commercial banks (4010), insurance (4030) and real estate (4040). The vulnerability of diversified financials (4020) peaked in 2008, 2009, 2011, and 2013, after which time it started to decline. The vulnerability of other industries peaked in 2008-2009 and declined thereafter. Starting from 2007 onward, the gap between vulnerability of diversified financials (4020) and those other industries became significantly large. That is, the vulnerability of diversified financials (4020) were at least three times greater than the vulnerabilities of the other three industries.

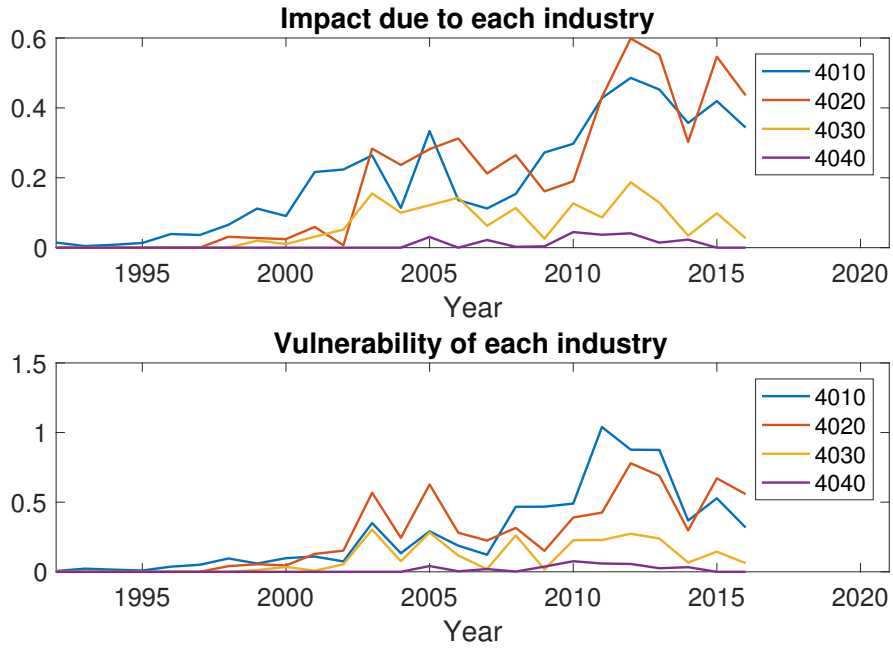

Figure 8.13: West Asia: Time-varying impact due to each industry and vulnerability of each industry for West Asia.

West Asia is a relatively small region comprising Georgia, Kazakhstan, Russia, Turkey, and Ukraine. Most financial companies in West Asia are commercial banks (4010) and diversified financials (4020), which are the two most impactful and vulnerable industries of the region. While the impact and vulnerability of insurance (4030) are rather sizable over the sample period, those of real estate (4040) are insignificant.

The biggest industry by number of companies in the Middle East was diversified financials (4020) in 1992-1997, commercial banks (4010) in 1998-2009 and diversified

financials (4020) in 2010-2016. The most impactful industry corresponded with the one comprising the largest number of companies at a given time period. That is, commercial banks (4010) was the most impactful in 1998-2004 and 2006-2008 while diversified financials (4020) the most impactful in 1992-1997, 2005, and 2009-2016. Diversified financials (4020) was the most vulnerable industry in all years except 2003-2004. There were roughly half as many insurance companies as the number of companies in the largest industry over the sample period. The impact and vulnerability of insurance (4030) is thus approximately half of the top industry. The impact and vulnerability of real estate (4040) began to rise in 2005, peaked in 2010, and declined thereafter to a value close to zero in 2016.

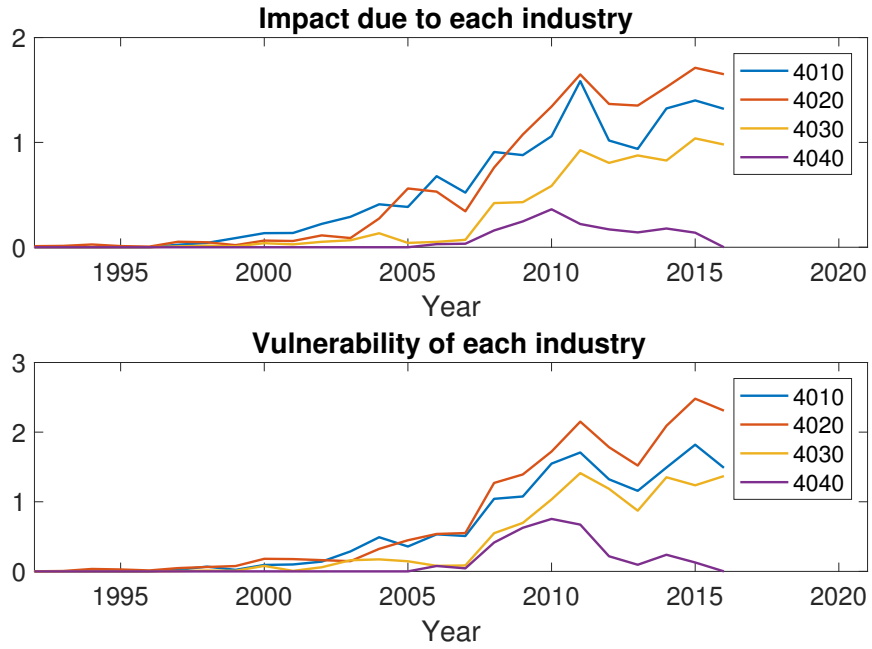

Figure 8.14: Middle East: Time-varying impact due to each industry and vulnerability of each industry for the Middle East.

South Asia had roughly the same number of commercial banks and diversified financial companies from 1992 to 2010, after which time the number of diversified financial companies increased exponentially. In 2016, there were five times as many diversified financial companies as commercial banks. As such, the most impactful and vulnerable industries were both commercial banks (4010) and diversified financials (4020) in 1992-2010, after which period diversified financials (4020) was the most impactful and vulnerable industry. The number of insurance companies in South Asia

were negligible until 2010 when it rose quickly to roughly 75 percent of that of commercial banks throughout the period from 2011 to 2016. As a consequence, the impact and vulnerability of insurance (4030) increased substantially after 2010. The number of real estate companies was negligible over the entire sample period, resulting in the industry's small impact and vulnerability.

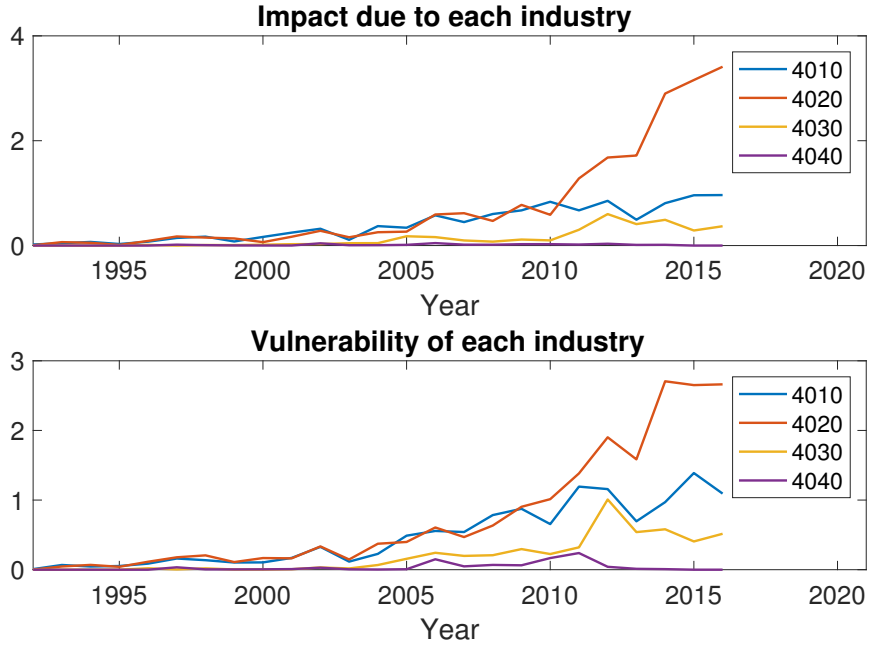

Figure 8.15: South Asia: Time-varying impact due to each industry and vulnerability of each industry for South Asia.

East Asia was dominated by banks for ten years between 1990 to 2000, after which the number of diversified financial companies exceeded that of banks and continued to increase sharply. The number of banks in East Asia remained unchanged around roughly 120-150 banks throughout the entire sample period from 1990 to 2016. There were much fewer number of insurance and real estate companies than banks and diversified financials over the sample period. The most impactful and vulnerable industry in East Asia was diversified financials (4020) except in 1993-1998 when banks (4010) was the most impactful. Despite having much fewer number of companies than banks (4010), insurance (4030) and real estate (4040) have relatively significant impact on the region and are quite vulnerable.

Prior to 1995, banks (4010) was the industry that had the largest number of companies in Southeast Asia's financial sector. Between 1995 and 2004, there were roughly

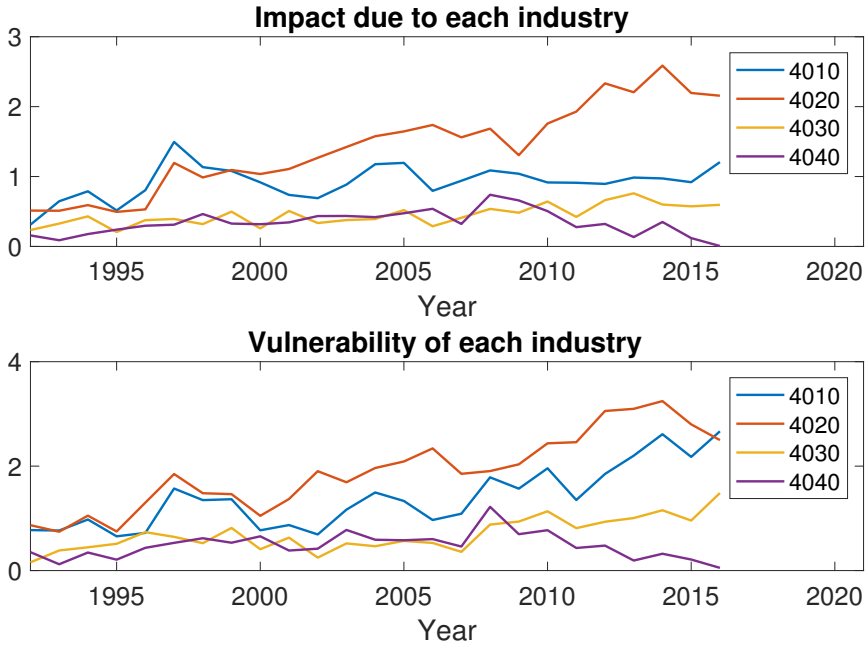

Figure 8.16: East Asia: Time-varying impact due to each industry and vulnerability of each industry for East Asia.

the same number of banks and diversified financials, after which the number of diversified financials started to increase significantly. Diversified financials (4020) was the most impactful industry throughout the entire sample period (1990-2016) and was also the most vulnerable industry throughout the entire sample period except in 1990-1995 and in 1998.

Before 2005 Australia had more real estate companies than any other types in the financial sector, after which time the number of companies in diversified financials (4020) started to increase exponentially and the industry became the largest by number of companies. The impact of real estate (4040) was not significantly larger than those of other industries even during the period between 1992-2005 when there were many more real estate companies than the other types. Diversified financials (4020) was the most impactful from 2003 onward and the most vulnerable from 1996 onward.

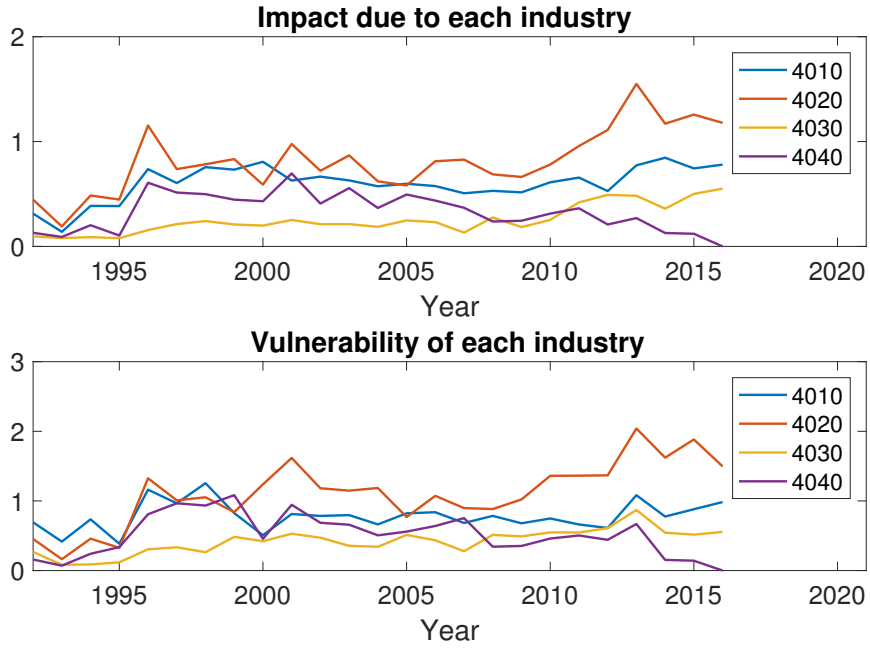

Figure 8.17: Southeast Asia: Time-varying impact due to each industry and vulnerability of each industry for Southeast Asia.

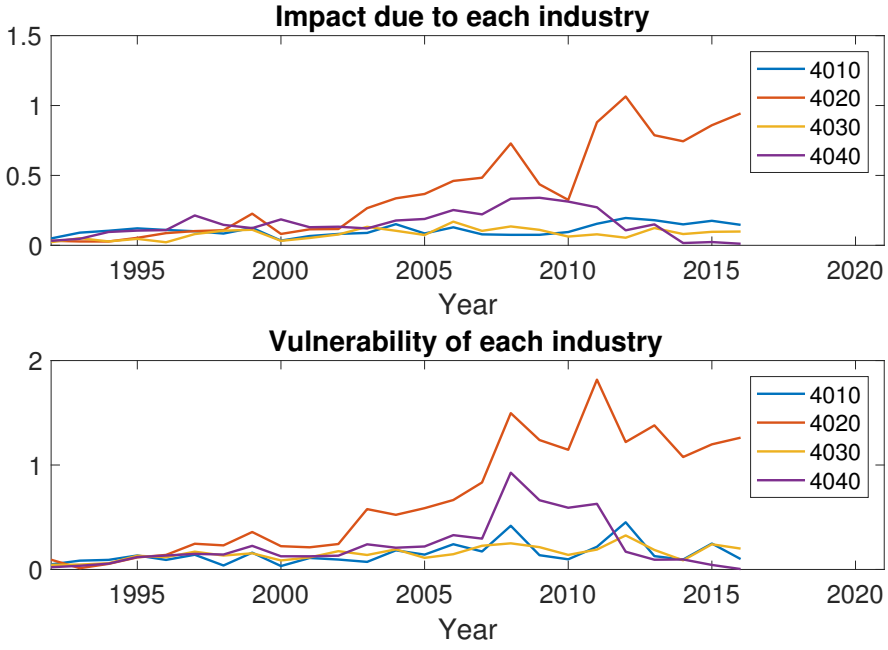

Figure 8.18: Australia: Time-varying impact due to each industry and vulnerability of each industry for Australia.

8.5 Conclusion

In this chapter we measure interdependency between four industries of the global financial sector: banks, diversified financials, insurance, and real estate. We analyzed weekly stock returns in two full samples (1990-1999, 2000-2016) and 25 rolling windows, each covering 3 years from 1990 to 2016. Five interdependency metrics are computed: number of links, conditional mutual information, conditional transfer entropy, impact, and vulnerability.

In both two full samples, banks and diversified financials were the two most influential industries in the context of temporal interconnectivity. Conditional transfer entropy was the largest from banks to diversified financials, followed by that from diversified financials to banks, banks to insurance, and insurance to banks, with the lowest transfer entropies between insurance and real estate. In terms of contemporaneous interdependency, banks and diversified financials had the highest mutual information followed by banks and insurance.

In rolling-window analysis, we find that banks outnumbered the other types of financial institutions between 1990 and 2010, after which diversified financial companies outnumbered the others. The number of banks increased steadily from 1990 to 2010 and declined thereafter, the number of real estate companies increased slowly from 1990 to 2000 and declined from 2000 onward. Over the entire sample period from 1990 to 2016, the number of diversified financial companies increased rapidly while the number of insurance companies increased relatively slowly. North America, South America, and Africa are the regions in which banks were the most numerous but for the other regions, diversified financial companies were the most numerous.

In terms of impact and vulnerability, banks had the highest impact and vulnerability in North America and in the US for all years and in South America for most years. This is consistent with the findings in Billio et al. [2012] where banks transmit more shocks than other types of financial institutions. Diversified financials generally had the highest impact and vulnerability in Europe, the Middle East, South Asia, East Asia, Southeast Asia, and Australia. In Africa and West Asia, banks and diversified financials took turns being the highest impactful and vulnerable industry.

Chapter 9

General Conclusions

This research measures time-varying connectivity in the global financial network using two frameworks. First, we keep all links in the global financial network and measure connectedness in the full network using improved vector autoregresion (VAR) and forecast error variance decomposition (FEVD). Second, we sparsify the links in the global financial network using the novel, information filtering networks-based algorithm called LoGo and measure connectedness in the sparse network using conditional transfer entropy and mutual information.

In the first empirical analysis, we use our improved VAR to measure time-varying connectedness within each of the three banking systems—North America, the European Union, and Southeast Asia using banks' stock returns from 2005 to 2016. Our improved VAR applies exponential weights onto the data in each rolling window, with more recent data points receiving higher weights than data points that are further in the past. In addition, we used ridge regression to estimate the parameters of our VAR model, in order to mitigate the curse of dimensionality.

The time-varying connectedness obtained from our improved VAR indicates that there are temporal changes in the systemic risk in the three banking systems, with peaks during major crisis events and troughs during normal periods. In general, the level of total connectedness in the North American banking system was the highest, followed respectively by those of the EU, and ASEAN banking systems. This indicates that the North American banking system was the most interconnected, in which shocks were more likely to be transmitted from one institution to another than in the EU and ASEAN.

We perform Granger causality test to investigate lead-lag relationships among the

three regions' connectedness and find that the North American network connectedness has predictive power on the EU network connectedness and the EU network connectedness has predictive power on the ASEAN network connectedness. We also perform linear and non-linear transfer entropy tests to validate our Granger causality test results. The non-linear test results are consistent with those from the linear test, demonstrating robustness. We found that there is a significant net information transfer from North America to the EU, from North America to ASEAN and from the EU to ASEAN.

To mitigate survival bias, we analyze rolling windows of data featuring between 1,680 to 4,396 companies in the global financial sector from 1990 to 2016. As a result, we have time-varying, high dimensional datasets that have many more variables than observations. To deal with the curse of dimensionality, we model sparsity in our network using the LoGo algorithm, which breaks down a large problem of estimating a high dimensional covariance matrix into significantly simpler problems involving estimating much smaller matrices. This quality makes the LoGo algorithm suitable to analyze high dimensional datasets where large standard errors and overfitting are a predominant issue.

In modeling sparsity, we divide our study into two parts. First, we categorize the global financial companies by economic region and compute mutual information, transfer entropy, and derive measures of impact and vulnerability from transfer entropy for each economic region.

We find that other than North America and Europe, the number of financial companies in each region increased over time. The number of companies in North America reached its plateau just before the Dotcom bubble, after which it slowed down and dropped after the Global Financial Crisis. In Europe, the number of companies peaked prior to the eurozone crisis in 2009, after which it dropped sharply.

The economic regions were more interconnected during crises, e.g., the Asian crisis in 1997-1999, and the subprime crisis and Global Financial Crisis in 2006-2008 than during normal periods, e.g., 1990-1992. Over time, more economic regions became interconnected as evidenced by the increase in the number of links between the regions. North America and Europe were connected to all other economic regions in all rolling windows and the link between the two regions was much stronger than those between all other regions.

Based on our impact and vulnerability measures, North America and Europe were the most dominating regions, having significantly higher impact and vulnerability than the others. East Asia and Southeast Asia were the third and fourth most impactful and vulnerable regions until 2007, after which the Middle East, South Asia and Australia began to emerge.

Second, we categorize the global financial companies by industry and compute the same metrics, i.e., number of links, mutual information, transfer entropy, impact and vulnerability for each industry. We also perform a more granular analysis by dividing each economic region into industries and compute impact and vulnerability for each industry within the economic region. We found that banks had the highest impact and vulnerability in North America in all years and in South America in most years throughout the entire sample period from 1990 to 2016. Diversified financials generally had the highest impact and vulnerability in Europe, the Middle East, South Asia, East Asia, Southeast Asia, and Australia. In Africa and West Asia, banks and diversified financials took turns being the most impactful and vulnerable industry.

Lastly, we show that the network connectedness measure computed from transfer entropy of the sparse network and that computed from the FEVD of the full network are similar. While both measures could correctly identify past crisis periods, the measure computed from transfer entropy demonstrates much clearer peaks during major crisis events, e.g., the Global Financial Crisis, the European sovereign debt crisis, the US credit downgrade, and the Libor scandal. This suggests that the sparse network increases the signal-to-noise ratio in the data and improves the interpretability of the connectedness measure, allowing us to make better inference than the full network.

The connectedness metrics obtained throughout this research capture both direct and indirect links between the financial institutions. This differs from the findings in existing work that uses bilateral exposure information e.g. interbank lending data to infer network connectedness because such data reflect only direct connectedness between the banks. Indirect connectedness arisen from factors such as similarity in business models, trading, investment and risk management strategies, and common exposures to economic fluctuations are not captured in the literature on bilateral exposures.

The main contributions of this thesis are in both the methodologies and actual empirical analyses. On the methodology part, we propose technical improvements to

the VAR-FEVD which lead to superior results compared to the standard VAR. We also add to the graphical lasso literature by providing an empirical proof that the algorithm yields unreliable results for our large datasets and illustrate that the novel LoGo-TMFG algorithm leads to better outcome in this case. In addition, we propose "impact" and "vulnerability" which are computed from conditional transfer entropies as additional connectednesss metrics. On the empirical analysis part, we apply VAR-FEVD on unique datasets and conduct causality tests on the resulting total connectedness metrics, which provides valuable insight on the lead-lag relationship between connectedness in different economic regions. Moreover, we analyze the entire global financial network using LoGo-TMFG, which is the first both in terms of the dataset and application of the algorithm, resulting in new, useful findings.

Our research findings are beneficial especially for policy makers, e.g., the central banks, who can use our connectedness metrics to enhance systemic risk monitoring. The insight from our research findings and methodologies used can also benefit those who work in the macro research or macro trading desks at a bank, asset manager, or trading firm. In addition, the methodologies used in our research can be applied to other sequential datasets beyond financial data.

9.1 Critiques

While we believe our research contributes significantly to the systemic risk literature, it is not without a flaw. A drawback of mutual information and transfer entropy which are key metrics in this research is that they are unit-free which requires using the metrics in a relative, rather than absolute, fashion. That is, transfer entropy from A to B is of magnitude 4 means nothing until we compare it to, say, transfer entropy from C to B. If transfer entropy from A to B is greater than transfer entropy from C to B, it means more information flows from A to B more than from C to B. In contrast, the connectedness measure computed from the forecast error variance decomposition (FEVD) allows for a more convenient interpretation. That is, $FEVD_{A->B}$, which has a value between 0 and 1, can be read as a proportion in the uncertainty of B that is contributed by A.

In addition, the results of both the VAR-FEVD and LoGo-TMFG algorithms are more robust at aggregate levels—system-wide, region-wide and industry-wide—rather than at the pairwise level. Other areas of improvement are listed in the Section 9.2

below.

9.2 Futher research

The material presented in this thesis can be extended in a number of directions. Firstly, the applications of the VAR-FEVD and LoGo-TMFG algorithms are not limited to the financial sector. On the contrary, the algorithms could straightforwardly be extended to measure interconnectedness between various other sectors, such as manufacturing, energy, transportation, pharmaceuticals, and healthcare, to name a few. It is also possible to use the VAR-FEVD methodology on other sequential datasets that demonstrate autoregressive properties; while the author believes that the LoGo-TMFG algorithm has wider applications with respect to types of data.

Secondly, we use ridge regression on the VAR-FEVD in order to deal with high dimensional datasets; however, other estimation techniques such as the lasso could also be applied onto the VAR-FEVD methodology. The well-known lasso regression method is likely to enable the VAR-FEVD to better handle wide datasets because the lasso performs both variable selection and regularization while ridge regression does only regularization. In addition, the lasso will put insignificant VAR coefficients to zero, allowing for better estimation of the pairwise connectedness measure which will enhance the interpretability of the pairwise results.

Lastly, the analyses in this thesis are not of predictive nature but both the VAR-FEVD and LoGo-TMFG algorithms are capable of performing predictive analysis. The ability to forecast future levels of connectivities will be useful for many parties including the financial institutions and regulators in preventing disastrous financial crises from taking place.

Appendix A

Partial correlation vs. forecast error variance decomposition

A.1 Partial correlation

If X and Y are correlated with a third variable Z, X and Y may be correlated simply because they are correlated with Z. Partial correlation allows measuring the correlation between X and Y that is not due to their both being correlated with Z.

If X, Y and Z are jointly Gaussian variables. u_X and u_Y are the residuals from the following linear regressions

$$X = a_1 Z + u_X \tag{A.1}$$

$$Y = a_2 Z + u_Y \tag{A.2}$$

Partial correlation of X and Y given Z is given by

$$\rho_{X,Y \cdot Z} = \frac{u_X' u_Y}{\sqrt{(u_X' u_X)(u_Y' u_Y)}} \tag{A.3}$$

In a VAR(1) model in which each of the variables X_1, X_2 and X_3 is a function of its own first lag and the first lags of the other variables, we have

$$X_{1,t} = a_{11} X_{1,t-1} + a_{12} X_{2,t-1} + a_{13} X_{3,t-1} + u_{1,t} \tag{A.4}$$

$$X_{2,t} = a_{21} X_{1,t-1} + a_{22} X_{2,t-1} + a_{23} X_{3,t-1} + u_{2,t} \tag{A.5}$$

$$X_{3,t} = a_{31} X_{1,t-1} + a_{32} X_{2,t-1} + a_{33} X_{3,t-1} + u_{3,t} \tag{A.6}$$

Partial correlation of X_1 and X_2 given $Z = \{X_{1,t-1}, X_{2,t-1}, X_{3,t-1}\}$ is

$$\rho_{X_1,X_2 \cdot Z} = \frac{u_1' u_2}{\sqrt{(u_1' u_1)(u_2' u_2)}} \tag{A.7}$$

A.2 *h*-step ahead FEVD

The derivation of the *h*-step ahead FEVD start with the actual value y_{t+h} and the *h*-step ahead forecast value for y_t given the information at time *t*

$$y_{t+h} = \mu + \Theta_0 w_{t+h} + \Theta_1 w_{t+h-1} + \Theta_2 w_{t+h-2} + \ldots + \Theta_h w_t + \ldots \tag{A.8}$$

$$y_t(h) = \mu + \Theta_h w_t + \Theta_{h+1} w_{t-1} + \ldots, \tag{A.9}$$

and the *h*-step ahead forecast error

$$y_{t+h} - y_t(h) = \Theta_0 w_{t+h} + \Theta_1 w_{t+h-1} + \ldots + \Theta_{h-1} w_{t+1}. \tag{A.10}$$

In matrix form

$$\begin{aligned}
\begin{bmatrix} y_{1,t+h} - y_{1,t}(h) \\ y_{2,t+h} - y_{2,t}(h) \\ \vdots \\ y_{K,t+h} - y_{K,t}(h) \end{bmatrix} &= \begin{bmatrix} \theta_{11,0} & \theta_{12,0} & \ldots & \theta_{1K,0} \\ \theta_{21,0} & \theta_{22,0} & \ldots & \theta_{2K,0} \\ \vdots & & & \\ \theta_{K1,0} & \theta_{K2,0} & \ldots & \theta_{KK,0} \end{bmatrix} \begin{bmatrix} w_{1,t+h} \\ w_{2,t+h} \\ \vdots \\ w_{K,t+h} \end{bmatrix} \\
&+ \begin{bmatrix} \theta_{11,1} & \theta_{12,1} & \ldots & \theta_{1K,1} \\ \theta_{21,1} & \theta_{22,1} & \ldots & \theta_{2K,1} \\ \vdots & & & \\ \theta_{K1,1} & \theta_{K2,1} & \ldots & \theta_{KK,1} \end{bmatrix} \begin{bmatrix} w_{1,t+h-1} \\ w_{2,t+h-1} \\ \vdots \\ w_{K,t+h-1} \end{bmatrix} + \ldots \\
&+ \begin{bmatrix} \theta_{11,h-1} & \theta_{12,h-1} & \ldots & \theta_{1K,h-1} \\ \theta_{21,h-1} & \theta_{22,h-1} & \ldots & \theta_{2K,h-1} \\ \vdots & & & \\ \theta_{K1,h-1} & \theta_{K2,h-1} & \ldots & \theta_{KK,h-1} \end{bmatrix} \begin{bmatrix} w_{1,t+1} \\ w_{2,t+1} \\ \vdots \\ w_{K,t+1} \end{bmatrix}.
\end{aligned} \tag{A.11}$$

The h-step ahead forecast error for y_j is

$$\begin{aligned} y_{j,t+h} - y_{j,t}(h) &= \theta_{j1,0} w_{1,t+h} + \theta_{j2,0} w_{2,t+h} + \ldots + \theta_{j1,h-1} w_{1,t+1} + \ldots + \theta_{jK,h-1} w_{K,t+1} \\ &= \sum_{i=0}^{h-1} \left(\theta_{j1,i} w_{1,t+h-i} + \ldots + \theta_{jK,i} w_{K,t+h-i} \right) \\ &= \sum_{k=1}^{K} \theta_{jk,0} w_{k,t+h} + \ldots + \theta_{jk,h-1} w_{k,t+1} \big). \end{aligned} \tag{A.12}$$

The MSE of $y_{j,t}(h)$ is

$$\mathbb{E}\left((y_{j,t+h} - y_{j,t}(h))^2 \right) = \sum_{k=1}^{K} (\theta_{jk,0}^2 + \ldots + \theta_{jk,h-1}^2) = \sum_{i=0}^{h-1} \sum_{k=1}^{K} \theta_{jk,i}. \tag{A.13}$$

The contribution to the forecast error variance (or the MSE of the h-step ahead forecast) of variable y_j that is due to the innovation w_k (a one-standard deviation shock to the variable k) is $\theta_{jk,0}^2 + \theta_{jk,1}^2 + \ldots + \theta_{jk,i}^2 = \sum_{i=0}^{h-1} (e_j' \theta_i e_k)^2$.

$$FEVD_{jk,h} = \frac{\sum_{i=0}^{h-1} (e_j' \theta_i e_k)^2}{\sum_{i=0}^{h-1} \sum_{k=1}^{K} \theta_{jk,i}^2} = \frac{\sum_{i=0}^{h-1} (e_j' \theta_i e_k)^2}{MSE(y_{j,t}(h))}. \tag{A.14}$$

Appendix B

Rolling-window analysis

B.1 Sparse regional networks: Interregional links

Figures B.1, B.2, B.3, B.4, B.5, B.6, B.7, and B.8 plot respectively the number of links from South America, Africa, West Asia, the Middle East, South Asia, East Asia, Southeast Asia, and Australia to the other economic regions and the number of links in the opposite direction for 25 rolling windows between 1990 and 2016.

The numbers of links are conditional transfer entropies computed using sparse inverse covariance matrix which is estimated using LoGo-TMFG algorithm. In general, the number of intra-regional and inter-regional links in all abovementioned regions increased over time from 1990 to 2016.

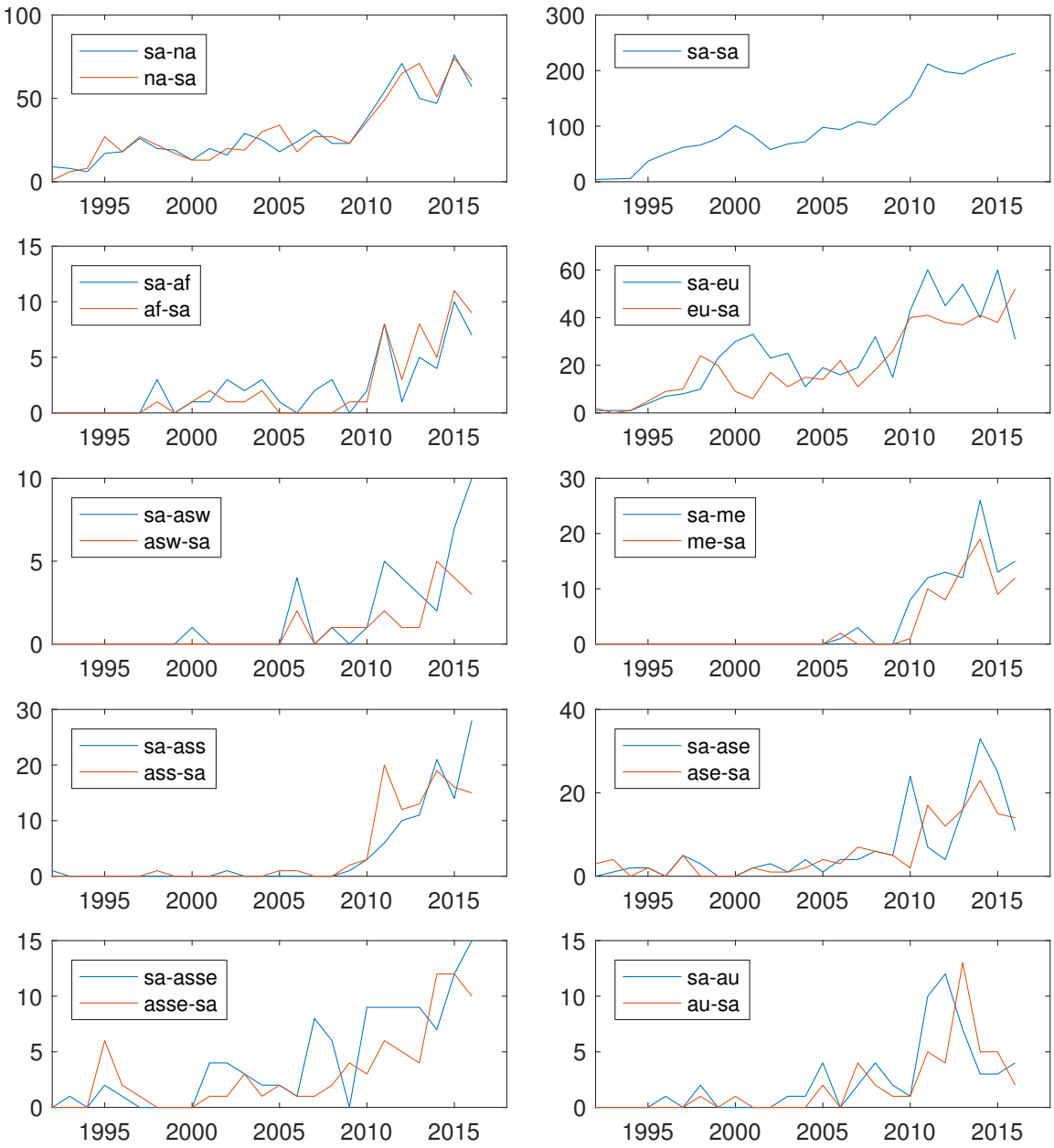

Figure B.1: South America: Number of links from South America to the other economic regions and vice versa for 25 rolling windows between 1990 and 2016. In general, the number of links between financial companies within South America and between South American companies and those in the other regions increased over time, with the largest increase in 2010. South America is connected with North America the most, followed by Europe, and East Asia.

Figure B.2: Africa: Number of links from Africa to the other economic regions and vice versa for 25 rolling windows between 1990 and 2016. The number of links between financial companies within Africa and between African companies and those in the other regions generally increased over time, with the largest increase in 2011. Africa was connected with North America the most, followed by Europe, and South Asia.

Figure B.3: West Asia: Number of links from West Asia to the other economic regions and and vice versa for 25 rolling windows between 1990 and 2016. West Asia was connected with Europe the most, followed by North America. The number of links between West Asia and the others increased over time, with the most significant increase in 2010.

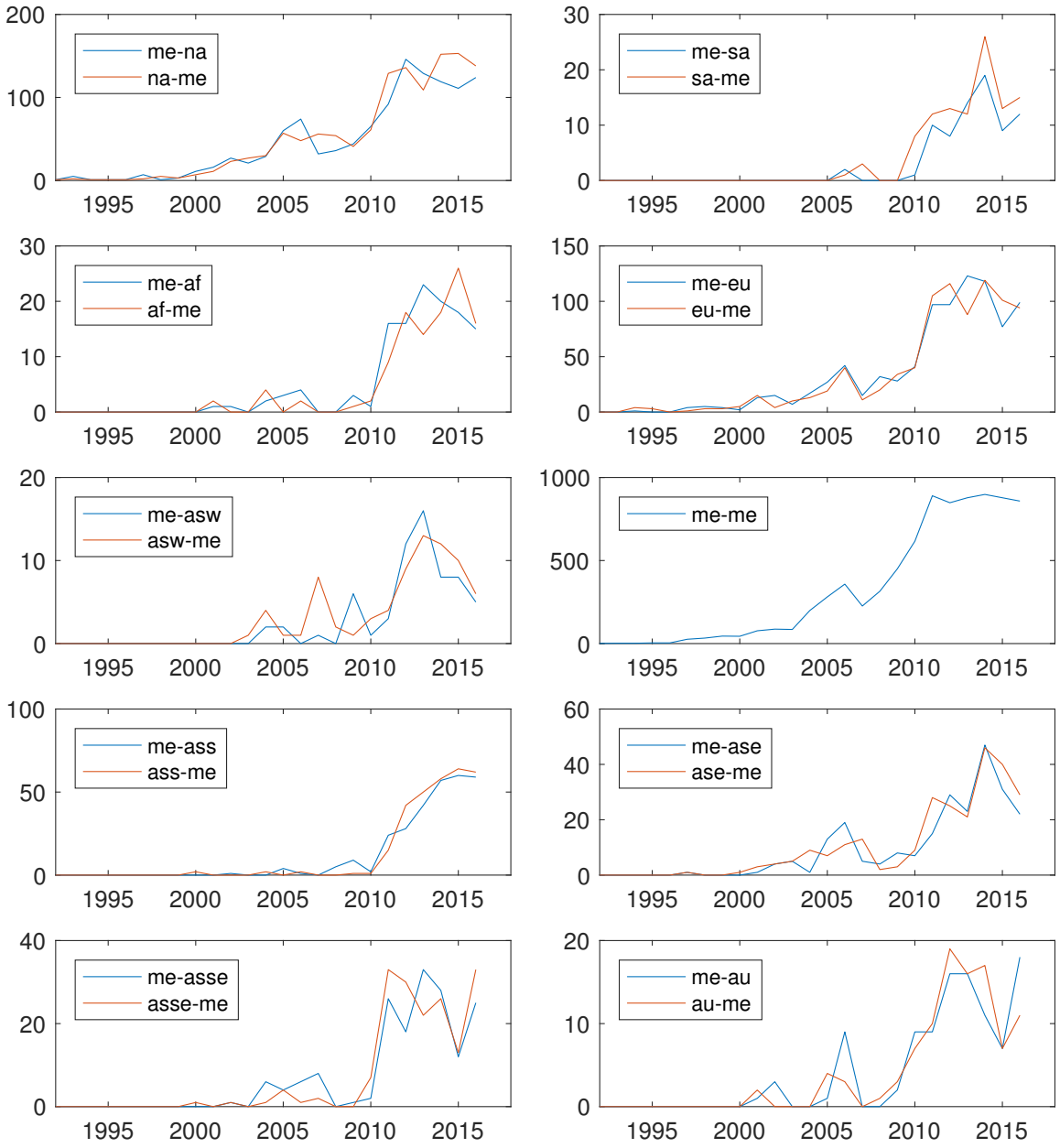

Figure B.4: The Middle East: Number of links from the Middle East to the other economic regions and and vice versa for 25 rolling windows between 1990 and 2016. The Middle East was connected with North America the most, followed by Europe and South Asia. The number of links between the Middle East and the other regions increased over time, with the most rapid increase in 2010 but a slight drop in 2014. In general, the number of intra-regional links within companies in the Middle East increased over time, with the most significant increase between 2007 and 2010.

Figure B.5: South Asia: Number of links from South Asia to the other economic regions and vice versa for 25 rolling windows between 1990 and 2016. South Asia was connected with North America the most, followed by Europe, the Middle East and East Asia. The number of links between South Asia and the other regions increased over time, with the most rapid increase in 2010 but a slight drop in 2014. The number of intra-regional links within companies in the South Asia increased over time, with a sharpe rise between 2005 and 2015.

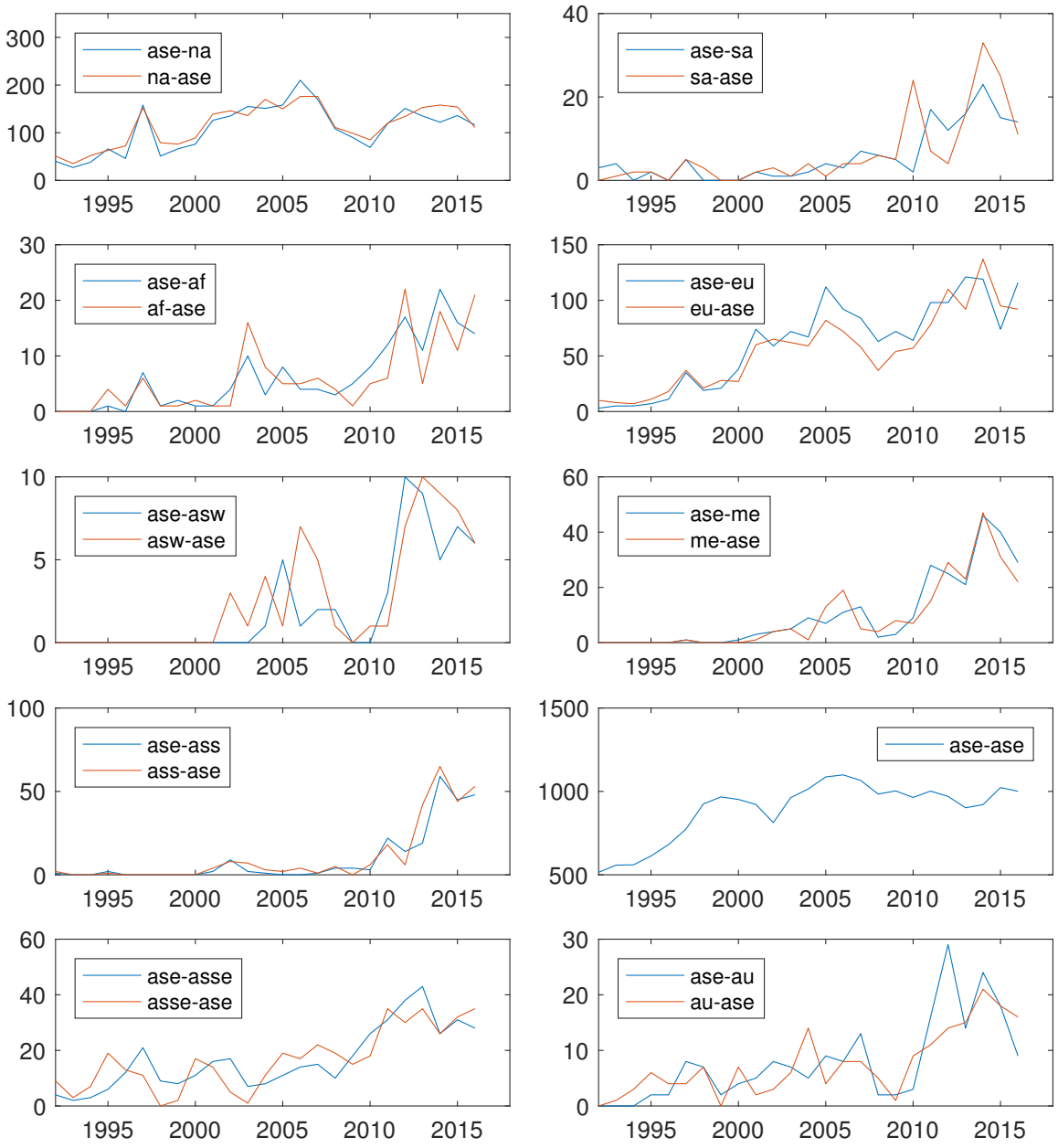

Figure B.6: East Asia: Number of links from East Asia to the other economic regions and vice versa for 25 rolling windows between 1990 and 2016. East Asia was connected with North America the most, followed by Europe and Southeast Asia. The number of links from and to East Asian financial companies (both inter-regional and intra-regional) increased over time.

Figure B.7: Southeast Asia: Number of links from Southeast Asia to the other economic regions and vice versa for 25 rolling windows between 1990 and 2016. Southeast Asia was connected with North America the most, followed by Europe and East Asia. The number of links from and to Southeast Asia increased over time, with the most rapid increase occuring around 2004 and 2010 for Southeast Asia vs. North America and Southeast Asia vs. Europe. For Southeast Asia vs. other regions, the number of links increased the most rapidly in 2010.

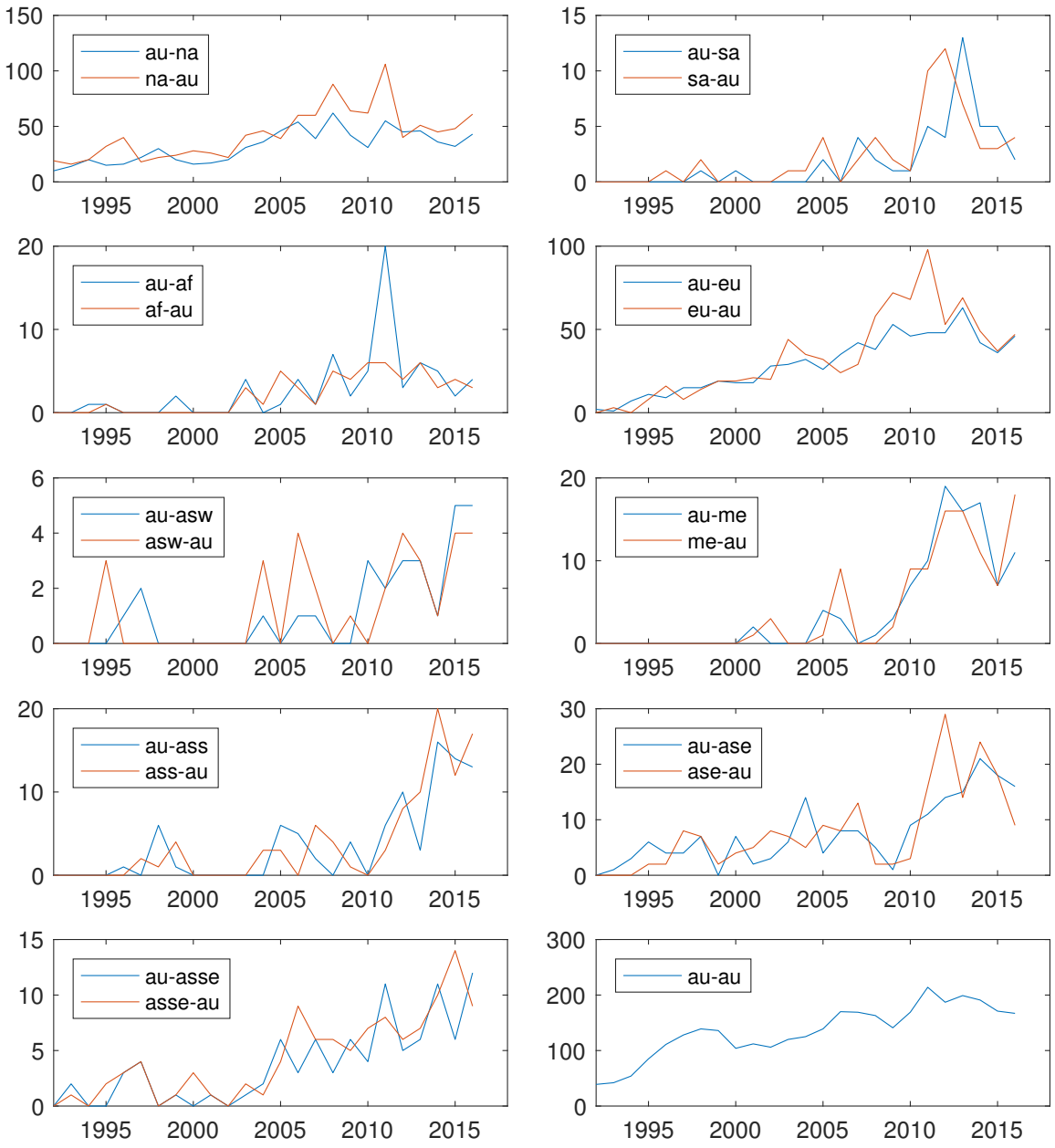

Figure B.8: Australia: Number of links from Australia to the other economic regions and vice versa for 25 rolling windows between 1990 and 2016. Australia was connected with North America the most, followed by Europe and East Asia. The number of links between the Australia and the other regions increased over time, with the most rapid increase occuring around 2005 and 2010.

B.2 Sparse industrial networks: Additional data summary

Figure B.9: Time-varying average annualized log returns by industry in all ten economic regions of the world between 1990 and 2016.

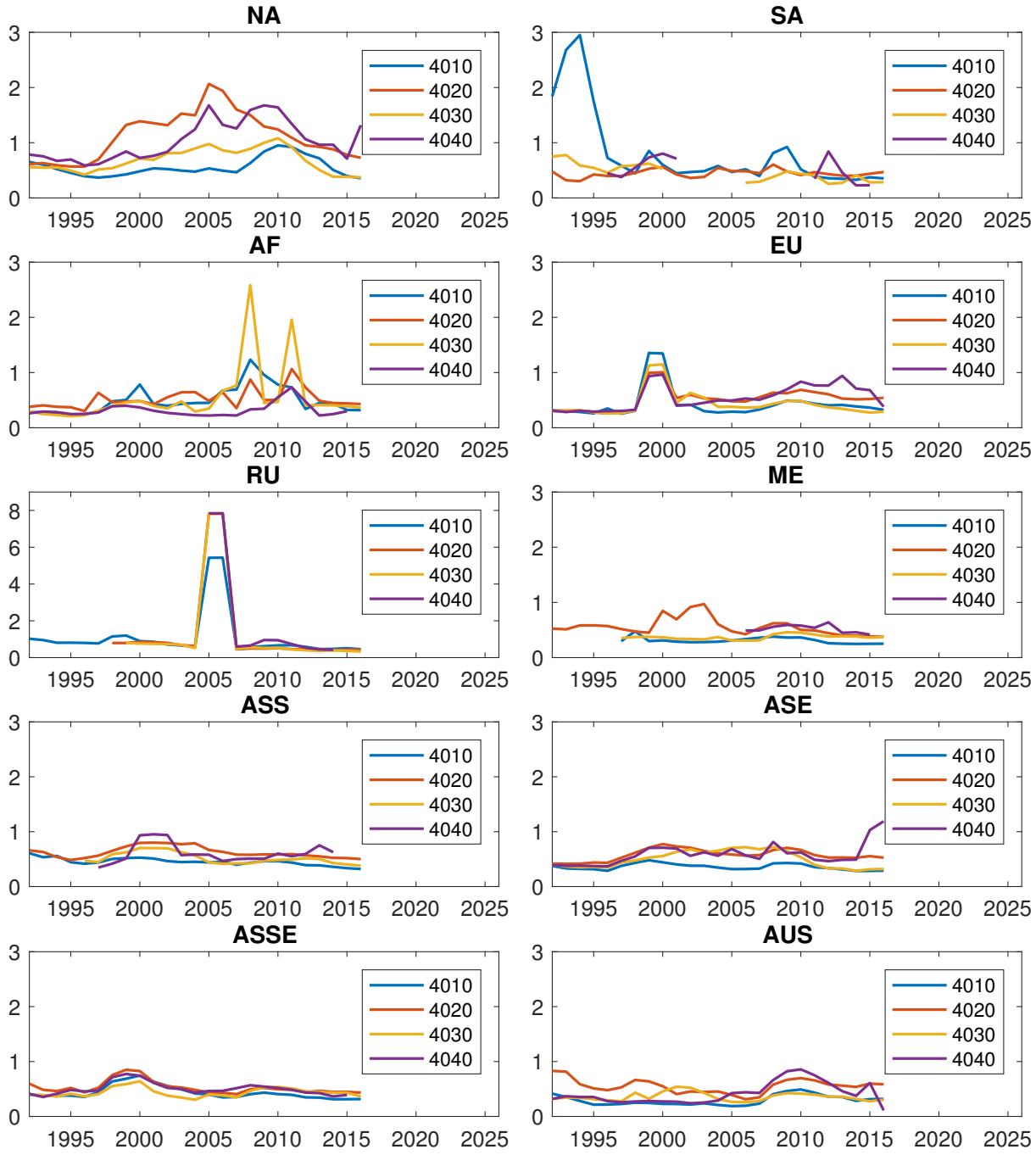

Figure B.10: Time-varying average annualized average standard deviations by industry in all ten economic regions of the world between 1990 and 2016.

Table B.1: Number of financial companies in each industry globally for all 25 three-year periods between 1990-2016, where 4010 is banks, 4020 is diversified financials, 4030 is insurance, and 4040 is real estate

	4010	4020	4030	4040	Total
1990-92	861	364	271	184	1680
1991-93	899	408	283	198	1788
1992-94	913	446	309	213	1881
1993-95	959	525	338	253	2075
1994-96	1080	588	349	333	2350
1995-97	1125	634	335	347	2441
1996-98	1162	695	356	365	2578
1997-99	1239	731	349	368	2687
1998-00	1317	798	344	385	2844
1999-01	1511	815	337	369	3032
2000-02	1503	846	340	350	3039
2001-03	1537	965	354	346	3202
2002-04	1554	1030	365	340	3289
2003-05	1579	1119	389	338	3425
2004-06	1643	1196	396	341	3576
2005-07	1632	1213	377	298	3520
2006-08	1624	1256	373	290	3543
2007-09	1664	1366	386	276	3692
2008-10	1709	1448	391	263	3811
2009-11	1784	1828	503	281	4396
2010-12	1746	1834	532	228	4340
2011-13	1701	1884	537	167	4289
2012-14	1661	2017	545	126	4349
2013-15	1632	2090	544	77	4343
2014-16	1593	2159	542	16	4310

References

A.R. Admati, P.M. DeMarzo, M.F. Hellwig, and P. Pfleiderer. Fallacies, irrelevant facts, and myths in the discussion of capital regulation: Why bank equity is not socially expensive. *SSRN working paper*, pages 1–70, 2013.

T. Adrian and M. K. Brunnermeier. CoVaR. *The American Economic Review*, 106(7): 1705–1741, 2016.

F. Allen and A. Babus. Networks in finance. *Wharton Financial Institutions Center Working Paper No. 08-07.*, 2008.

F. Allen and D. Gale. Financial contagion. *The Journal of Political Economy*, 108(1): 1–33, 2000.

A. Alter and A. Beyer. The dynamics of spillover effects during the european sovereign debt turmoil. *Journal of Banking and Finance*, 42:134–153, 2014.

N. Antonakakis. Exchange return co-movements and volatility spillovers before and after the introduction of euro. *Journal of International Financial Markets, Institutions and Money*, 22(5), 2012.

B. Awartani and A. I. Maghyereh. Dynamic spillovers between oil and stock markets in the gulf cooperation council countries. *Energy Economics*, 36:28–42, 2013.

O. Banerjee, L.E. Ghaoui, and A. d'Astremont. Model selection through sparse maximum likelihood estimation for multivariate gaussian or binary data. *Journal of Machine Learning Research*, 9:485–516, 2008.

European banks. Banking and nothingness: Europe's dithering banks are losing ground to their decisive american rivals. http://www.economist.com/news/finance-and-

economics/21674778-europes-dithering-banks-are-losing-ground-their-decisive-american-rivals-banking, October 2017. Accessed: 2017-03-11.

M. Bardoscia, S. Battisson, F. Caccioli, and G. Caldarelli. Debtrank: A microscopic foundation for shock propagation. *PLoS ONE*, 10(7):1–13, 2015.

W. Barfuss, G.P. Massara, T. Di Matteo, and T. Aste. Parsimonious modeling with information filtering networks. *Physical Review E*, 2016.

L. Barnett, A.B. Barrett, and A.K. Seth. Granger causailty and transfer entropy are equivalent for gaussian variables. *Physical Review Letters*, 103:238701, 2009.

J. Batson, D. A. Spielman, and N. Srivastava. Twice-ramanujan sparsifiers. *SIAM Rev*, 56(2):315334, 2014.

S. Battiston, M. Puliga, R. Kaushik, P. Tasca, and G. Caldarelli. DebtRank: Too central to fail? financial networks, the FED and systemic risk. *Scientific Reports*, 2:1–6, 2012.

N. Beale, D. G. Rand, H. Battey, K. Croxson, R. M. May, and M. A. Nowak. Individual versus systemic risk and the regulator's dilemma. *Proceedings of the National Academy of Sciences*, 108(31):12647–12652, 2011.

R. E. Bellman. *Adaptive Control Process: A Guided Tour*. Princeton University Press, 1961.

A.A. Benczúr and D.R. Karger. Approximating s-t minimum cuts in $\tilde{O}(n^2)$ time. In *Proceedings of the Twenty-eighth Annual ACM Symposium on Theory of Computing*, STOC '96, pages 47–55, New York, NY, USA, 1996.

M. Billio, M. Getmansky, A.W. Lo, and L. Pelizzon. Econometric measures of connectedness and systemic risk in the finance and insurance sectors. *Journal of Financial Economics*, 104(3):535–559, 2012.

C. M. Bishop. *Pattern Recognition and Machine Learning*. Springer, 2006.

K. Brecht. How U.S. and EU capital markets are different. http://openmarkets.cmegroup.com/10431/how-u-s-and-eu-capital-markets-are-different, October 2015. Accessed: 2017-03-11.

C. Brownlees and R. Engle. SRisk: A conditional capital shortfall measure of systemic risk. *Review of Financial Studies*, 30(1):48–79, 2016.

V. Bubák, E. Kočenda, and F. Žikeš. Volatility transmission in emerging european foreign exchange markets. *Journal of Banking & Finance*, 35(11):2829–2841, 2011.

F. Caccioli, M. Shrestha, C. Moore, and J.D. Farmer. Stability analysis of financial contagion due to overlapping portfolios. *Journal of Banking & Finance*, 46:233–245, 2014.

F. Caccioli, J.D. Farmer, N. Foti, and D. Rockmore. Overlapping portfolios, contagion, and financial stability. *Journal of Economic Dynamics and Control*, 51:50–63, 2015.

C. Caceres, V. Guzzo, and M. Segoviano Basurto. Sovereign spreads: Global risk aversion, contagion or fundamentals? *IMF working papers*, pages 1–29, 2010.

S. Carbo-Valverde, D. Marques-Ibanez, and F. Rodriguez-Fermandez. Securitization, bank lending and credit quality: The case of spain. *ECB working paper*, (1329), 2011.

F. Chau and R. Deesomsak. Does linkage fuel the fire? The transmission of financial stress across the markets. *International Review of Financial Analysis*, 36:57–70, 2014.

P. Claeys and B. Vasicek. Measuring bilateral spillover and testing contagion on sovereign bond markets in europe. *Journal of Banking & Finance*, 46:151 – 165, 2014.

R. Cont, A. Moussa, and E.B. Santos. Network structure and systemic risk in banking systems. *SSRN working paper*, 2010.

F. Corsi, S. Marmi, and F. Lillo. When micro prudence increases macro risk: The destabilizing effects of financial innovation, leverage, and diversification. *Operations Research*, 64(5):1073–1088, 2016.

H. Degryse and G. Nguyen. Interbank exposure: An empirical examination of systemic risk in the belgian banking system. 2004.

M. Demirer, F.X. Diebold, L. Liu, and K. Yilmaz. Estimating global bank network connectedness. *Applied Econometrics*, 33(1):1–15, July 2017.

F.X. Diebold and K. Yilmaz. Measuring financial asset return and volatility spillovers, with application to global equity markets. *The Economic Journal*, 119:158–171, 2009.

F.X. Diebold and K. Yilmaz. Better to give than to receive: Predictive directional measurement of volatility spillovers. *International Journal of Forecasting*, 28:57–66, 2012.

F.X. Diebold and K. Yilmaz. On the network topology of variance decompositions: Measuring the connectedness of financial firms. *Journal of Econometrics*, 182:119–134, 2014.

F.X. Diebold and K. Yilmaz. *Financial and Macroeconomic Connectedness*. Oxford University Press, 2015a.

F.X. Diebold and K. Yilmaz. Trans-Atlantic equity volatility connectedness: U.s. and european financial institutions, 2004-2014. *Journal of Financial Econometrics*, forthcoming:1–47, 2015b.

D. Dungey, R. Fry, B. Gonzales-Hermosillo, and V.L. Martin. Empirical modelling of contagion: a review of methodologies. *Quantitative Finance*, 5(1):9–24, 2005.

L. Eisenberg and T.H. Noe. Systemic risk in financial systems. *Management Science*, 47(2):236–249, 2001.

M.R. Fengler and K.I.M. Gisler. A variance spillover analysis without covariances: What do we miss? *Journal of International Money and Finance*, 51:174–195, 2015.

J. Friedman, T. Hastie, and R. Tibshirani. Sparse inverse covariance estimation with the graphical lasso. *Biostatistics*, 9:432–441, 2008.

I. Fujiwara and K. Takahashi. Asian financial linkage: Macro-finance dissonance. *Pacific Economic Review*, 17:1:136–159, 2012.

C.H. Furfine. Interbank exposures: Quantifying the risk of contagion. *Journal of Money, Credit and Banking*, 35:111–128, 2003.

P. Gai and S. Kapadia. Contagion in financial networks. In *Proceedings of the Royal Society of London A: Mathematical, Physical and Engineering Sciences*, page rspa20090410. The Royal Society, 2010.

S. Garry and J. Carlos Moreno-Brid. Is a new era of growth on the horizon for Latin America? *World Economics Association Newsletter*, 5(6):1–16, December 2015.

M-V Geraci and J-Y Gnabo. Measuring interconnectedness between financial institutions with bayesian time-varying vector autoregressions. *Journal of Financial and Quantitative Analysis*, 53(3):13711390, 2018. doi: 10.1017/S0022109018000108.

J. Geweke. Measurement of linear dependence and feedback between multiple time series. *Journal of the American statistical association*, 77(378):304–313, 1982.

C. W. J. Granger. Investigating causal relations by econometric models and cross-spectral methods. *Econometrica*, 37(3):424–438, 1969.

William H. Greene. *Econometric Analysis*. Prentice Hall, 2003.

O. Heinavaara, J. Leppa-Aho, Corander J., and Honkela A. On the inconsistency of l1-penalised sparse precision matrix estimation. *BMC Bioinformatics*, 17, 2016.

X. Huang, I. Vodenska, S. Havlin, and H. E. Stanley. Cascading failures in bi-partite graphs: Model for systemic risk propagation. *Scientific Reports*, 3(1219):1–8, 2013.

S. Klößner and S. Wagner. Exploring all var orderings for calculating spillovers? yes, we can!a note on diebold and yilmaz (2009). *Journal of Applied Econometrics*, 29 (1):172–179, 2014.

G. Koop, M.H. Pesaran, and S.M. Potter. Impulse response analysis in nonlinear multivariate models. *Journal of Econometrics*, 74(1):119–147, 1996.

O. Ledoit and M. Wolf. Nonlinear shrinkage estimation of large-dimentional covariance matrix. *The Annals of Statistics*, 40(2):1024–1060, 2012. URL `http://www.jstor.org/stable/41713664`.

Z. Liu, S. Quiet, and B. Roth. Banking sector interconnectedness: what is it, how can we measure it and why does it matter? *Bank of England Quarterly Bulletin*, Q2 2015.

A. Lucas, B. Schwaab, and X. Zhang. Conditional euro area sovereign default risk. *Journal of Business & Economic Statistics*, 32(2):271–28, 2014.

H. Lutkepohl. *New Introduction to Multiple Time Series Analysis*. Springer-Verlag Berlin Hidelberg New York, 2006.

S. Martinez-Jaramillo, O.M. Perez, F.A. Embriz, and F. Lopez-Gallo. Systemic risk, financial contagion and financial fragility. *Journal of Economic Dynamics & Control*, 34:2358–2374, 2010.

D.J. Masson. Commercial banking in the U.S. versus canada. *Graziadio Business Review*, 2007.

D.G. McMillan and A.E.H. Speight. Return and volatility spillovers in three euro exchange rates. *Journal of Economics and Business*, 62:79–93, 2010.

E. Nier, J. Yang, T. Yorulmazer, and A. Alentorn. Network models and financial stability. *Journal of Economic Dynamics and Control*, 31:2033–2060, 2007.

Y. Onaran. U.S. banks bigger than GDP as accounting rift masks risk. https://www.bloomberg.com/news/articles/2013-02-20/u-s-banks-bigger-than-gdp-as-accounting-rift-masks-risk, February 2013. Accessed: 2017-03-12.

M.H. Pesaran and Y. Shin. Generalized impulse response analysis in linear multivariate models. *Econometrics Letters*, 58(1):17–29, 1998.

F. Pozzi, T. Di Matteo, and T. Aste. Exponential smoothing weighted correlations. *The European Physical Journal B*, 85: 175:1–21, 2012.

D.E. Rapach, J.K. Strauss, and G. Zhou. International stock return predictability: What is the role of the united states? *The Journal of Finance*, 68(4):1633–1662, 2013.

M. Rohleder, H. scholz, and M. Wilkens. Survivorship bias and mutual fund performance: Relevance, significance, and methodical differences. *Review of Finance*, 15 (2):441–474, 2010.

H. Rue and L. Held. *Gaussian Markov Random Fields: Theory And Applications (Monographs on Statistics and Applied Probability)*. Chapman & Hall/CRC, 2005. ISBN 1584884320.

T. Schreiber. Measuring information transfer. *Physical Review Letters*, 85:461–464, Jul 2000. doi: 10.1103/PhysRevLett.85.461.

C.E. Shannon. A mathematical theory of communication. *The Bell Labs Technical Journal*, 27:379–423, 1948.

R.J. Shiller. From efficient markets theory to behavioral finance. *The Journal of Economic Perspectives*, 17(1):83–104, 2003.

C.A. Sims. Macroeconomics and reality. *Econometrica*, 48:1–48, 1980.

P. Smaga. The concept of systemic risk. *Systemic Risk Center Special Paper No 5*, pages 1–68, 2014.

D. Spielman and S. Teng. Spectral sparsification of graphs. *SIAM Journal on Computing*, 40(4):9811025, 2011.

D.A. Spielman and N. Srivastava. Graph sparsification by effective resistances. 2009.

R.S. Tsay. *Analysis of financial time series*. Wiley & Sons, 2010.

S. Tungsong, F. Caccioli, and T. Aste. Relation between regional uncertainty spillovers in the global banking system. *Journal of Network Theory in Finance*, 4(2):1–23, 2018.

C. Upper. Simulation methods to assess the danger of contagion in interbank markets. *Journal of Financial Stability*, 7(3):111–125, 2011.

C. Upper and A. Worms. Estimating bilateral exposures in the german interbank market: Is there a danger of contagion? *European Economic Review*, 48(4):827–849, 2004.

M. Verleysen and D. François. The curse of dimensionality in data mining and time series prediction. In *Proceedings of the 8th International Conference on Artificial*

Neural Networks: Computational Intelligence and Bioinspired Systems, pages 758–770, Berlin, Heidelberg, 2005. Springer-Verlag.

R.A. Weigand. A tale of two banking systems: the performance of us and european banks in the 21st century. *Investment Management and Financial Innovations*, 2015.

W. White. The implications of the FTA and NAFTA for Canada and Mexico. Technical report, Bank of Canada, 1994.

A.D. Wyner. A definition of conditional mutual information for arbitrary ensembles. *Information and Control*, 38(1):51–59, 1978.

K. Yilmaz. Return and volatility spillovers among the east asian equity markets. *Journal of Asian Economics*, 21:304–313, 2010.

P. Zhao and B. Yu. On model selection consistency of lasso. *Journal of Machine Learning Research*, 7:2541–2563, 2006.

X. Zhou, W. Zhang, and J. Zhang. Volatility spillovers between the chinese and world equity markets. *Pacific-Basin Finance Journal,*, 20, 2012.